AIAA 2019-2020 General Aviation Trainer Aircraft Family

Team Member	AIAA Number	Signature
Grant Godfrey	856024	
Brio Ratzlaff	977334	
Francisco Caceres	986195	
Thomas Kennedy	1069261	
Tyler Schwallie	998659	
Team Advisor		
Dr. Ron Barrett	022393	

Table of Contents

List of Symbols

Symbol	**Definition**	**Unit**
a	Acceleration	ft/s^2
A	Aspect Ratio	~
b	Wingspan	ft
BFSC	Brake Specific Fuel Consumption	(lbm/hr)/ lbf
B.L.	Butt Line	in
c	Chord	ft
c_f	Skin Friction Coefficient	~
C_D	Drag Coefficient	~
$C_{D,o}$	Parasite Drag Coefficient	~
C_L	Lift Coefficient	~
DF	Design Features	~
DR	Design Requirements	~
e	Oswald Efficiency Factor	in
F.S.	Fueselage Station	ft/s^2
g	Acceleration of Gravity	~
j	Feature Weight	~
k	Feedback Gain	~
LL	Low Lead	~
M	Mission	~
n	Number	hp
P	Power	lbf/ft^2
P	Pressure	lbf/ft^2
q	Dynamic Pressure	ft^2
S	Wing Area	%
S.M.	Static Margin	ft/s
V	Velocity	lbf
W	Weight	in
W.L.	Water Line	lbf/ft^2
W/S	Wing Loading	
Greek Symbols		~
α	Angle of Attack	$slug/ft^3$
β	Side Slip	degree
η	Efficiency	~
ρ	Air Density	
Γ	Dihedral	
Δ	Change in	

Subscripts

ac	Aerodynamic Center
b	Butterfly Tail
c/4	Quarter Chord
clean	Clean Configuration
cr	Critical
crew	Aircraft Crew
d	Drag
DB	Base Drag
DBA	Aft Body Base Drag
dyn	Dynamic
e	Empty
etent	Empty Tentative
f	Fuel
f	Fuselage
fc	Fineness Ratio
ff	Fuel Fraction
got	Value Have
i	Indicated Number
i	Inboard
l	2D Lift
l design	Design Lift
L	3D Lift
m	Moment
max	Maximum Value
max need	Maximum Needed
n	Yawing Moment
n	Indicated Number
need	Needed Value
o	Outboard
etent	Tentative Operating Empty
p	Propeller
pl	Payload
root	Planform Root
s	Static
t	Tire
tip	Planform Tip
to	Takeoff
tfo	Trapped Fuel and Oil
w	Wing
wf	Wing Fuselage

Acronyms

AIAA	American Institute of Aeronautics and Astronautics
CAD	Computer Aided Design
C.G.	Center of Gravity
FAA	Federal Aviation Administration
FADEC	Full Authority Digital Engine Controller
IFR	Instrument Flight Rules
OF	Objective Function

PID	Proportional, Integral, Derivative
RFP	Request for Proposal
STAMPED	Statistical Time and Market Predictive Engineering Design
VFR	Visual Flight Rules

List of Tables

List of Figures

1. Introduction, Mission Specifications and Profiles

This report was constructed to fulfill all the requirements set forth by the 2019-2020 American Institute of Aeronautics and Astronautics (AIAA) Request for Proposal (RFP) for a General Aviation Trainer Aircraft family (Ref. 1). The RFP can be found directly here.

1.1. Introduction

It has been noted that the commercial airline industry will soon see a shortage of pilots as the current generation of pilots age and reach the mandatory retirement age of 65 (Ref. 2). Traditionally filled by freshly separated military pilots, the reduction in numbers of the military has led to less pilots seperating and filling those slots, forcing airlines to seek pilots with civilian based training. With nearly 20,000 cockpit seats estimated to open up, a new set of General Aviation aircraft will be needed to properly train civilian pilots to meet the needs for both regional and national carriers. The current, most popular pilot trainer, the Cessna 172 has not seen a major redesign since its release in 1956. This leaves the market open for an economic family of aircraft that can compete with the available options in both, price, functionality and purpose designed to optimize pilot training. The following sections in this chapter will highlight the requirements, mission profiles, and a brief overview of the design process.

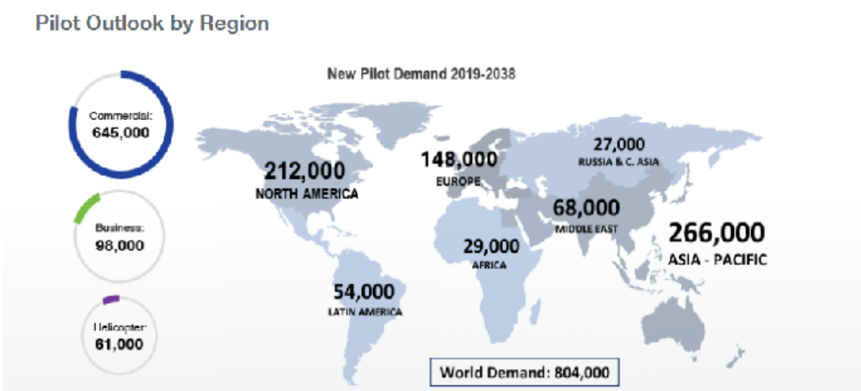

Figure 1.1 Boeing Pilot Outlook 2019-2038 (Ref. 3)

1.2. Mission Specification

Mandatory Design requirements set forth by the AIAA General Aviation Trainer Aircraft Family RFP and are listed below (Ref. 1):

- Capable of taking off and landing from runways (asphalt or concrete);
- Capable of VFR and IFR flight;
- Meets applicable certification rules in FAA 14 CFR Part 23.

Table 1.1 represents specifications that can vary between the two aircraft

Table 1.1 General Aviation Trainer Aircraft Family (Ref. 1)

	Single-engine	Multi-Engine
Crew	1 Pilot required, 2-Pilot (dual Instruction) Capable	
Passenger	1+	3+
Takeoff distance	<1500 ft	<2500 ft
Landing Distance	<1500 ft	<2500 ft
Endurance	>3 hr	> 4 hr
Ferry Range	>800 nmi	>1000 nmi
Service Ceiling	>12000 ft	>18000 ft
Certification category	Utility	Normal

1.3. Mission Profile

Each aircraft in the general aviation trainer aircraft family will have similar mission profiles with varying take off, ferry range and landing distances as shown in Table 1.1. Figure 1.2 represents the flight profile for the aircraft family.

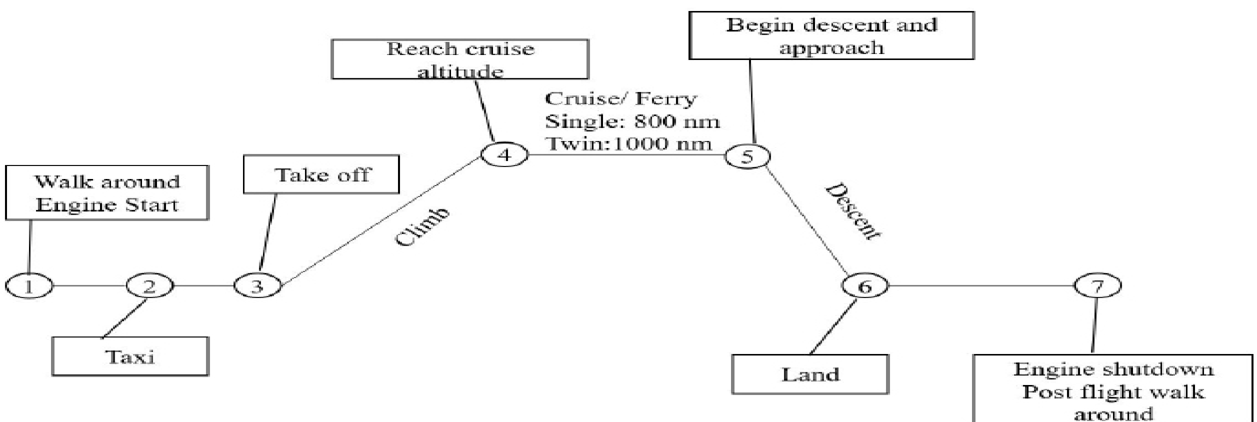

Figure 1.2 Mission Profile

1.4. Overall Design Methods and Procedures

The methods outlined in the eight-part Aircraft Design Series by Dr. Jan Roskam were utilized by the authors with supplemental instruction by Dr. Ron Barrett (Ref. 4). Hand calculations were used to verify all design and sizing choices. The design process is listed below:

i.) Identify Mission Specifications and Profile;

ii.) Historical Review;

iii.) Stamped Analysis;

iv.) Weight Sizing;

v.) Wing and Powerplant sizing.

2. Historical Review

The purpose of this chapter is to give insight on aircraft currently used by pilot training institutions. This will guide Super Aerial Bros in making appropriate design choices to ensure the viability of the future aircraft trainer family. This section looked at two single engine aircraft and two twin engine aircraft

2.1. Cessna 172 Skyhawk

The Cessna 172 Skyhawk is the staple of aviation training and is the most popular general aviation aircraft on the market (Ref. 5). Introduced in 1956 the Cessna 172 has undergone only minor design changes, but has seen multiple engines, interior and avionic updates that have kept the aircraft competitive. The Cessna Skyhawk forgiving stall characteristics, low landing speeds, reliability and low acquisition costs have led Embry-Riddle Aeronautical University to grow and update their fleet with the purchase of 60 new Skyhawks for pilot training (Ref. 6). Between 2005-2018, 2243 Cessna Skyhawks have been sold (Ref. 7).

Figure 2.1 Cessna 172 Skyhawk (Ref. 5)

2.2. Cirrus SR20

The Cirrus SR 20 is another popular single engine aircraft chosen by training institutions such as Purdue Polytechnic Institute and Western Michigan University (Ref. 8,9). The SR20 was the first General aviation light aircraft with full composite construction as well as an emergency parachute. The higher acquisition cost and higher fatality rates (1.6/100,000 flight hours) early in the aircraft life caused aircraft sales of the SR20 to drastically trail the Cessna 172 (Ref. 7, 11). Between 2005-2018, 935 aircraft have been sold (Ref. 7).

Figure 2.2 Cirrus SR20 (Ref. 10)

2.3. Diamond DA 42

The twin engine Diamond DA42 was introduced in 2004 By Diamond Aircraft Industries in Austria. It was the first new twin engine design produced in over 25 years. The Austro AE 300 turbo diesel engines are certified to run on either Jet A-1 or diesel each with their own full authority digital engine controller (FADEC). With a cruise fuel combustion of 10.4 gal/hr, its efficiency and

Figure 2.3 Diamond DA 42 (Ref. 13)

safety record have made it a prime choice for twin engine training for Embry-Riddle Aeronautical University. 901 DA 42 have been sold from 2005-2018 (Ref. 7).

2.4. <u>Piper Seminole</u>

The Piper Seminole, operated by Purdue Polytechnic Institute and the University of North Dakota, two prominent flight schools, was introduced in 1979 (Ref. 8, 11). Also known as the PA-44, it was developed from the single engine Piper Cherokee and is known for it's reliability and low operating cost. Despite the manufacture touting it as the twin engine trainer of choice, from 2005-2018, only 263 Piper Seminoles have been sold, significantly trailing the DA42 (Ref. 7)

Figure 2.4 Piper Seminole (Ref. 14)

2.5. <u>Summary and Recommendations</u>

2.5.1. <u>Summary</u>

A summary of comparable aircraft characteristics are in Table 2.1.

Table 2.1 Comparrison of Historical Aircraft (Ref. 1, 8, 9, 10)

	Cessna 172	Cirrus SR20	Diamond DA 42	Piper Seminole
Engines	1xIO-36-L2A	1xIO-390-C3B6	2xAE 300	2xO-360-A1H6
Max Airspeed (kias)	163	165	197	202
Max Cruise (ktas)	124	155	176	162
Stall Speed (kcas)	48	57	61	57
Maximum Range (nm)	640	620	1215	700
Payload (lbf)	870	1031	1299	1191
Maximum Occupants	4	5	4	4
Take off distance (ft)	1630	1685	1391	2200
Landing Distance (ft)	1335	2636	1148	1490
Service Ceiling (ft)	14000	17500	18000	15000

2.5.2. <u>Recommendations</u>

The authors recommend that the characteristics that make the reviewed aircraft popular should be analyzed and then used to guide the design of the Super Aerial Bros aircraft family.

3. Objective Function, Variable Weights and Objective Functiong

This chapter is used to optimize the design of the two general aviation trainer aircraft using an objective function. The objective function was derived from the RFP (Ref. 1).

3.1. Objective Function Variables and Weights

The objective function variables are separated into two categories design requirements and design features. The design requirements are represented in Table 3.1.

Table 3.1 Design Requirements Variable and Weight (Ref. 1)

Design Requirement(DR_n)	Single Engine	Multi Engine	Number(n)
Taking off and landing from runways(asphalt or concrete)			1
Capable of VFR and IFR flight			2
Meets applicable certification rules in FAA 14 CFR Part 23			3
Engine/Propulsion system available in the year 2025			4
Crew	1 Pilot Required, 2-Pilot (Dual Instruction) Capable		5
Passengers	1+	3+	6
Takeoff Distance	< 1500ft	< 2500ft	7
Landing Distance	< 1500ft	< 2500ft	8
Endurange	> 3 hr	> 4 hr	9
Ferry Range	> 800 n mi	> 1000 n mi	10
Service Ceiling	> 12,000 ft	> 18,000 ft	11
Certification Category	Utility	Normal	12

The design features are different from the design requirements. The design features are not on a binary scale, instead are given a weight. The design features were chosen based off the company strategy and the RFP (Ref. 1). The weight of each design feature was calculated based on a discussion with Nelson Krueger at the Lawrence Municipal Airport (Ref. 15). The design features are shown in Table 3.2.

Table 3.2 Design Feature Variables and Weight

Design Feature (DF_i)	Number (i)	Weight (j_i)
Operating Cost	1	0.75
Acquisition Cost	2	0.80
Interchangeable Parts	3	0.60
Aesthetics	4	0.40
Reliability	5	1.00
Semi-autonomous Flight	6	0.20
Flight in known Icing Conditions	7	0.40
Fit within T-Hanger	8	0.50

3.2. Objective Function

The objective function was designed to take the design requirements and design features and assign a numeric value to the potential design. The objective function was designed using two product operators. The first product operator uses the design requirements. This product operator yields a one if all the design requirements are met and a zero if one of the requirements are not satisfied. The second product operator uses the design features. This product operator weighs the potential designs based on the weights of the design features and allow the authors to compare all the potential design configurations shown in Chapter 7. The objective function is shown in Equation 3.1.

$$OF = \prod_{1}^{n}(DR_n) \times \prod_{1}^{i}(1 + j_i \times DF_i)$$

Eq. 3.1 Objection Function

3.3. Summary and Recommendations

3.3.1. Summary

The design requirements outlined in the RFP and the design features selected by the authors was used to compare the potential configurations.

3.3.2. Recommendations

The authors recommend that more subject experts are consulted to iterate the objective function.

4. STAMPED Analysis Techniques

The purpose of this chapter is to perform Statistical Time and Market Predictive Engineering Design (STAMPED) analysis based on the methods outlined in Ref. 16.

4.1. STAMPED Analysis

To facilitate the design process and obtain market parameters and trends, STAMPED analysis was employed in selecting preliminary design variables. All aircraft data was gathered from Ref. 17.

Data such as weight, power, velocity, and geometrical aspects of 26 single engine and twin-engine aircraft were gathered, ranging from aircraft manufactured from 1940 to 2019. With nearly 80 years worth of time-tested data, preliminary aircraft sizing parameters such as empty weight to takeoff weight ratio (W_e/W_{to}), maximum lift to drag ratio $(L/D)_{max}$, power loading (W/P), wing area (S), and wing loading (W/S) can be extrapolated and calculated and the results graphed and analyzed (Ref. 15). For example, (W_e/W_{to}) can be graphed with respect to time, or year, as shown in Figure 4.1 for single engine trainers. Figure 4.1 shows that the average (W_e/W_{to}) of single engine trainers is 0.64, with a standard deviation of 0.526. Designers can plot the trendlines and obtain the

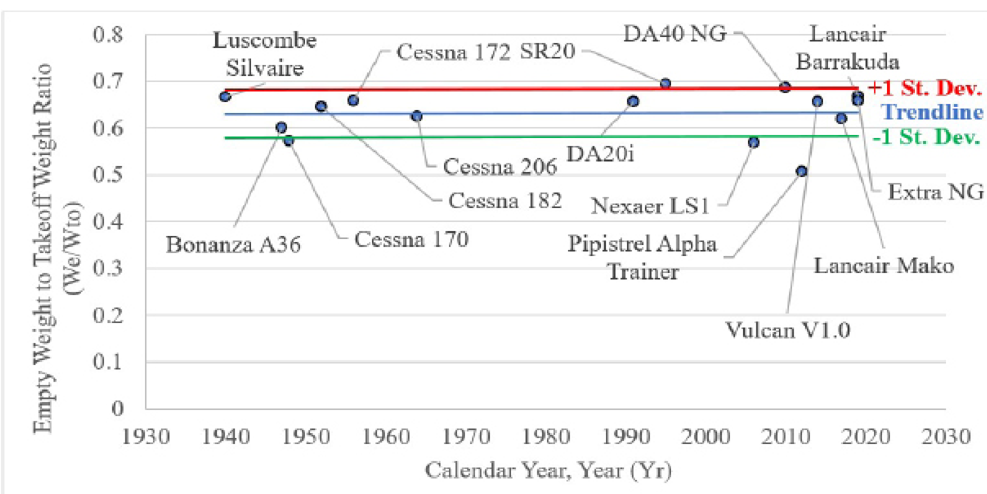

Figure 4.1 Single Engine Trainer Empty Weight to Takeoff Weight Ratio through Time

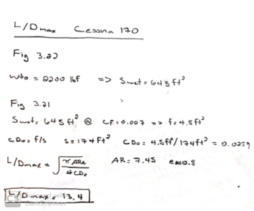

Click Small Figures To Expand Hand Calculations

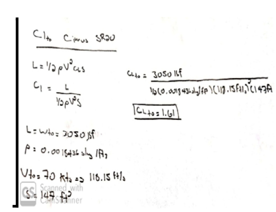

required data for their own designs and can decide to take aggressive or conservative approaches by following the standard deviation trendlines. The Super Aerial Bros design philosophy opted for a less risky approach thus general linear trendlines were used to extrapolate design parameters. Trendlines for $(L/D)_{max}$, (W/P), (W/S), and (S) were also generated as shown in Figure 4.2 through Figure 4.5 respectively.

Table 4.1 tabulates the selected design parameters obtained from STAMPED data for single engine aircraft. Data from twin engine aircraft was analyzed using the same procedure as single engine aircraft, the data is tabulated in Table 4.2. The variables in Table 4.1 and Table 4.2 can then be combined with the design methods in Dr. Jan Roskam's Airplane Design Part I: Preliminary Sizing of Airplanes (Ref. 4) to obtain solid design variables, congruent with modern day market and industry trends. The processes used to size the aircraft in the following chapters will continue to reference Table 4.1 and Table 4.2.

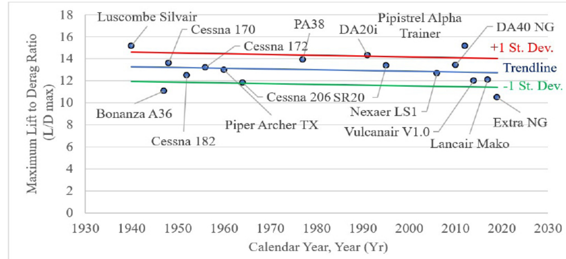

Figure 4.2 Single Engine Trainer Maximum Lift to Drag Ratio through Time

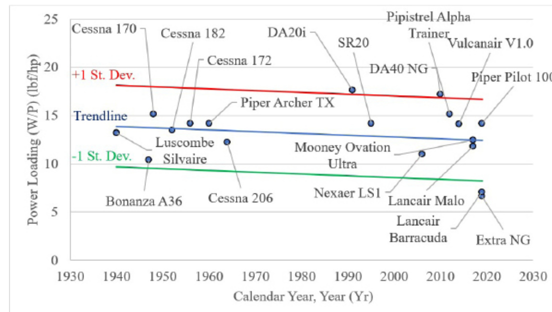

Figure 4.3 Single Engine Trainer Power Loading through Time

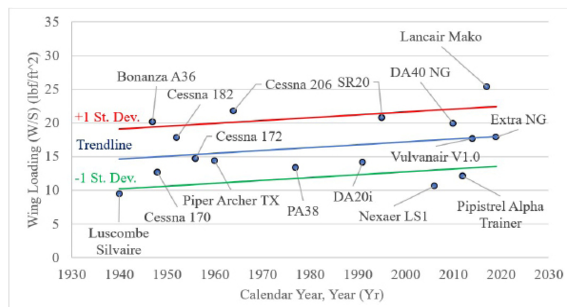

Figure 4.4 Single Engine Trainer Wing Loading through Time

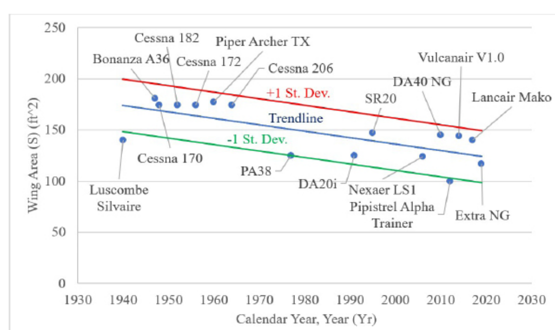

Figure 4.5 Single Engine Wing Area through Time

4.2. Summary and Recommendations

4.2.1. Summary

STAMPED analysis was performed to find initial design parameters listed in Table 4.1 and Table 4.2. The values found will drive initial design characteristics.

Table 4.1 Single Engine Trainer Preliminary Design Parameters

Design Variable	Value	Units
(W_e/W_{to})	0.64	(~)
$(L/D)_{max}$	12.6	(~)
(W/P)	12.2	lbf/hp
(W/S)	18.17	lbf/ft^2
S	120	ft^2

Table 4.2 Twin Engines Trainer Preliminary Design Parameters

Design Variable	Value	Units
(W_e/W_{to})	0.70	(~)
$(L/D)_{max}$	15.6	(~)
(W/P)	18.0	lbf/hp
(W/S)	23.6	lbf/ft^2
S	192	ft^2

4.2.2. Recommendations

The authors recommend using more aircraft to encompass more accurate data trends.

5. Aircraft Weight Sizing

The purpose of this chapter is to detail the process performed for the initial weight sizing of the single and twin engine aircraft based on the methods in Ref. 4.

5.1. Weight Sizing

Weight sizing was performed according to the method outlined in Ref. 4 and in the hand calculations below. Requirements affecting aircraft weight sizing are presented in Table 5.1. Reserve fuel is assumed to be accounted for in the range and endurance requirements. Sizing for each of the two aircraft was performed for two conditions: required range, and required endurance. Sample calculations for single engine weight sizing are shown in pop-up hand calculations below.

Table 5.1 Requirements Impacting Weight Sizing (Ref. 1,17)

FAR 23	Single Engine		Twin Engine	
Weight Limit, W_{limit} (lbf)	Range, R (nmi)	Endurance, E (hr)	Range, R (nmi)	Endurance, E (hr)
19000	800	3	1000	4

The single engine sizing process was as follows. For weight sizing, range, and endurance, the payload weight (W_{pl}) was set to a weight for two crewmembers plus baggage for each. The crewmember and baggage weights are assigned as per the Federal Aviation Administration (FAA). The crewmember with a baggage weight of 240 lbf was found in Table 2.3 of Ref. 18. An initial estimated takeoff weight ($W_{to\text{-}guess}$) of 2650 lbf was used based on STAMPED analysis. Weight fractions for every phase of the mission profile was assigned according to Table 2.1 of Ref. 4. Values for phase five weight to phase four weight (W_5/W_4) were calculated using Breguet range and endurance equations based on the RFP requirements, respectively. Brake specific fuel consumption (BSFC) and propeller efficiency (η_p) were taken from Table 2.2 of Ref. 4 while the maximum lift to drag ratio $(L/D)_{max}$ and cruise velocity (V_{cr}) were found using STAMPED analysis. Values used in Breguet calculations are listed in Table 5.2.

Click to Enlarge

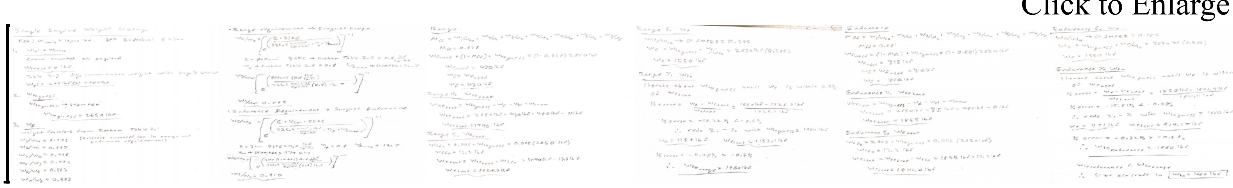

Table 5.2 Values for Breguet Equations (Ref. 4, 16)

Type	V_{cr} (kts)	η_p(~)	BSFC (lbf/hp-hr)	$(L/D)_{max}$ (~)
Single	174	0.8	0.6	12.7
Twin	170	0.82	0.6	12.9

The multiplication of all weight fractions yields the mission fuel fraction (M_{ff}) which used in conjunction with $W_{toguess}$ yielded the used fuel weight ($W_{f\text{-}used}$). Since reserve fuel is accounted for in range and endurance requirements W_{fused} is equivalent to the fuel weight (W_f). Tentative operating empty weight (W_{oetent}) is found by subtracting W_f and W_{pl} from $W_{toguess}$. Weight of trapped fuel and oil (W_{tfo}) is assumed to be 0.5% of $W_{toguess}$. Subtracting W_{tfo} from W_{oetent} gives tentative empty weight (W_{etent}). Empty weight to takeoff weight ratio (W_e/W_{to}) is found using STAMPED analysis and when multiplied by $W_{toguess}$ it yields the empty weight (W_e).

Once the above weight values were found, the process is repeated; iterating about $W_{toguess}$ until W_e is within 0.5% of W_{etent}. This yields the proper takeoff weight (W_{to}) for preliminary aircraft weight sizing. The process is identical for both the single and twin engine aircraft.

5.2. Summary and Recommendations

5.2.1. Summary

Major conclusions from Chapter 5 include takeoff weight, empty weight, and fuel weight values that are required for the single and twin engine aircraft to meet range and endurance requirements. Aircraft weights are tabulated in Table 5.3.

5.2.2. Recommendations

The authors recomend a wider range of data in the STAMPED analysis to better estimate initial empty weight.

Table 5.3 Weight Sizing Results

Type	Single	Twin
W_{Crew} (lbf)	0	0
W_{pl} (lbf)	480	480
W_{to} (lbf)	1660	4610
$W_{f\,used}$ (lbf)	198	464
W_f (lbf)	198	464
W_{tfo} (lbf)	8.3	15.7
W_e/W_{to} (~)	0.585	0.69
W_e (lbf)	971	2160
W_1/W_{to} (~)	0.995	0.992
W_2/W_1 (~)	0.997	0.996
W_3/W_2 (~)	0.998	0.996
W_4/W_3 (~)	0.992	0.9
W_5/W_4 (~)	0.91	0.888
W_6/W_5 (~)	0.993	0.992
W_7/W_6 (~)	0.993	0.992
M_{ff} (~)	0.881	0.8517

6. Wing and Powerlant Sizing

The purpose of this chapter is to perform wing and powerplant sizing based on the methods in Ref. 4. The following constraints were used:

- Stall Speed: <61 kts per FAR23;
- Takeoff Distance: <1500 ft (single engine) and <2500 ft (twin engine);
- Landing Distance: <1500 ft (single engine) and <2500 ft (twin engine).

Using those constraints, Eq. 3.6 from Ref. 4 was used to determine the take off parameters. From Eq. 3.6, the takeoff parameters for single engine aircraft was determined to be 145.6 lbf^2/ft^2*hp and 219.3 lbf^2/ft^2*hp for twin engine. The hand calculations are in the pop up windows located at the end of the chapter.

The authors then manipulated Eq 3.2 from Ref. 4 so that the limit of power loading can be found on a power loading vs wing loading graph for each engine configuration. The hand calculations can be found in the popup calculations at the end of the chapter.

Using those two equations, MATLAB was used to generate a plot to properly size both a single engine and twin engine aircraft. Following a conservative design approach, a $C_{L\,Max\,to}$ in the middle of the range specified by Ref. 4 was selected. Preliminary sizing was done in Chapter 4. The $C_{L\,Max\,to}$ for single engine must be no smaller than 1.5; for twin engine must be no smaller than 1.8. Because these are minimum values, the wing loading must be greater than 18 lbf/ft^2 for single engine and 23 lbf/ft^2 for twin engine. Similarly, the power loading must be greater than 12 lb/hp for single engine and 15 lb/hp for twin engine. The wing loading was graphed against the power loading including the $C_{L\,Max\,to}$ to find the required loading to design the aircraft about. These graphs are represented for the single engine and the twin engine in Figure 6.1 and Figure 6.2 respectively.

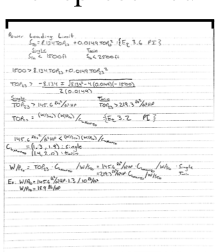

Click to Enlarge

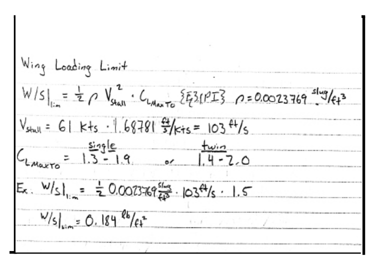

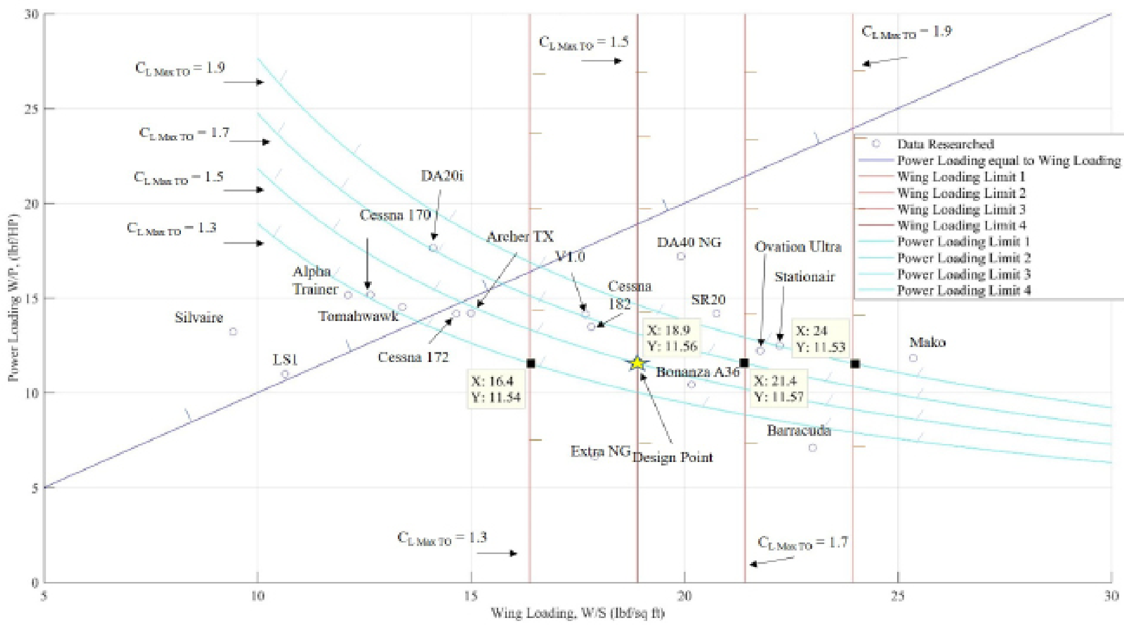

Figure 6.1 Single Engine Wing Loading

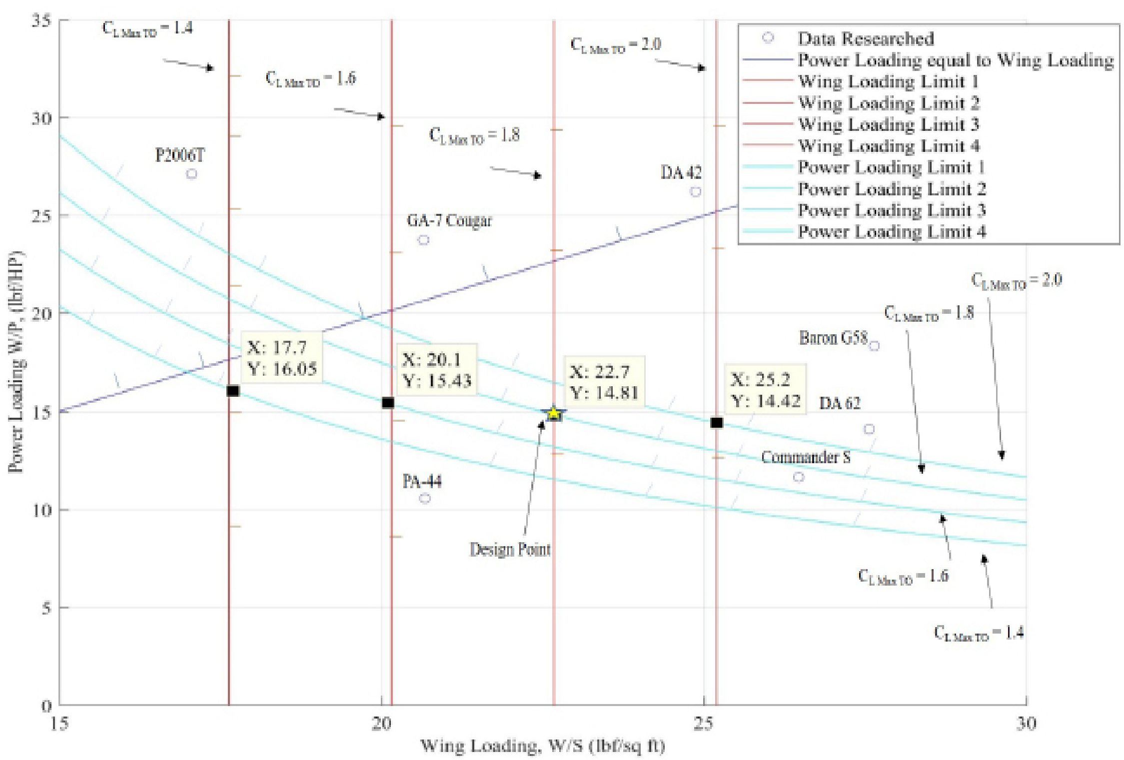

Figure 6.2 Twin Engine Wing Loading

6.1. <u>DRAG POLAR ESTIMATION</u>

Equation 3.19 from Ref. 4 was used to estimate the approximate drag polar at low speeds. It was assumed that aspect ratio would equal ten and the induced drag coefficient would equal 0.8. As the design is very similar to the Cessna 172, the Cessna 172 estimated wetted area and equivalent parasite area were used to estimate zero lift drag coefficient using Eq 3.20. The values found were 0.014 for single engine and 0.018 for twin engine. The calculations for these values are represented in the hand calculations.

6.2. <u>Summary and Recommendations</u>

6.2.1. <u>Summary</u>

The authors conclude the values for preliminary wing and powerplant sizing shown in Table 6.1 and Table 6.2.

Table 6.1 Wing and Powerplant Sizing Characteristics for Single Engine

W/S (lbf/ft^2)	W/P_{to} (lbf/HP)	$CL_{max\ TO}$	C_{Do}
18.9	11.6	1.5	0.014

Table 6.2 Wing and Powerplant Sizing Characteristics for Twin Engine

W/S (lbf/ft^2)	W/P_{to} (lbf/HP)	$CL_{max\ TO}$	C_{Do}
22.7	14.8	1.8	0.018

6.2.2. <u>Recommendations</u>

The authors recommend that:

i.) Due to the same expected maximum coefficient of lift, the required take off and landing runway length should be the same;

ii.) The initial drag polar found is an estimation and should be recalculated once the final aircraft design is set.

Click to Enlarge

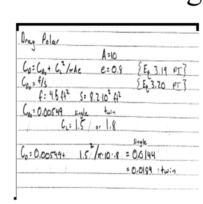

7. Class I Configuration Matrix and Initial Down Selection

The purpose of this chapter is to outline the factors that will drive the aircraft design and to select a final configuration that will best meet the requirements put forth by the RFP. The methods contained in Ref. 20 were used.

7.1. Considerations of Major Design Impacts

The steps laid out by Ref. 20 was to first review the specifications put forth by the RFP. From those requirements, the items that greatest drive the design must be more heavily considered. The design driving requirements were:

- Passengers: 1+ for single engine, 3+ for twin engine;
- Interchangeability of parts between twin and single engine aircraft;
- Lower acquisition and maintenance cost;
- Fit into a traditional T-Hangar;
- Certification under FAR 23.

7.2. Comparative study of Similar Aircraft

The historical review of aircraft in Chapter 2, and aircraft included in the STAMPED analysis. Chapter 4 both analyzed and discussed multiple aircraft that are all currently used as training aircraft. Therefor, these aircraft have very similar mission profiles that both the RFP outlined and that Super Aerial Bros is designing for. The Cessna 172 Skyhawk and the Diamond Aircraft DA42 were both selected by Embry Riddle to add too and replace their aging aircraft fleet. The Cessna 172 Skyhawk has been the primary single engine aircraft used for training, and therefor its mission profile is identical to the specification Super Aerial Bros designed towards. Characteristics that have made the 172 Skyhawk successful are low stall speeds, low acquisition and maintenance cost and its inherent stability. These characteristics were considered by Super Aerial Bros in the design of the aircraft family. The only complaints by a seasoned aircraft instructor, Nelson Krueger located at the Lawrence Municipal Airport, is the limited ground visibility during ground operations. This was caused by the instrument panel height being too tall and seat height being unable to adjust to give proper ground visibility during ground operations. This complaint on the Cessna 172 will be considered in the design of the Super Aerial Bros aircraft family. The Diamond Aircraft DA42 has also been selected by multiple training institutions for twin engine and complex aircraft training because of its low fuel consumption, fuel flexibility and reliability.

7.3. Configuration Sweep and Selection

7.3.1. Concept of Operations

The Super Aerial Bros aircraft family are used as standard general aviation aircraft. It operates from paved surface runways and has a takeoff distance of less than 1500 ft and 2500 feet for the single and twin-engine aircraft respectively. The respective aircraft conduct both short familiarization flights and cross-country flights with flight legs longer than 50 nm from the origin (Ref. 21). All flights would be conducted under VFR or IFR with each aircraft capable of 2- Pilot (Dual Instruction) piloting and carrying a total of four occupants. The single engine aircraft will have under 200 hp. The single engine has fixed landing gear to ensure it can be used for initial pilot training and no addition pilot ratings would be needed. The twin-engine aircraft is considered a complex aircraft and used as the second aircraft in the training pipeline.The conecpt of operartion is shown in Figure 7.1.

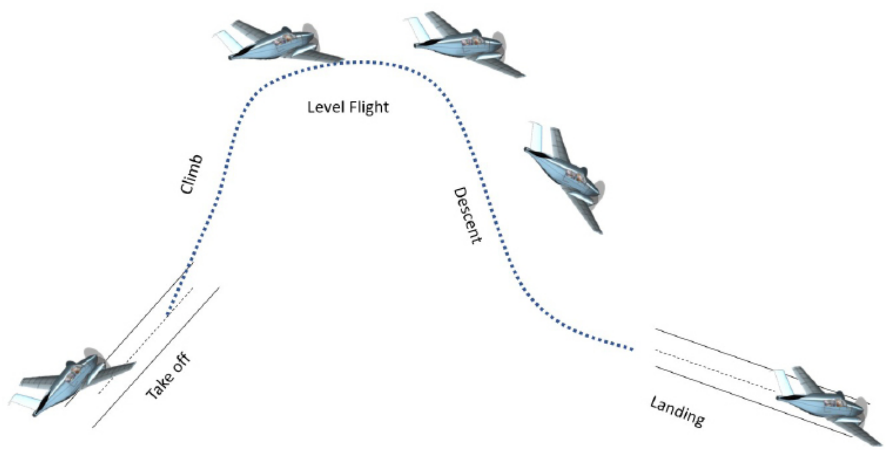

Figure 7.1 Concept of Operation of Trainer Aircraft

7.3.2. Selection of the Overall Configuration

7.3.2.1. Aircraft Category

The single engine propeller and twin-engine propeller aircraft descriptions of aircraft categories contained in Airplane Design Part II by Dr. Roskam best suit the aircraft designed by Super Aerial Bros (Ref .20). These aircraft fall under FAR 23 utility and normal certification for the single engine and twin engine respectfuly.

7.3.2.2. Configuration Sweep

The following eight designs in Figure 7.2 were created using Intuitive Aircraft Design, a MATLAB plugin. More traditional designs were faced off against each other based on the input by Nelson Krueger (Ref. 15). Mr. Krueger suggested that a traditional designed aircraft with a traditional control scheme focusing on stability and reliability would be vital to the success of the aircraft family. Two nontraditional designs were also considered.

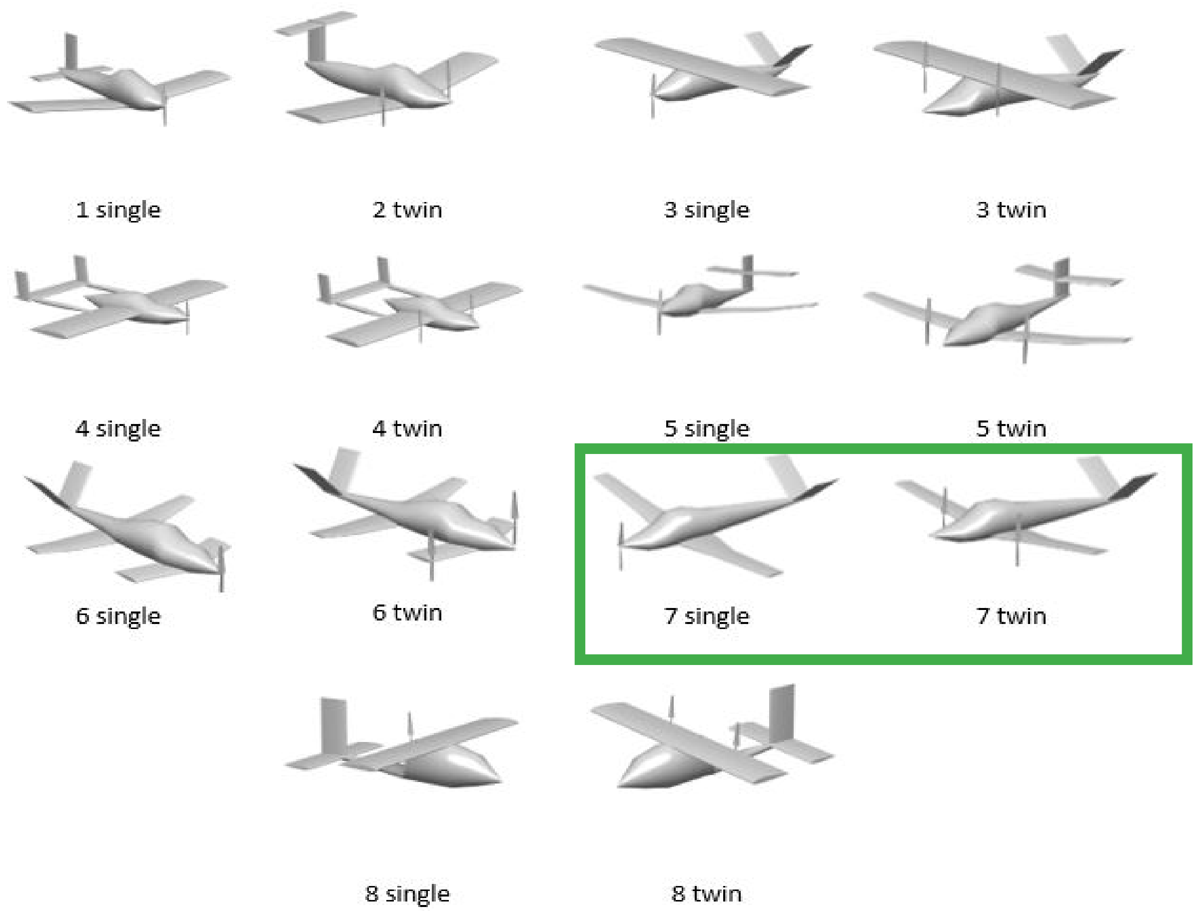

Figure 7.2 Configuration Sweep

7.3.2.3. Configuration Downselection

With the design weighting in Chapter 3 considered, design 7 best suits the objectives of Super Aerial Bros. The disqualifying factors for the other designs are listed in Table 7.1

Table 7.1 Disqualifying Design Features

Design	Disqualifying reasons
1	similar to existing aircraft in the training market
2	similar to existing aircraft in the training market
3	unable to take advantage of wing in ground effect
4	complex manufacturing, additional structural weight, may not fit in a T-Hanger
5	similar to existing aircraft in the training market
6	complex manufacturing, additional structural weight, challenging to manage CG
8	complex manufacturing, additional structural weight, challenging to manage CG

7.4. Configuration Summary and Recommendations

7.4.1. Summary

The configuration of the general aviation aircraft family will have the following characteristics:

- Low wing to facilitate wing in ground effect;
- Dihedral to improve open-loop Dutch Roll stability;
- Tapered wing to increase performance and aspect ratio;
- Tractor style motors for improved C.G. location and ease of maintenance;
- V-tail to reduce wetted area and empennage weight.

The selected designs are shown in Figure 7.3

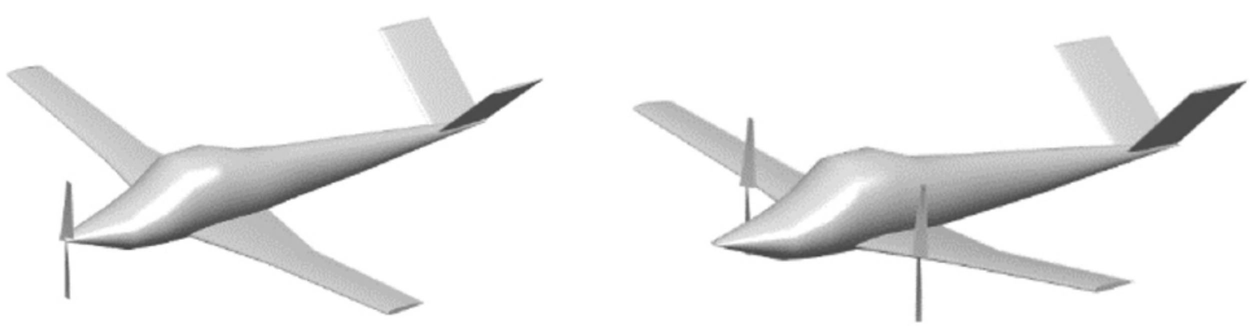

Figure 7.3 Selected Configuration

7.4.2. Recommendations

The authors recommend that:

i.) Multiple design should be carried through the initial design process to have a more in-depth comparison of advantages and disadvantages;

ii.) A larger design sweep is used.

8. Cockpit and Fuselage Layout Designs

The purpose of this section is to discuss the general layout of the cockpit and fuselage including visibility lines, control areas, and the general shape of the outer mold line. Layout in this section follows the general method as presented by Dr. Roskam in Airplane Design Part II (Ref. 20) and Airplane Design Part III (Ref. 23). Design considerations for the cockpit layout of the two aircraft trainer family are as follows:

- Identical fuselage between single and twin engine variants;
- Structural depth of 1.5 in;
- Accommodate 6 ft 7 in male and 20th percentile female pilots;
- Accommodate two 95th percentile male passengers;
- Two abreast seating;
- Capable of four total persons at 190 lbf each;
- Capable of 4 bags at 16 lbf and 50 linear inches (24 in x 16 in x 10 in) each.

8.1. Cockpit Layout Considerations

Using identical fuselages between the twin and single variants keeps manufacturing cost low through the principle of economies of scale. Roskam recommends reserving a depth of 1.5 in from the outer mold line of the aircraft for structure (Ref. 20). Accommodating a 20th percentile female is standard design practice while accommodating a 6 ft 7 in male will widen the market of the Super Aerial Bros trainer family to larger customers such as National Basketball Association athletes. Carrying four persons meets the RFP requirement while designing the trainer family for 95th percentile male passengers ensures a wider utility outside of the commercial pilot training market. The average flight crewmember and carry-on baggage weights are 190 lbf and 16 lbf respectively (Ref. 19). A 50 linear inch carry-on bag is the standard airline checked bag size (Ref. 23).

The cockpit was sized from human models created in Siemens NX. The male pilot and female pilot were located with a reference point of the left and right eyes, respectively. Eyes were referenced to the windshield with an x-axis distance of 23.6 in for the male pilot and 19.7 in for the female pilot. Seats were then placed to support the pilots following Figure 2.7 of Ref. 22 as a general guideline. Seats translate forward and aft and elevate up and down as well as recline to accommodate wide variety of pilot sizes. Left and right side sticks are also adjustable to pilot size. Vision guidelines were then plotted from the pilot eyes according to the visibility pattern of Figure 2.18 in Ref. 22. Finally, the two 95th percentile male passengers and their seat were located along

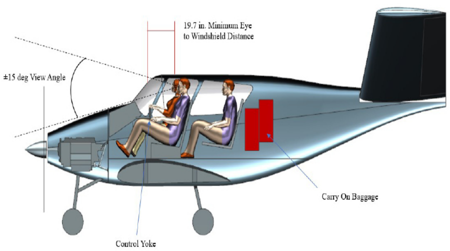

Click to Enlarge

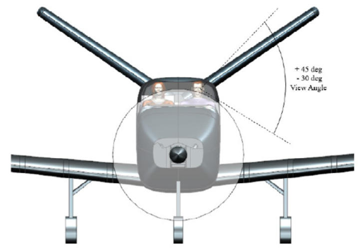

Figure 8.1 Cockpit Layout Side (Not to Scale)

Figure 8.2 Cockpit Layout Front (Not to Scale)

8.2. Fuselage Layout

After cockpit layout, the engine for the single engine variant was placed at the nose below the 15 degree pilot visibility line. With the engine placed, the outer mold line was wrapped around the placed persons, payloads, and components. Isometric, side, and top views are shown in Figure 8.3 through Figure 8.5, respectively. Tail upsweep was designed to the 15 degree rule to prevent flow separation and allow for takeoff rotation (Ref. 20). Fuselage fineness ratio (l_f/d_f) is 5.2, giving a fuselage drag coefficient due to cross-sectional area (C_{DB}) of 0.75 as according to Figure 3.1 of Ref. 22. Aft body fineness ratio (l_{fc}/d_{fc}) was calculated to be 3.0, giving an aft body base drag coefficient (C_{DBA}) of 0.25 as according to Figure 3.3 of Ref. 22. Lastly, windows were cut in accordance with plotted pilot visibility lines. Actual pilot visibility for the male pilot is shown in Figure 8.6.

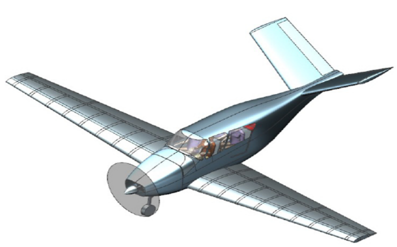

Figure 8.3 Fuselage ISO (in) (Not to Scale)(Click to Enlarge)

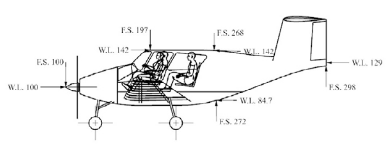

Figure 8.4 Fuselage Side (in) (1:80)(Click to Enlarge)

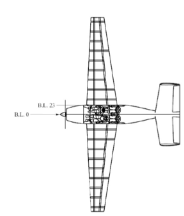

Figure 8.5 Fuselage Top (in) (1:80)(Click to Enlarge)

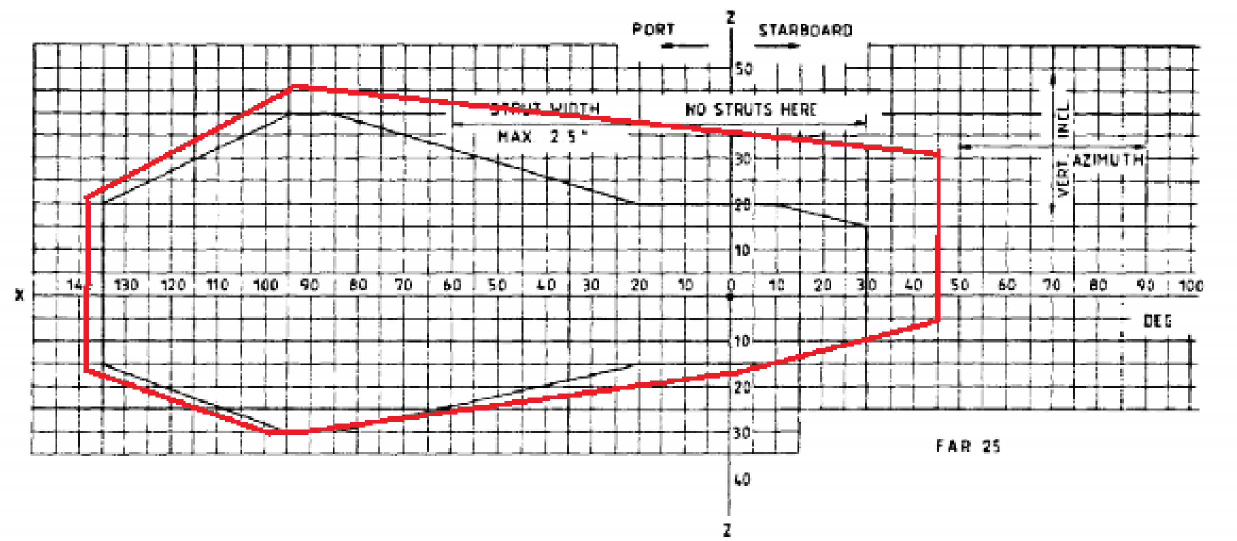

Figure 8.6 Pilot Cockpit Visibility (Ref. 23 Pg 27)

8.3. Summary and Recommendations

8.3.1. Summary

The authors conclude that the fuselage between the single and twin variants will be identical with the exception of the nose. Both cockpits will accommodate up to four persons ranging in size from 6 ft 7 in to 62 in in height. Salient fuselage and cockpit values are presented in Table 8.1.

Table 8.1: Fuselage Salient Characteristics

l_f (in)	w_f (in)	h_f (in)	d_f (in)	l_{fc} (in)	d_{fc} (in)	l_f/d_f (~)	C_{DB} (~)	l_{fc}/d_{fc} (~)	C_{DBA} (~)
300	48	58	58	145	48	5.2	0.75	3.0	0.25

8.3.2. Recommendations

The authors recommend aesthetics of the aircaft be improved and that a cargo access door be added in future iterations.

9. Layout Design of the Propulsion Installation

The purpose of this section is to discuss the engine selection process based on the power requirements found in Chapter 6. The installation of the engines and sizing of the propeller will be discussed. The procedures in Ref. 20 were followed.

9.1. Selection of the Propulsion System

The propulsion system selected for the single engine aircraft and the twin were naturally aspirated reciprocating engines with a propeller. The single engine aircraft engine chosen was the Lycoming IO-360-B2F with a 72 inch diameter, two blade fixed pitch propeller with an estimated propeller efficiency of 0.85. The twin engine aircraft engine chosen was the Lycoming IO-360-B1F with a 56 inch diameter three blade constant speed propeller with an estimated propeller efficiency of 0.85. These engines were chosen based off the requirements laid out in the RFP. The following requirements in Table 9.1 were considered in the engine selection.

Table 9.1 Engine Requirements

Requirement	Singe-Engine	Multi-Ending
Takeoff Distance	< 1500 ft	< 2500 ft
Endurance	> 3 hr	> 4 hr
Service Ceiling	> 12,000 ft	> 18,000 ft

A preliminary flight envelope was generated for the single engine and the twin engine aircraft. The single engine aircraft flight envelope spans 0 feet to 12,000 feet with velocity ranging from Mach 0.1 to Mach 0.3. The twin engine aircraft flight envelope spans 0 feet to 18,000 feet with velocity ranging from Mach 0.1 to Mach 0.4. The flight envelopes were plotted over Figure 5.1 in Ref. 20 to determine the initial type of engine that could be used. This overlay is shown in Figure 9.1,and displayed the ability to use piston engines with propellers for the propulsion system.

The engines were sized based on the required take off power. The power at takeoff (P_{to}) was calculated using W/P_{to}. W/P_{to} was calculated using TOP_{23} of 145.6 lbs^2/ft^2 hp, $CL_{max\ to}$ of 1.8, and W/S_{to} of 23 lb/ft^2 initially calculated in Chapter 6. The calculation is shown in the hand calculation pop-up at the end of the chapter. The single engine P_{to} needed was calculated to be 161 hp. The twin engine P_{to} needed was calculated to be 308 hp which results in 154 hp per engine. These P_{to} values lead to the decision of using the Lycoming IO-360-B2F engine for the single engine aircraft and the Lycoming IO-360-B1F for the twin aircraft. The selection of the Lycoming IO-360-B1F/B2F was chosen to help reduce the maintenance of the engines due to the engine of the single engine aircraft and the twin engine aircraft having similar components. Additionally the Lycoming IO-360 engines are reliable engines used on numerous general aviation aircraft.

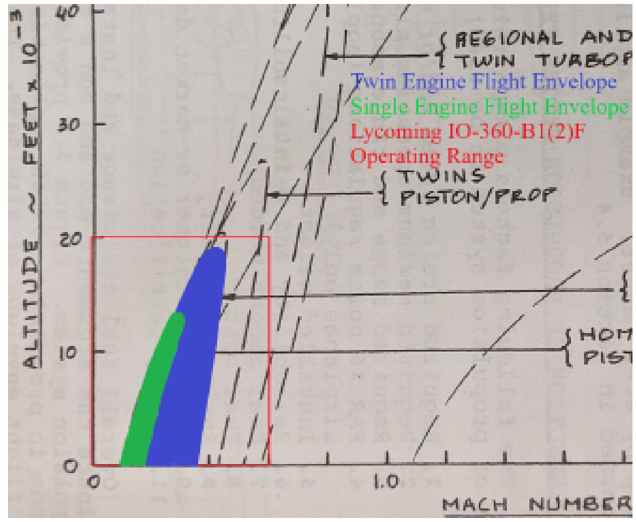

Figure 9.1 Flight Envelope with respect to Speed and Altitude (Ref. 20)

The engines selected were then verified to function within the flight envelope and the endurance requirement. The engine was verified using the Operator's Manual for the Lycoming IO-360 engine (Ref. 24). Figure 3.22 from Reference 24, represents the Sea Level and Altitude Performance and is shown in Figure 9.2. The flight envelope overlay showed that the engine will perform at the altitudes needed in the flight envelope of the single and the twin engine aircraft. The red outline represents the flight envelope.

The endurance of the aircraft was checked by using the fuel consumption of the engine and the fuel weight for each aircraft. The fuel weight was converted into gallons of 100LL avgas, then the volume of the fuel was divided by the fuel consumption of the engine to give the endurance. This was calculated at 65 percent throttle cruise. The

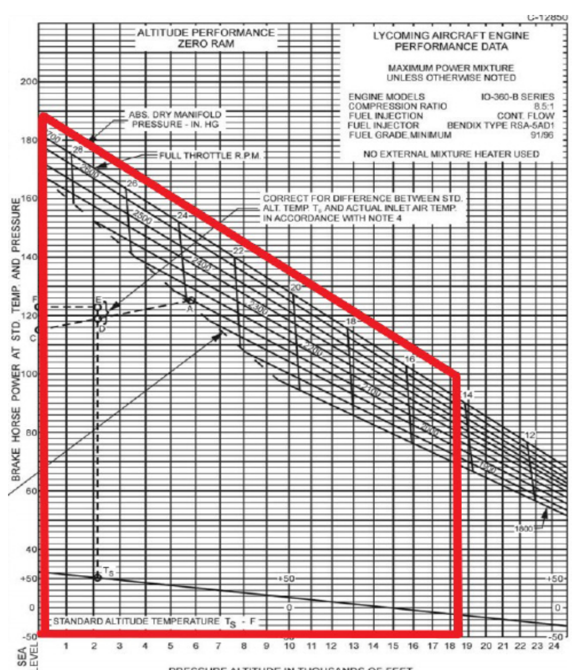

Figure 9.2 Engine Operating Altitude (Ref. 24)

endurance of the single engine aircraft is 3.88 hrs and the endurance of the twin engine aircraft is 5.18 hrs. These calculations are represented in the hand calculations at the end of this section.

For the single engine aircraft, Equation 5.1 in Ref. 20 was used to find the power loading per blade of the two bladed propeller. The single engine power loading per blade resulted in 3.18 hp/ft2. This value was compared to the range of single engine FAR23 certified aircraft found in Table 5.2 in Ref. 20 of 2.0-3.9 .The twin engine power loading per blade resulted in 3.77 hp/ft^2. This value was compared to the range of twin engine FAR23 certified aircraft found in Table 5.4 in Ref. 20 of 2.8-4.8 .The calculated values are shown in the hand calculations at the end of the chapter.

9.2. <u>Installation of the Propulsion System</u>

The Lycoming IO-360-B1F/B2F engine with mounting bracket is represented in Figure 9.3.

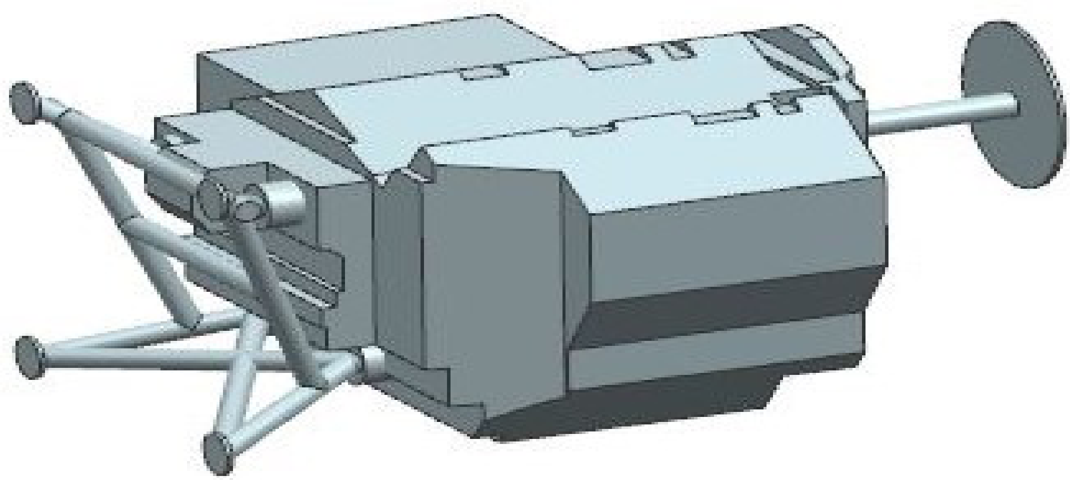

Figure 9.3 Engine with Mounting Bracket (Ref. 24) (Not to Scale)

The engine will be mounted using a truss system on the nose of the aircraft. For the single engine aircraft the engine will be mounted directly onto the firewall located aft of the engine. The truss system attaches to each of the four mounting locations. The twin engine aircraft engines are located on each wing with the same truss system as the single engine connecting to the spar of the wing.

The engine location and installation of the Lycoming IO-360-B2F for the single engine aircraft is shown in Figure 9.4. The engine locations and installation of the Lycoming IO-360-B1F for the twin engine aircraft is shown in Figure 9.5.

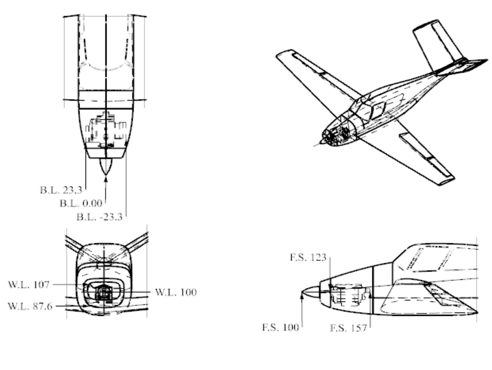

Figure 9.4 Single Engine 3-View (in)
Isometric Not to Scale
3-View Enlarges to Scale 1:40

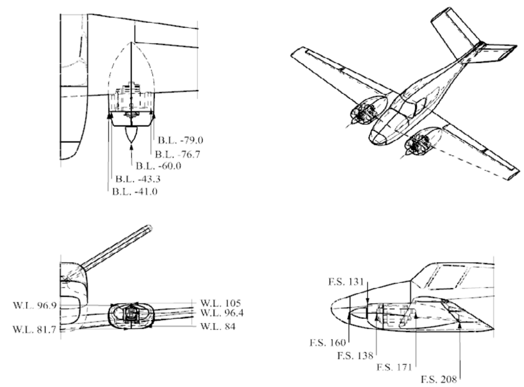

Figure 9.5 Twin Engine 3-View (in)
Isometric Not to Scale
3-View Enlarges to Scale 1:40

9.3. <u>Summary and Recommendations</u>

9.3.1. <u>Summary</u>

The propulsion system for the single engine aircraft uses a Lycoming IO-360-B2F engine mounted on the nose using a fixed pitch propeller with two blades with a diameter of 72 inches. The propulsion system for the twin engine aircraft uses two Lycoming IO-360-B1F engines one mounted on each wing using variable pitch propellers with three blades with a diameter of 56 inches. The propellers will be selected by the owners but must have an efficiency of 0.85. The Lycoming IO-360-B1E/F has a weight of 300 lbs and a specific fuel conspumption of 0.49 lbm/hpH.

9.3.2. <u>Recommendations</u>

The authors recommend that:

i.) A higher fidelity CAD model is developed;

ii.) A diesel engine variant is found for increased fuel availability;

iii.) Additional analysis is developed for the truss structure;

iv.) A range of propellers is selected for customer convenience.

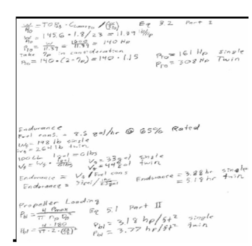

Click Here to Expand

10. Class I Wing Layout Design

The purpose of this chapter is to perform a preliminary analysis for wing layout. This includes the overall geometry of the wing along with lateral control devices. To make the aircraft more affordable, a single wing design capable of flying the single and twin-engine variant. The procedure found in Ref. 20 was used.

10.1. Overall Structure

A cantilever wign design was chosen due to its simplistic structure and ease of manufacturability. Additionally, a braced wing causes interference drag. More drag requires more thrust and therefore a more powerful power plant.

10.2. Overall Wing and Fuselage Arrangement

A low wing design was chosen for the aircraft. This would result in lower speeds and/or coefficient of lift to takeoff or land. Table 10.1 compares characteristics of high, mid, and low wings which were also considered for the authors' decision.

Table 10.1 Wing Characteristic Comparison

	High Wing	Mid Wing	Low Wing
Interference Drag	2	1	3
Lateral Stability	1	2	3
Visibility from Cabin	1	2	3
Landing Gear Weight	3	2	1

10.3. Wing Geometry Data

Wing geometry data was analyzed and shown in Table 6.2 and Table 6.3 from Ref 20. Figure 10.1 and Figure 10.2 display the graphed data from the tables listed from Ref. 20. A NACA 4415 airfoil was chosen. This airfoil produces a trailing edge stall which means the stall is not sudden and takes more time to coalesce into a full stall on the aircraft. Additionally, a gradual stall allows a training pilot to have more time to react. Table 1.2 contains characteristics of the airfoil given a Reynold's number of 2.7 million. Data used to approximate those values are found in Ref. 25.

Figure 7.1 from Ref. 20 was used to solve for the critical Mach number at the mean geometric chord of five feet. To do so the following values were found: Reynold's number, section coefficient of lift, thickness ratio of the airfoil, and aspect ratio. Eq 7.4 from Ref. 20 was used to solve for

Reynold's number (2.7 million) and Eq 6.1 from Ref. 20 to find the coefficient of lift during cruise (0.31). A given thickness ratio of 0.15 for the NACA 4415 from Ref. 25 was used. The final characteristic of the wing needed to solve for the critical Mach number was the aspect ratio. From the data shown in Figure 10.2, the authors' design vector sets the aspect ratio at eight. The final approximate characteristics of the airfoil are shown in Table 10.2.

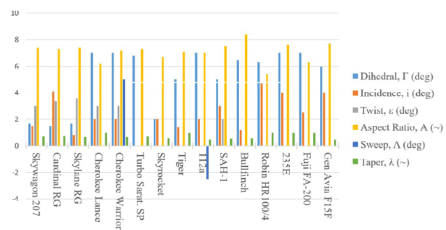

Figure 10.1 Single Engine Wing Geometric Data (Ref. 20) (Click to Enlarge)

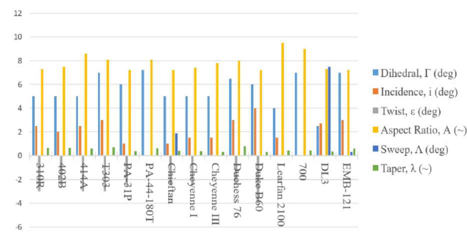

Figure 10.2 Single Engine Wing Geometric Data (Ref. 20) (Click to Enlarge)

10.4. Lateral Control Device Layout and Wing Fuel Volume

CAD was used to develop a preliminary design of the wing and lateral control device layout. Aileron sizing was done using Table 8.3 from Ref. 20. Values were chosen such that the airplane variants would be competitive in the market as well as have good control over lateral stability. Figure 10.3 through Figure 10.5 show important features of the wing involving buck line, fuselage station, and water line respectively. Eq 6.2 from Ref. 20 was used to calculate the wing fuel volume. CAD was used to find the approximate wing fuel volume. The authors decided to use a conservative approach with determining the wing fuel volume such that the smaller volume found was used: 80 ft^3. This value was found using CAD.

Click Image to Enlarge Hand Calculations

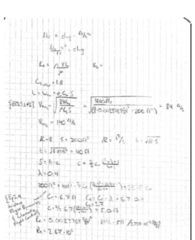

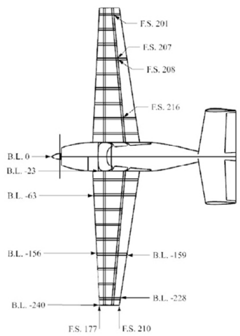

Figure 10.3 Butt Line of Wing Enlarge to Scale 1:80 (in)

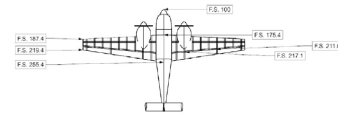

Figure 10.4 Fuselage Station of Wing Enlarge to Scale 1:125 (in)

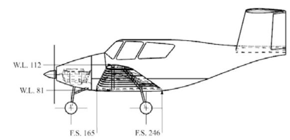

Figure 10.5 Water Line of Wing Enlarge to Scale 1:125 (in)

10.5. Summary and Recommendations

10.5.1. Summary

The authors conclude the following characteristics for the wind planform design shown in Table 10.2 and Table 10.3.

Table 10.2 Airfoil Characteristics

C_d	$C_{l\,design}$	M_{crit}
0.0072	1.5	0.67

Table 10.3 Wing Characteristics

λ_w	Γ_w (deg)	i_w (deg)	ε_w (deg)
0.4	5.8	2	-1.7
b (ft)	A	c_r (ft)	c_t (ft)
40	8	6.7	2.7
S_a/S	b_a in/out	c_a in/out	V_{wf} (ft^3)
0.062	~0.62/0.93	~ 0.26/0.26	80

10.5.2. Recommendations

The authors recommend that the structural sizing be more thoroughly analyzed. Additionally, rounded wingtips should be implemented to minimize wing drag.

11. High Lift Devices

The purpose of this chapter is to explain the design of the high lift devices of the single engine and twin-engine aircraft using Roskam's Airplane Design Part II (Ref. 20).

11.1. Design of High Lift Devices

Flaps increase the lift coefficient to meet its takeoff or landing criteria. As such, the wing's lift coefficient must first be determined to find what flap type and size will complement the needed lift coefficients. Since the single and twin aircraft will share the same wing, the flaps were designed based on the twin engine lift coefficients as they were higher than the single engine's. Flap design was based on Equation 11.1.

$$C_{l\,(max\,need)} - C_{l\,(max\,got)} = \Delta C_{l\,(max\,flap)}$$ **Equation 11.1**

Were $C_{L\,(max\,need)}$ is the required lift coefficient, $C_{L\,(max\,got)}$ is the lift coefficient that the aircraft has, and $\Delta C_{L\,(max\,flap)}$ is the needed lift coefficient addition to obtain the lift requirements. The required lift coefficients were found during the preliminary sizing of the aircraft in Chapter 9. The landing lift coefficient and the takeoff lift coefficient have the same value of 1.8. The aircraft lift coefficient can be calculated based on the lift coefficients at the aircraft tip and root which were calculated by finding the Reynold's Number at the respective location using Figure 7.1 from (Ref. 20). With the set aircraft's lift coefficient, the lift requirements can be found. Table 11.1 tabulates the salient lift coefficients.

Table 11.1 Salient Lift Coefficients (Twin Engines)

$C_{l\,root}$	$C_{l\,tip}$	$C_{L\,got}$	$\Delta C_{l\,clean}$	$\Delta C_{l\,to}$	$\Delta C_{l\,L}$	$\Delta C_{l\,need}$
1.70	1.45	1.43	0.375	0.394	0.394	1.75

Plain flaps were found to be sufficient to provide the required lift coefficient with a flap chord to wing chord ratio (c_f/c) of 0.3, recommended by (Ref. 20). The span stations, η_i and η_o were placed after the rib following the engine for the twin engine configuration and adjacent to the aileron to increase the efficiency. The location of the flap would result in a wing-flap area (S_{wf}) of 75 ft^2. Table 11.2 provides the final flap configuration parameters. The chosen flap configuration would allow an ΔC_l need of 1.99 at 40° flap deflection for the twin engine trainer. A 32 degree flap deflection will get the minimum ΔC_l need of 1.77 for the twin engine trainer while the single engine trainer, following the same methodology, requires 15 degree flap deflection for a ΔC_l needed of 1.2. Table

11.3 provides the lift coefficient at different flap deflections. Figures 11.1-11.4 show the flap fuselage, butt line, and water line stations. Figure 11.4 shows the twin engine aircraft off axis view with flaps.

Table 11.2 Flap Design Characteristics

Flap Type	n_i (%)	n_o (%)	S_{wf} (ft^2)	c_f/c
Plain	26	65	75	0.3

Table 11.3 Lift Coefficient at Flap Deflection

δf (°)	ΔCl(need)
10	0.803
20	1.41
30	1.69
40	1.99
50	2.33
60	2.36

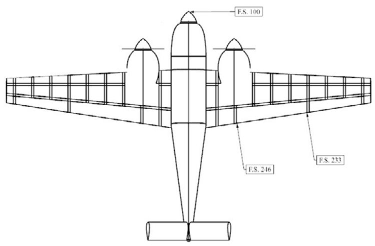

Figure 11.1
Plain Flap Fuselage Station Enlarge to Scale 1:80 (in)

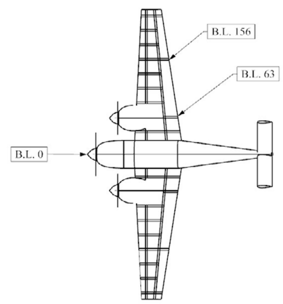

Figure 11.2 Plain Flap Butt Line Stations Enlarge to Scale 1:80 (in)

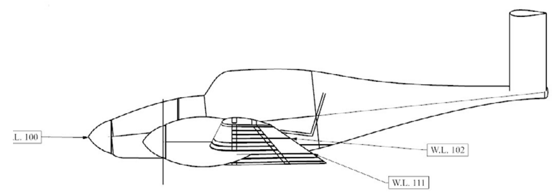

Figure 11.3 Plain Flap Water Line Stations Enlarge to Scale 1:50 (in)

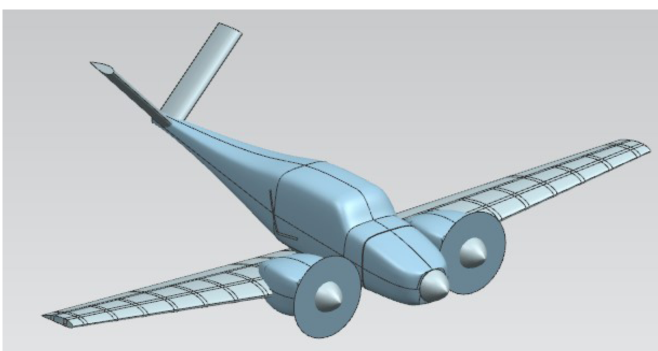

Figure 11.4 Plain Flap Off-Axis View (Not to Scale)

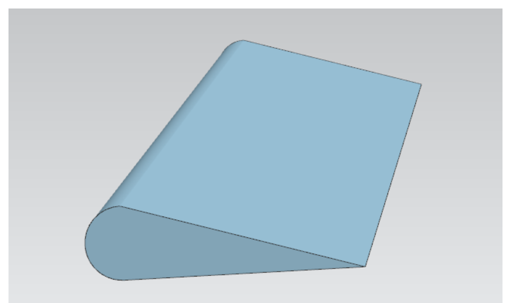

Figure 11.5 Plain Flap Cross-Section (Not to Scale)

11.2. Summary and Recommendations

11.2.1. Summary

The flaps are located at a span station of 26% and 65% with a flap chord to wing chord ratio of 0.3 to meet the lift requirements. The flaps will not need to be fully extended to achieve the lift requirements with 32 degree flap deflection being sufficient to land and takeoff on the twin engine and 15 degree for the single engine.

11.2.2. Recommendations

The authors recommend that a stability analysis is performed to fully determine if the flap configuration is sufficient to meet both aircraft requirements.

Click to Enlarge

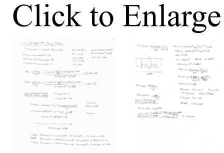

12. Class I Design on the Empennage

The purpose of this chapter is to detail the design process of the empennage. The design method used is based from Roskam's Airplane Design Part II (Ref. 20) and recommendations from Dr. Barrett. Salient characteristics will be presented alongside technical drawings of the empennage.

12.1. Empennage Design Procedure

From the initial Class I configuration in Chapter 7, it was determined that the aircraft would have a V tail, also known as a butterfly tail, controlled by fly-by-wire system. A V tail reduces wetted area and empennage weight. Aircraft such as the Beechcraft Bonanza and the Cirrus SF50 both incorporate V tails (Ref. 26, 27). Ref. 20 provides a Class I empennage design for V tails by designing an equivalent horizontal and vertical tail and projecting their characteristics to find the equivalent V tail. The V tail will be designed to function for both the single and twin-engine aircraft.

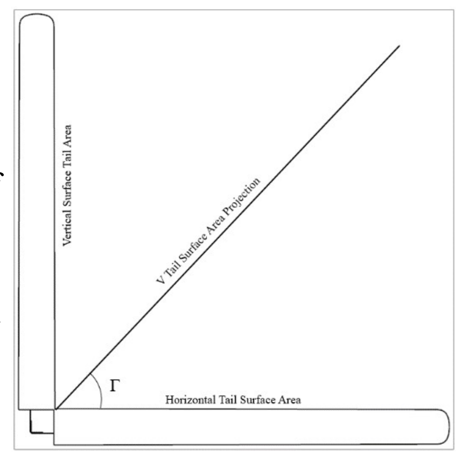

Figure 12.1 V Tail Projection (Click to Enlarge)

Ref. 20 provides data for twin engine and single engine aircraft which can be used to calculate design parameters of the empennage such as wetted area, aspect ratio, incidence and sweep angle. To approximate the design of the V tail, an equivalent design for a virtual horizontal and vertical tail was first determined and then projected into a V tail from initial C.G. estimations. Based on historical aircraft, a horizontal tail volume coefficient of 0.838 and a vertical tail volume coefficient of 0.068 were chosen. From the volume coefficients, the virtual horizontal tail and vertical tail areas was calculated and used to find the V tail dihedral angle (Γ_b) and projected into the actual V tail area. Figure 12.3 provides a schematic of the projection of the horizontal and vertical tail into the V tail.

Aspect ratio and taper ratios were chosen based on additional historical data from Ref. 20, the Beechcraft Bonanza, and the Cirrus SF50 (Ref. 26 and 27). Ref. 20 recommended the use of a symmetric airfoil therefore the NACA 0012 airfoil was chosen. The V tail would also compromise a ruddervator which would have a V tail chord to ruddervator chord ratio of 0.3. Figure 12.4 shows the designed V tail and Table 12.1 tabulates the salient V tail characteristics. Additional top, side and front views including F.S., B.L., and W.L. are included in Figures 12.4, 12.5, and 12.6.


Click to Enlarge
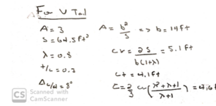

Table 12.1 Salient Empennage Characteristics

S_b (ft^2)	Γ_b (°)	Airfoil	AR	λ_b	i_b (°)	$\Delta_{c/4\,b}$ (°)	X_b (in)	$\underline{c}_b$ (ft)
64.5	33.7	NACA 0012	3	0.8	0	8	170	4.6

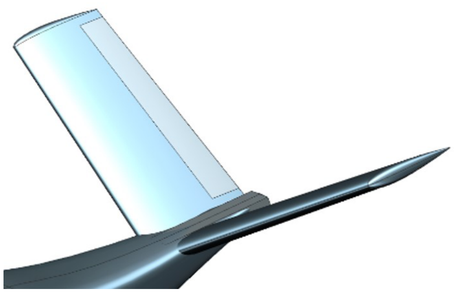
Figure 12.2 V Tail Off Axis View (Not to Scale)

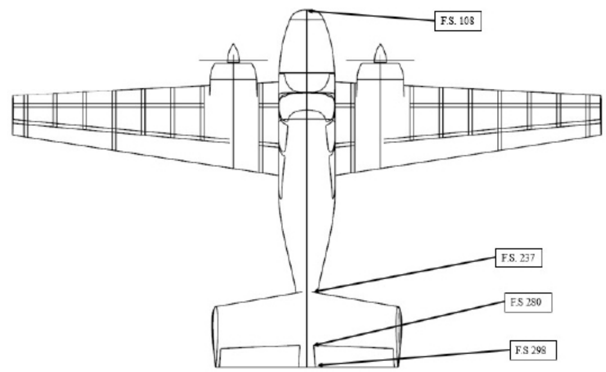

Figure 12.3 V Tail Fuselage Station (in) (Click to Enlarge) (1:80)

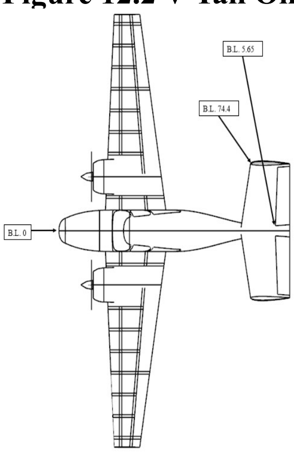

Figure 12.4 V Tail Butt Line Station (in) (Click to Enlarge) (1:50)

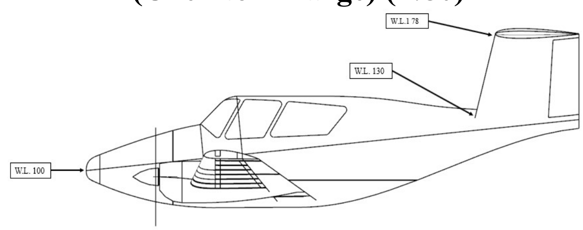

Figure 12.5 V Tail Water Line Station (in) (Click to Enlarge) (1:50)

12.2. Summary and Recommendations of Empennage Design and Characteristics

12.2.1. Summary

The empennage consists of a NACA 0012 V tail with a wetted area of 64.5 ft^2, an aspect ratio of three, and a dihedral angle of 33.7°. The V tail was designed to be integrated on both the single and twin-engine aircraft, such as the wings, to minimize complexity and costs.

12.2.2. Recommendations

The authors recommend that a dynamic analysis of the empennage be performed using AAA or AVL to optimize the design of the empennage.

13. Class I Landing Gear Design

The purpose of this chapter is to explain the design of the landing gear for the single and twin-engine aircraft using the methods outlined in Chapter 9 of Roskam's Design Part II (Ref. 20).

13.1. Landing Gear Design Procedure

The landing gear was designed based off the single engine aircraft due to the aircraft having the furthest aft C.G. location of the two aircraft. The gear was designed as a tricycle gear due to tricycle gear being more stable and needing no additional certification to be operated. The single engine was designed for fixed gear and the twin engine was designed to be retractable to maintain competitiveness in the market and avoid a high drag profile.

The landing gear was designed to adhere to a 15 degree tip-over angle, 15 degree rotation angle, 55 degree lateral tip over angle (demonstrated by a 35 degree inverted cone), and a five degree lateral ground clearance based on the requirements in Ref. 20. These requirements are represented in Figure 13.1, Figure 13.2, Figure 13.3, and Figure 13.4 respectfully.

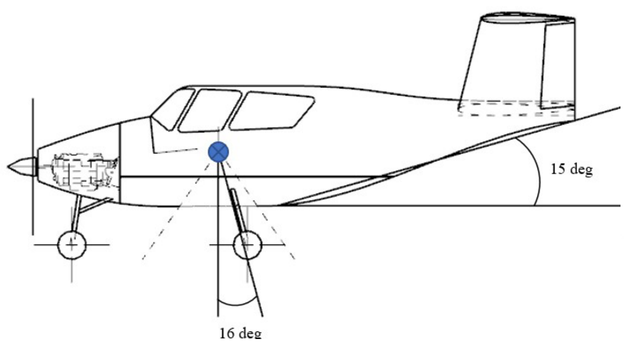

Figure 13.1 Landing Gear Side View 1 (in) (Click to Enlarge)(1:50)

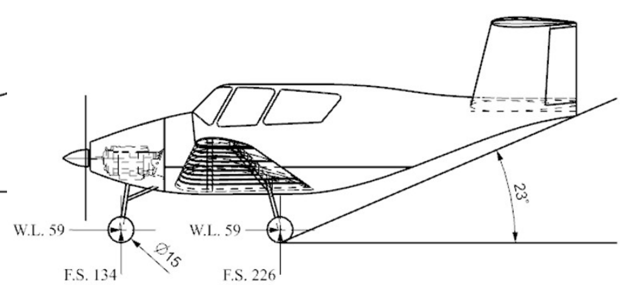

Figure 13.2 Landing Gear Side View 2 (in) (Click to Enlarge)(1:50)

Figure 13.3 Landing Gear Off-Axis View (Not to Scale)

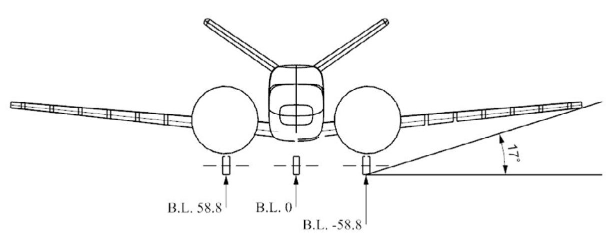

Figure 13.4 Landing Gear Front View (in) (Click to Enlarge)(1:100)

Equations 9.1 and 9.2 in Ref. 20 were used to calculate the loading on the nose gear and main gear respectfully. Using take off weight and empty weight of each aircraft, Table 9.1 in Ref. 20 recommends a nose tire to be a 15 in diameter 5 in wide 18 psi tire, and the main gear to be a 15 in diameter 6 in wide 28 psi tire for both aircraft. This calculation is shown in the hand calculations at the end of the chapter. Figure 13.5 shows the twin gear is able to fully fit into the fuselage in its retracted state.

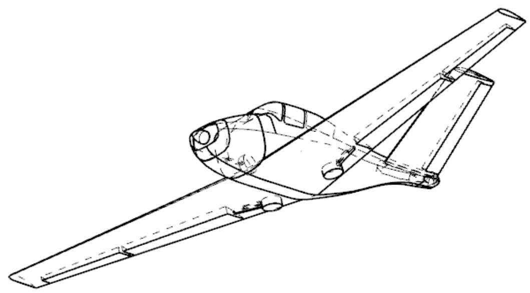

Figure 13.5 Landing Gear Twin Retracted
(Click to Enlarge)(Not to Scale)

13.2. Landing Gear Summary and Recommendations

13.2.1. Summary

Figure 13.6 shows the landing gear integrated on the aircraft satisfying the requirements laid out in section 13.1.

Figure 13.6 Landing Gear Aircraft Integration

Click to Enlarge

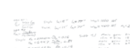

13.2.2. Recommendations

The authors recommend that pants are designed for the landing gear and a cost analysis performed.

14. Class I Weight and Balance Analysis

The purpose of this chapter is to outline the procedures for weight and balance as well as the initial component weight breakdown. The methods used are found in Ref. 20 and Ref. 28.

14.1. Preliminary Three View

Three views of the aircraft are shown with the locations of the major system components numbered. The numbers correspond to specific sub systems and are identified in Table 14.1 and Table 14.2.

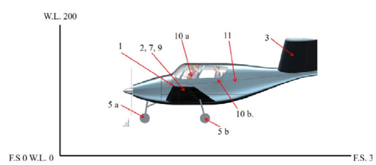

Figure 14.1 Single Side View (in) (Click to Enlarge)(1:80)

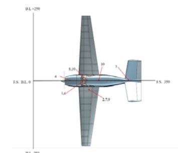

Figure 14.2 Single Top View (in) (Click to Enlarge)(1:80)

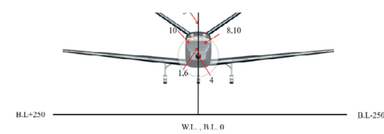

Figure 14.3 Single Front View (in) (Click to Enlarge)(1:100)

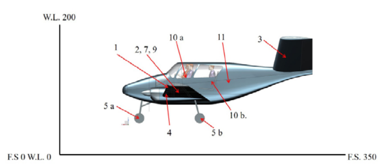

Figure 14.4 Twin Side View (in) (Click to Enlarge)(1:80)

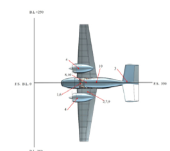

Figure 14.5 Twin Top View (in) (Click to Enlarge)(1:80)

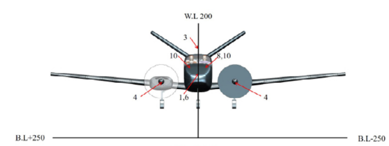

Figure 14.6 Twin Front View (in) (Click to Enlarge)(1:80)

14.2. Weight Breakdown and Weight and Balance Calculation

The components of the aircraft were broken down into 11 different sections outlined by Ref 20 and Ref 28. The initial empty and max takeoff weights for each aircraft were found in Chapter 5. Similar aircraft were found and the weight fractions of the corresponding components were used to estimate the weights of the unknown components for the Super Aerial Bros aircraft family. The C.G. location of each loading condition was found by the addition of baggage, fuel, and a maximum of 4 occupants to enable the creation of a C.G. excursion chart. Initially, the single engine aircraft had a 30 in. excursion. To remedy this, a larger empty weight was used. Weights and a single load case for each aircraft is shown in Table 14.1 and Table 14.2 for the single and twin-engine aircraft respectively.

Table 14.1 Single Engine Weight and Balance

Single Engine									
No.	Component	Wi	Xi	WiXi	Yi	WiYi	Zi	WiZi	Weight Fraction
		lbf	in	in-lbf	in	in-lbf	in.	in-lbf	%
1	Fuselage	272	185	50320	0	0	115	31144	21%
2	wing	230	190	43700	0	0	84	19320	18%
3	Empennage	172	365	62780	0	0	148	25456	13%
	Engine	300	140	42000	0	0	100	30000	23%
	Propeller	50	104	5200	0	0	100	5000	4%
	Landing Gear N.G.	23	140	3220	0	0	52	1196	2%
	M.G	50	226	11300		0	52	2600	4%
6	Fixed equip	200	178	35600	0	0	115	22900	15%
									100%
Empty Weight		1297							
	Trapped Fuel and Oil	8.3	204	1693.2	0		84	697.2	
8	Crew	200	204	40800.0	-10.5		115	23000	
9	Fuel (240 lbf max)	240	204	48960.0				0 0	
10	Passengers Front	200	204	40800.0	10.5		115	23000	
	Passengers Rear	400	235	94000.0	0		115	46000	
11	Baggage	160	253	40480.0			110	17600	
Weight		2505.3							
		Total Moment	520853.2	X C.G Location	207.9				

Table 14.2 Twin Engine Weight and Balance

Twin Engine									
No.	Component	Wi	Xi	WiXi	Yi	WiYi	Zi	WiZi	Weight Fraction
		lbf	in	inlbf	in	inlbf	in.	inlbf	%
1	Fuselage	272	178	48444	0	0	115	31162	13%
2	wing	324	190	61560	0	0	84	27216	15%
3	Empennage	173	365	63072	0	0	148	25574	8%
4	Engine	600	162	96900	0	0	100	60000	28%
	Propeller	100	114	11350	0	0	100	10000	5%
5	Landing Gear N.G	80	134	10720	0	0	52	4160	4%
	Landing Gear M.G	158	223	35234	0	0	52	8216	7%
6	Fixed equip	454	178	80741	0	0	115	51937	21%
									100%
Empty Weight		2160							
7	Trapped Fuel and Oil	15.7	204	3202.8	0		84		
8	Crew	200	204	40800	-10.5		115		
9	Fuel (464 lbf max)	464	204	94656	0		84		
10	Passengers Front	200	204	40800	10.5		115		
	Passengers Rear	400	238.5	95400	0		115		
11	Baggage	160	262	41920	0		110		
Weight		3600							
			Total Moment	724800	C.G Location	201.4			

The C.G excursions are shown in Figure 14.7 and Figure 14.8.

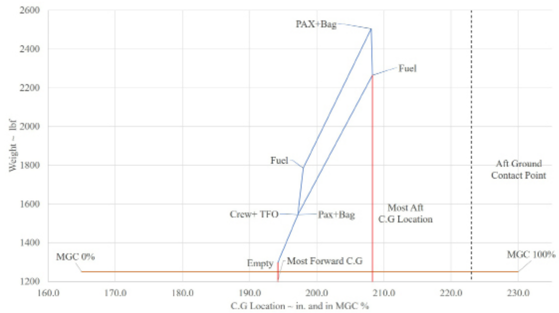

Figure 14.7 C.G Excursion Single

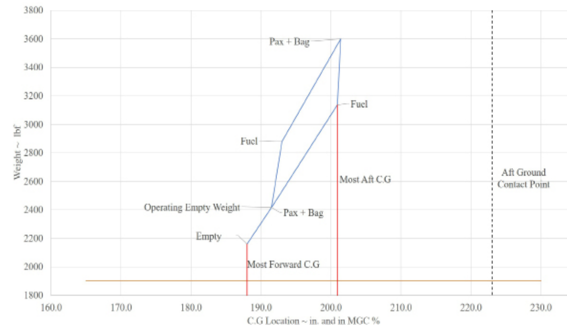

Figure 14.8 C.G Excursion Twin

Click to Enlarge

14.3. Summary and Recommendations

14.3.1. Weight and Balance Summary

Table 14.3 and Table 14.4 shows a summary of loading conditions, total weights and C.G. location.

Table 14.3 Single Engine Weight and Balance Summary

Weight and Balance Summary			
Condition	Weight (lbf)	CG location (in)	MGC %
empty	1297	195.9	0.41
Operating empty weight	1545	198.5	0.45
Takeoff Weight	1785	199.2	0.46
2 occupants	2025	200.8	0.48
3 occupants	2265	204.7	0.54
4 occupants	2505	207.9	0.59

Table 14.4 Twin Engine Weight and Balance Summary

Weight and Balance Summary			
Condition	Weight (lbf)	CG location (in)	MGC %
empty	2160	188	0.29
Operating Empty Weight	2416	191	0.35
Take Off Weight	2880	193	0.37
2 occupants	3120	195	0.40
3 occupants	3360	198	0.44
4 occupants	3600	201	0.49

14.3.2. Weight and Balance Recommendations

The authors recommend that the weight and balance chart be updated as additional component and structural weights are caclulated.

15. V-n Diagram

The purpose of this section is to construct a V-n diagram for the single-engine and twin-engine aircraft based on the methods shown in Ref. 20 and Ref. 28. Level flight and maneuvering were considered in the construction of the V-n diagrams of each aircraft.

15.1. Calculating V-n Diagram

The method described in Chapter 4 of Ref. 28 was used to calculated all the necessary components to build the V-n diagrams. The process is shown in the hand calculation at the end of this chapter. The components have been tabulated in Table 15.1.

Table 15.1 V-n Diagram Components

V-N Diagram				
SINGLE	$V_{s,1}$	V_a	V_c	V_d
	57.3 ft/s	112 ft/s	202 ft/s	253 ft/s
$n_{lim,pos}$	-	3.8	3.8	3.8
$n_{lim,neg}$	-	-1.52	-1.52	-1.52
n	1	-	-	-
$n_{lim,pos,gust}$	-	-	6.1	4.2
$n_{lim,pos,gust}$	-	-	-4.1	-2.2
TWIN	$V_{s,1}$	V_a	V_c	V_d
	71.6 ft/s	150 ft/s	290 ft/s	363 ft/s
$n_{lim,pos}$	-	4.4	4.4	4.4
$n_{lim,neg}$	-	-1.76	-1.76	-1.76
n	1	-	-	-
$n_{lim,pos,gust}$	-	-	6.6	4.5
$n_{lim,pos,gust}$	-	-	-4.6	-4.5

15.2. Presentation of V-n Diagram

In this section, the constructed V-n diagrams are presented. To construct the diagrams, the air density was assumed equal to that at sea level as to represent the maximum load factor possible at any point in flight. Additionally, the wing planform area is equal between the single-engine and twin-engine. Also, although the calculations show the cruise speed can be less than the one depicted on the V-n diagrams. The cruise speeds designed are to stay competitive within the general aviation market. To construct the final V-n diagram, a diagram for steady level flight was made and calculated maneuvering loads were superimposed. The Max load factor was then taken as the true expected load factor at any point within the flight. Figure 15.1 and Figure 15.2 show the V-n diagram with gust loading overlays.

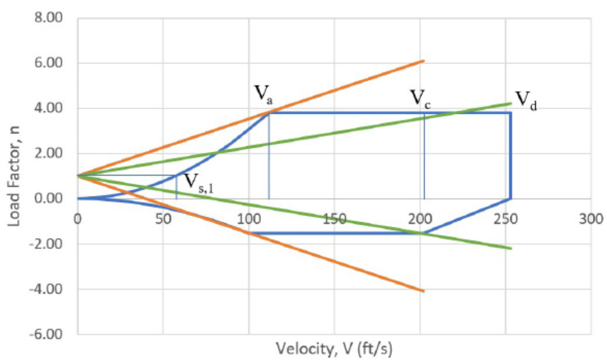

Figure 15.1 V-n Gust Diagram Overlay: Single Engine (Click to Enlarge)

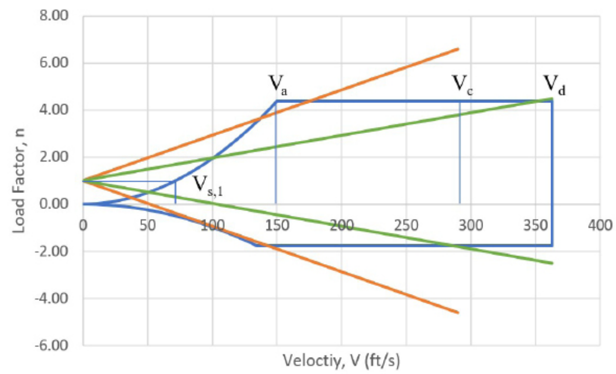

Figure 15.2 V-n Gust Diagram Overlay: Twin Engine (Click to Enlarge)

15.3. Summary and Recommendations

15.3.1. Summary

The authors conclude Figure 15.3 and Figure 15.4 to accurately depict the expect load factors for the single-engine and twin-engine aircraft throughout the flight.

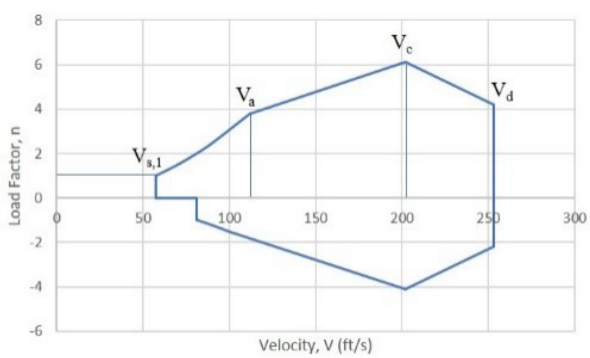

Figure 15.3 V-n Gust Diagram Single Engine (Click to Enlarge)

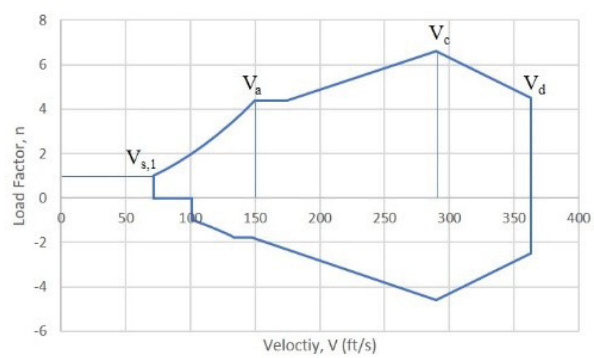

Figure 15.4 V-n Gust Diagram Twin Engine (Click to Enlarge)

15.3.2. Recommendations

The authors recommend the following:

i.) Pilots fly within the enclosed area of the V-n diagram;

ii.) As the design speed and CL_{α} are approximated, once they are properly calculated, the V-n diagrams should be reconstructed to be more accurate.

Click to Enlarge

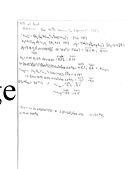

16. Class I Method for Stability and Control Analysis

The purpose of this chapter is to perform a Class I stability and control analysis on the twin and single engine aircraft to determine the stability of the aircraft based on the methods outlined in Chapter 11 of Ref. 20.

16.1. Static Longitudinal Stability

An X-plot was prepared to determine the proper size of the horizontal tail. A restriction set was that the horizontal tail area can not change by more than 10% compared to the preliminary size done in Chapter 12. The process followed is depicted in Chapter 11 of Ref. 20. The process was followed for a tail-aft airplane. The X-plots created are shown in Figures 16.1 and 16.2. The desired static margin was a minimum of 10%. To maintain a positive static margin for the single engine variant, a redesign to the weight management was done such that only 20 lbf of baggage per occupant is allowed in flight for max weight capabilities.

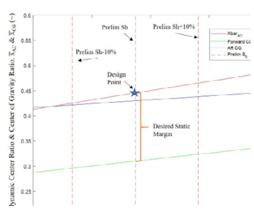

Figure 16.1 X-Plot Sizing Horizontal Tail Single Engine (Click to Enlarge)

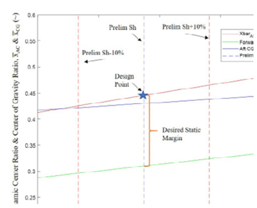

Figure 16.2 X-Plot Sizing Horizontal Tail Twin Engine (Click to Enlarge)

The variants were designed to be inherently stable. The single engine and twin engine aircraft are categorized in the 3.1.2 and 3.1.3 group given in Chapter 2 in Ref. 20. Chapter 11 of Ref. 20 allows for the calculation of the SAS feedback gain using the aft CG. The calculations for all information presented is given in Figures 16.3, 16.4, and 16.5 including multhop integration of the broken up aircraft.

16.2. Static Directional Stability

The process defined by Chapter 11 in Ref. 20 was followed to properly size the vertical tail projection of the V-tail for both aircraft. A X-plot was made to determine the vertical tail area such that $C_{n\,\beta}$ is greater than 0.001 deg^{-1}. The current design did not meet the needs such that $C_{n\,\beta}$ is greater than 0.001 deg^{-1}. A redesign was done such that the $C_{n\,\beta}$ exceeded or equaled 0.001 deg^{-1} by increasing the angle of the V-tail design. This is more thoroughly discussed in Chapter 18.

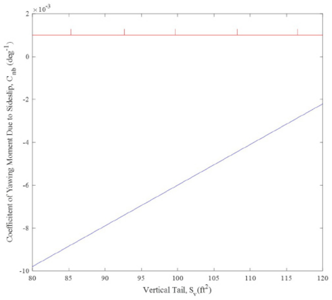

Figure 16.3 Coefficient of Yawing Moment due to Sideslip (Click to Enlarge)

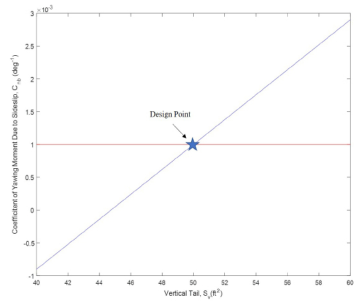

Figure 16.4 New Coefficient of Yawing Moment due to Sideslip (Click to Enlarge)

The required sideslip to rudder gain was calculated using the procedure shown in Chapter 11 in Ref. 20. Additionally, the maximum rudder deflection needed to counter a yawing moment due to single engine out was calculated using the procedure given in Section 11.3 in Ref. 20. The hand calculations are documented in the popup hand calcs.

16.3. Summary and Recommendations

16.3.1. Summary

The authors conclude the following characteristics for the twin and single engine aircrafts:

Table 16.1 Longitudinal Characteristics of Aircraft

Single Engine Static Margin, SM (%)		Twin Engine Static Margin, SM (%)	
Most Fwd CG	Most Aft CG	Most Fwd CG	Most Aft CG
12.2	0.92	13.0	1.1
SAS Feedback Gain, k_α (deg/deg)			
-0.38		-0.37	
Horizontal Tail Area, S_h (ft^2)			
57			

Table 16.2 Directional Characteristics of Aircraft

Vertical Tail Area for Stability, Sv (ft^2)	Sideslip to Rudder Feedback Gain, k_β (deg/deg)	Rudder deflection needed for Single Engine Out, δ_r (deg)
50.7	0	2.7

16.3.2. Recommendations

The authors recommend that another redesign of the horizontal tail projection of the V-tail be done such that a restriction on the amount of baggage per person can be increased by weight. If this is done, then another stability and control analysis should follow the redesign.

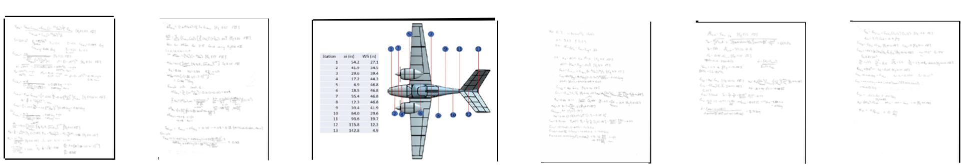

Click to Enlarge Hand Calculations

17. Class I Drag Polar and Performance Analysis

The purpose of this chapter is to provide a Class I Drag Polar and Performance Analysis of the single engine and twin-engine aircraft using Roskam's Airplane Design Part I Ref. 4.

17.1. Drag Polar Analysis with Wetted Area Breakdown

To calculate the drag polar of the single engine and twin-engine aircraft, the wetted area (S_{wet}) of each airplane component was computed, this included the wings, fuselage, empennage, and nacelles. Since the single engine and twin-engine aircraft share the same fuselage, wing, and empennage, the only difference between wetted areas between the single engine and twin-engine aircraft are the nacelles of the twin engine aircraft. The wetted area of the wings and the V tail was calculated using Ref. 4 methodology. The fuselage wetted area was calculated using a perimeter plot as shown in Figures 17.1. Table 17.1 shows the final wetted area calculations of each component.

With the calculated wetted areas, Ref. 4 provided the followed methodology to calculate the drag polars at cruise, takeoff, and landing. Table 17.2 provided the calculated drag characteristics including the total wetted area of the aircraft, the skin friction drag coefficient (c_f), the parasite area (f), and the clean zero lift drag coefficient (C_{Do}).

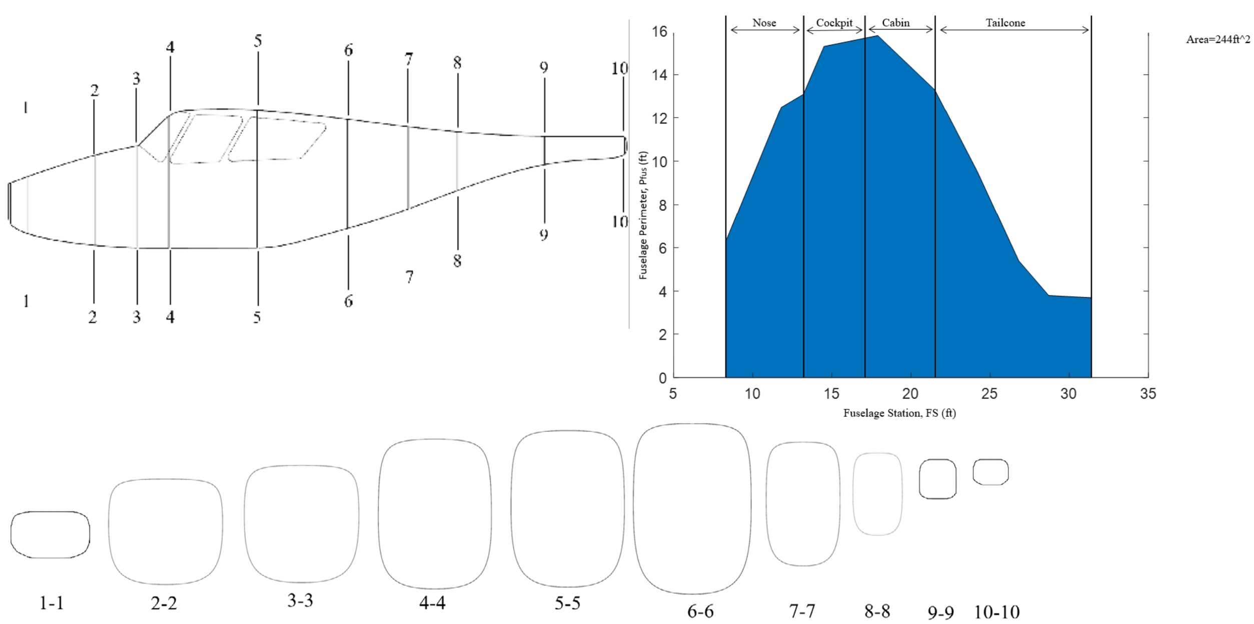

Figure 17.1 Fuselage Perimeter Plot

Table 17.1 Component Wetted Areas

Component	Wings	Fuselage	V Tail	Nacelles
S_{wet} (ft^2)	349	244	133	85

Table 17.2 Salient Drag Characteristics

Aircraft	**S_{wet} (ft^2)**	**c_f (~)**	**f (ft^2)**	**C_{Do} (~)**
Single Engine	726	0.004	3.4	0.017
Twin Engine	811	0.004	3.5	0.018

17.2. Summary and Recommendations

17.2.1. Summary

The results indicate that the drag polars are satisfactory since the calculated lift to drag ratios (L/D) are within 5% of the predicted L/D values obtained during the preliminary sizing of the aircraft thus no weight changes need to be performed as recommended by Ref. 4. The obtained L/D values show that the aircraft will be fuel efficient compared to STAMPED data from Chapter 4, minimizing the amount of emissions. As such, both the single engine and the twin engine aircraft are as environmentally friendly as possible. Table 17.3 provides L/D ratios at critical flight stages.

Table 17.3 L/D Values

Flight Condition	**L/D Single Engine**	**L/D Twin Engine**
Takeoff	9.75	8.86
Cruise	12.7	15.4
Landing	7.27	6.94

17.2.2. Recommendations

The authors recommend that the aircraft be manufactured as clean as possible to meet the skin friction coefficient requirement and that possible resizing of the aircraft components be considered to reduce wetted area.

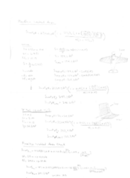

Click to Enlarge

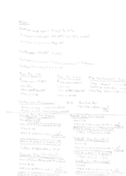

18. Analysis of Weight and Balance, Stability and Control and L/D Results

The purpose of this chapter is to analyze the effects of weight and balance, stability and control and L/D results that have been gathered through aircraft design process and to ensure they meet a set of requirements necessary for Class I design. The methods followed for this chapter are found in Ref. 20.

18.1. Impact of Weight and Balance and Stability and control results on the Design

In Chapter 14, weight and balance for multiple aircraft loading conditions were found. Each aircraft met the suggest for C.G excursion from Table 10.3 from Ref. 20. Each aircraft maintains a stable static margin through all loading conditions and has the appropriate directional stability and control.

18.2. Analysis of Critical L/D Results

The L/D values found during Class I design needed to be validated against the preliminary L/D estimation from Chapter 4. The aircraft was sized based on an L/D_{max} that was assumed to take place at cruise, therefor only the cruise L/D values were compared since it drove the Class I design. Table 18.1 and 18.2 show the single and twin-engine comparison respectfully.

Table 18.1 Single Engine Cruise L/D Comparison

Alt. (ft)	Weight	V ft/s	CL	CD	$(L/D_{Class\ I})$	$(L/D_{preliminary})$
8000	2505	202	0.68	0.054	12.68	12.6

Table 18.2 Twin Engine Cruise L/D Comparison

Alt.(ft)	Weight	V ft/s	CL	CD	$(L/D_{Class\ I})$	$(L/D_{preliminary})$
10000	3600	268	0.69	0.045	15.4	15.6

The difference between the preliminary and designed values are within 5% of each other and meet the requirements in Ref. 20.

18.3. Design Iterations Performed

Multiple iterative steps were required to have a Class I design that met desirable design criteria. The iterations performed are:

- Wing moved forward to reduce fuselage wetted area at the wing and fuselage intersecting point;

- Increased single engine aircraft empty weight from 974 to 1297 to reduce C.G excursion from 21 inches to 12 inches;
- Collapsed the rear fuselage slightly quicker to reduce fuselage wetted area and to increase aesthetic appeal;
- Moved the engines forward 6 inches on the twin engine aircraft to shift cg forward;
- Moved fuel stores in the wing forward 3 inches.;
- Moved the rear passengers for both aircraft forward 2.5 inches;
- V-Tail dihedral increased from 33.7 to 41.5 degrees to increase $C_{n\beta}$.

The iterations performed allowed for both aircraft to meet the necessary design requirements to continue past Class I design.

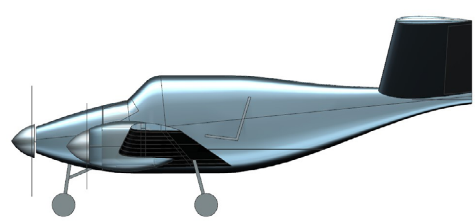

Figure 18.1 First Fuselage Iteration

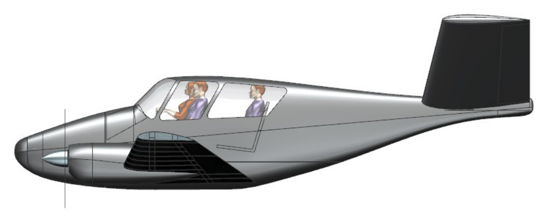

Figure 18.2 Latest Fuselage Iteration

18.4. Summary and Resommendations

18.4.1. Summary

The major findings of this chapter are:

- Both aircraft meet the L/D requirements and are within 5% of preliminary results.
- Multiple design iterations were performed to ensure C.G. excursion and S.M. were within acceptable ranges.

18.4.2. Recommendations

The authors recommend that:

- Both aircraft should have different wing and empennage sizing if cost was not a consideration to better control weight, C.G. excursion and S.M. travel;
- Additional iterations be performed to closer match preliminary sizing L/D.

19. Class I Aircraft Characteristics and Preliminary Three-View

This chapter presents a preliminary three-view and general aircraft characteristics for the single and twin aircraft.

19.1. Table of Class I Aircraft Characteristics

Table 10.1: Planform Characteristics

	Single		Twin	
	Wing	V-Tail	Wing	V-Tail
Area (in^2)	28800	9290	28800	9290
Span (in)	480	167	480	167
Mean Geometric Chord (in)	60	55.2	60	55.2
Aspect Ratio	8	3	8	3
Sweep Angle (deg)	0	8	0	8
Taper Ratio	0.403	0.8	0.403	0.8
Airfoil	NACA 4415	NACA 0012	NACA 4415	NACA 0012
Dihedral Anlge (deg)	5.8	33.7	5.8	33.7
Incidence Angle (deg)	2	0	2	0
Aileron Chord Ratio	0.3		0.3	
Ruddervator Chord Ratio	0.3		0.3	
Flap Chord Ratio	0.3		0.3	

Table 19.2: Fuselage Dimensions

	Single	Twin
Fuselage Length (in)	213	229
Maximum Fuselage Width (in)	46	46
Maximum Fuselage Height (in)	64	64

19.2. Class I Aircraft Description

The Super Aerial Bros single and twin engine V-tail aircraft are designed as a new generation of "all-purpose" pilot training aircraft. Both aircraft accommodate pilot statures ranging from 20th percentile females to 6 ft 7 in males and 95th percentile male rear passengers to provide a comfortable experience for a wide variety of consumers. Designed from the ground up with modern materials and a fly-by-wire system, the aircraft meet or surpass the FAR 23 standard. Identical fuselages (exception of nose and retractable landing gear), wings (exception of engines), empennages, and engines allow interchangeability of parts between the single and twin aircraft help to keep acquisition and maintenance costs low. Super Aerial Bros designed the single and twin aircraft with existing infrastructure in mind, ensuring each aircraft fits within a standard T-hangar. Figure 19.1 and 19.2 show the preliminary three-views of the single and twin engine aircraft.

19.3. Summary and Recommendations

19.3.1. Summary

The authors conclude that planform characteristics are as shown in Table 19.1 and fuselage dimensions are as shown in Table 19.2. Preliminary three-views of the single and twin engine aircraft are shown in Figure 19.1 and 19.2.

19.3.2. Recommendations

The authors recommend that the single and twin engine aircraft be named appropriately for ease of reference.

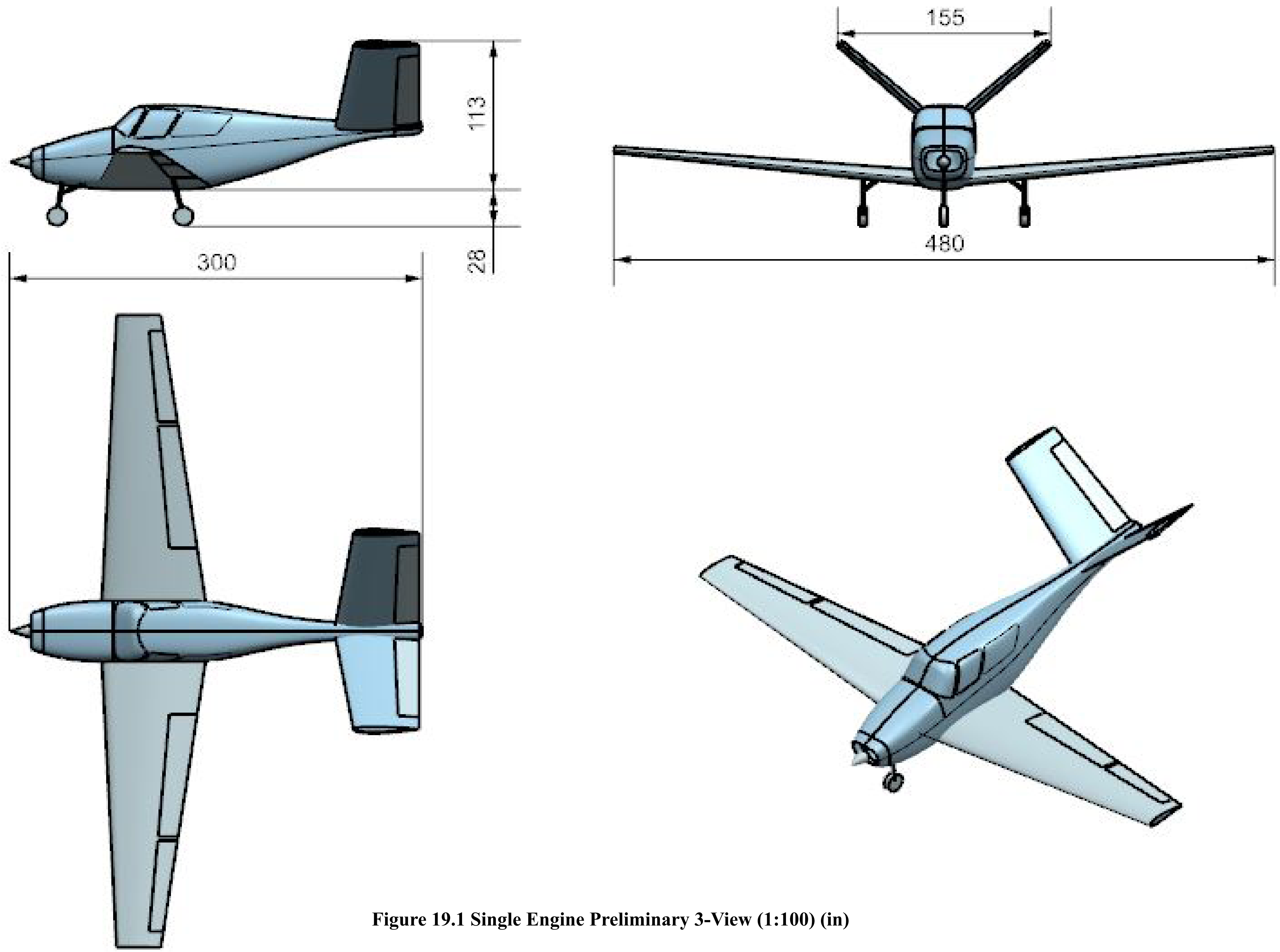

Figure 19.1 Single Engine Preliminary 3-View (1:100) (in)

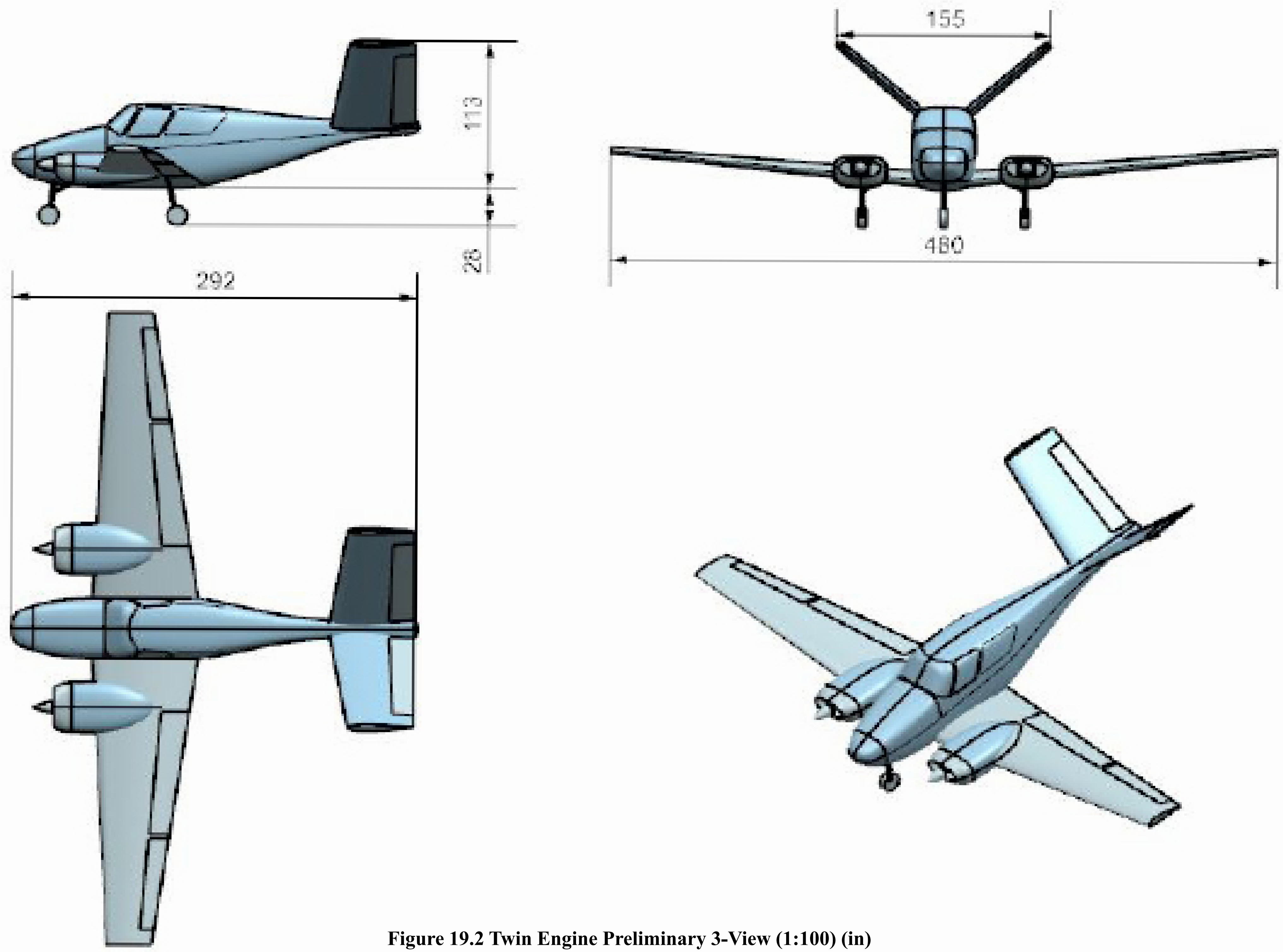

Figure 19.2 Twin Engine Preliminary 3-View (1:100) (in)

20. Description of Major Systems

The purpose of this chapter is to outline all major systems of the aircraft including flight control, fuel, electrical, hydraulic and environmental control systems. The methods to size and layout all major systems are found in Ref. 29.

20.1. List of Major Systems

Table 20.1 contains a list of all major systems contained in the Super Aerial Bros aircraft family. Additional component and system descriptions are contained in this chapter.

Table 20.1 List of Major Systems

System	Description
Flight Control	Flight Controller, Avionics, Actuator
Fuel	Tanks, Fuel Pumps, Cross Over Valve, Vent
Environmental Control	Heat Exchanger, Compressor, Blower
Electrical	Alternator, Primary Bus, Avionics Bus
Hydraulic	Reservoir, Lines, Brake Caliper

20.2. Description of the Flight Control System

The flight control system on each Super Aerial Bros aircraft will be a redundant fly by wire system utilizing a tuned PID controller. The Super Aerial Bros aircraft flight control systems consist of ailerons, flaps, and ruddervators. A fly by wire system was chosen for simplicity and weight savings. Each flight control system will have two electromechanical actuators with a maximum control surface deflection rate of 60 deg/sec. Actuator power requirements were sized from the twin engine variant: maintaining actuator size between variants will reduce cost. Actuators were sized so that a single actuator has sufficient power to control the entire surface in the event of an acutator failure. The power required for each control surface is listed in Table 20.2

Table 20.2 Control Surface Required Power

Control Surface	Power Required (Watts)
Flaps	667
Ailerons	38
Ruddervator	571

20.3. Description of the Fuel System

Fuel for each aircraft is stored within the wings outside of the fuselage outline. The required fuel capacity is evenly split between the two wings and the tank placement is such that a changing fuel load has minimal effect on C.G. Table 20.3 outlines the required fuel characteristics for each aircraft.

Table 20.3 Fuel Requirements

	Single Engine Aircraft	Twin Engine Aircraft
Max Fuel Flow(gal/hr)	13.1	25.2
Required Fuel Quantity (gal.)	40	78

The fuel system for each aircraft consists of aluminum fuel tanks that are connected to each other with fuel lines, electric fuel pumps and check valves as well as a tank selector to increase reliability and redundancy. Each tank has a fuel vent connected to the topmost part of the fuel tanks such that overfill can run out of the tanks and out the bottom of the wing. Each tank also maintains a fuel sampling point at the lowest tank location. Figure 20.1 and Figure 20.2 show the layout of the fuel system.

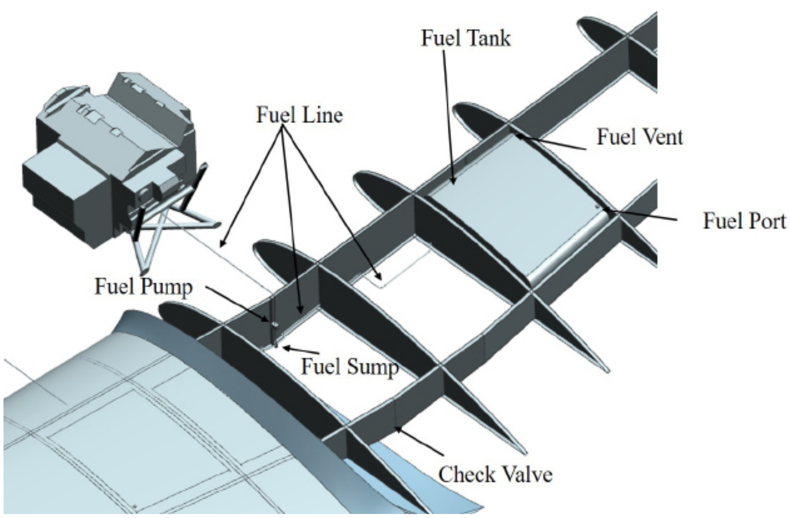

Figure 20.1 Single Engine Fuel System (Not to Scale)

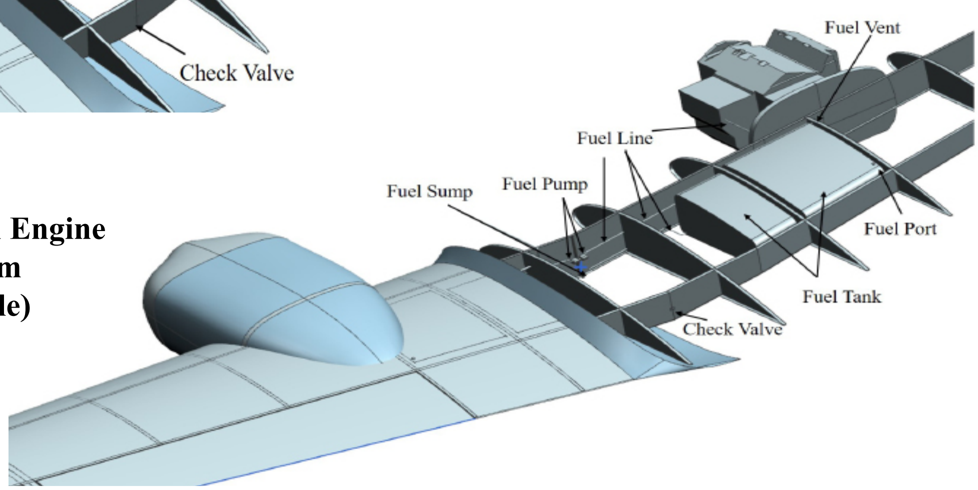

Figure 20.2 Twin Engine Fuel System (Not to Scale)

20.4. Description of the Electrical System

The electrical system for each aircraft in the family consists of a primary battery, a generator on each engine, and a smaller secondary avionics battery (internal to the avionics). The electrical system is broken into two separate electrical busses, a primary bus, and an avionics bus. The primary bus is used for engine start, battery charging, and landing gear extension and retraction. The avionics bus is used to power aircraft avionics and flight actuators. The separation ensures that the critical systems are isolated from each other and if a fault happens, it cannot travel.

To power the electrical system, a 2000-Watt generator is run from each engine. The twin engine aircraft would have a fully redundant power system with a generator on each engine, and a starting battery for each engine. A 28 Ampere Hour battery would provide complete system controlability for 10 minutes in the event of failure of both generators. The single engine would rely solely on the battery in the case of engine/generator failures. The power requirements for each individual component are listed in Table 20.4.

Table 20.4 Individual Power Requirements

Component	Electrical Load (Watts)
Avionics	300
Actuators	1276
Environmental Controls	200
Lights	10
Fuel pumps	50
Landing Gear	50
Total Power Required	1886

Figure 20.3 shows the electrical system on the aircraft. Figure 20.4 and Figure 20.5 show simplified electrical diagrams for the twin and single engine aircraft respectively.

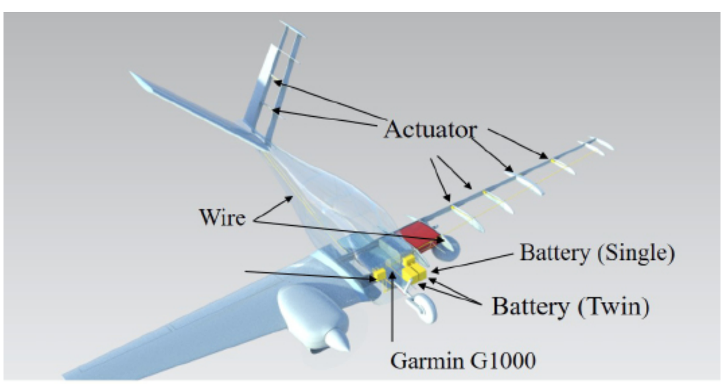

Figure 20.3 Electrical System (Not to Scale)

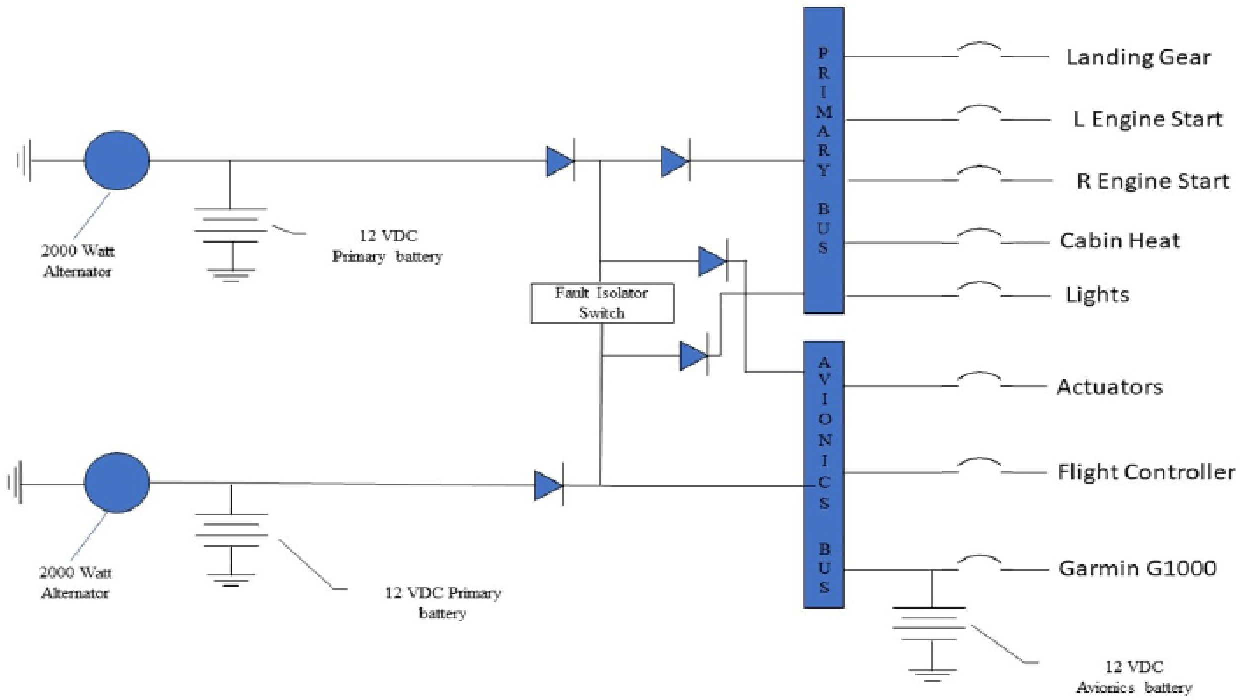

Figure 20.4 Twin Engine Electrical Diagram

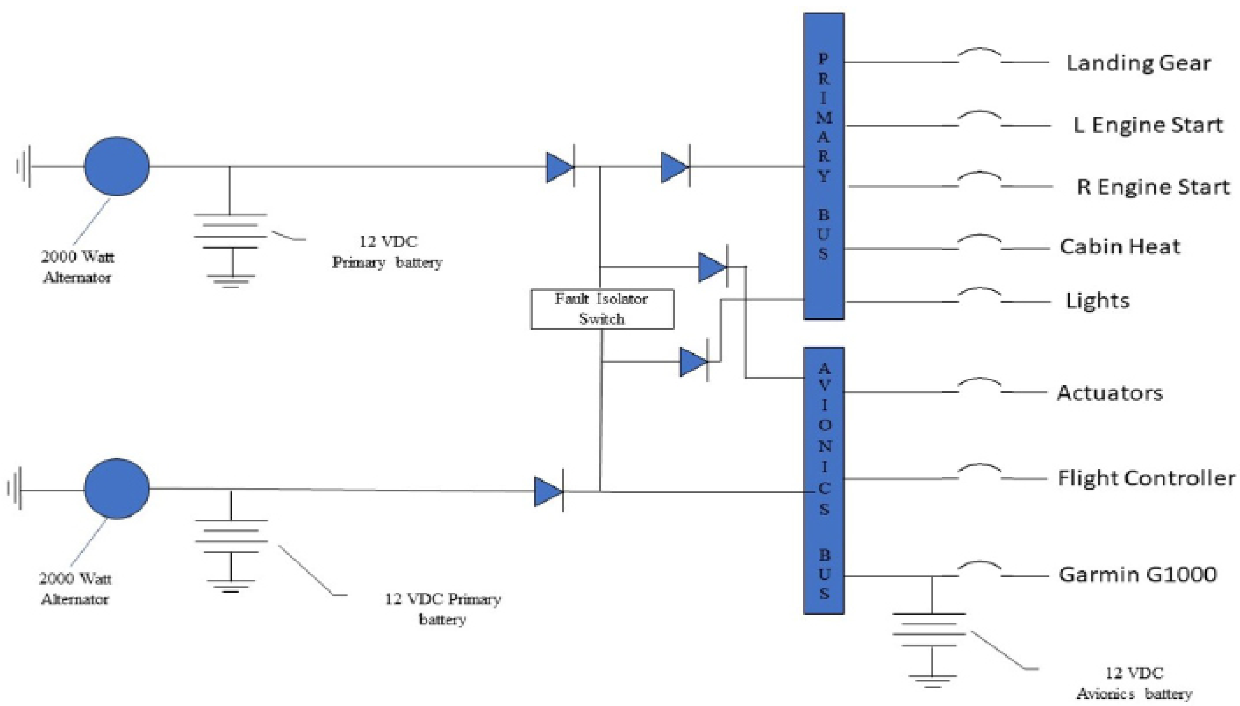

Figure 20.5 Single Engine Electrical Diagram

20.5. <u>Description of the Hydraulic System</u>

The hydraulic system on the Super Aerial Bros aircraft family is for actuation of the brakes located on the main landing gear. The system consists of brake calipers, a hydraulic reservoir and master cylinders for each set of pedals. The system is actuated by pressing the top of the rudder pedals, actuating the the caliber causing the brakes to engage. There is no other need for hydraulics on the aircraft family. Flight controls and landing gear utilize electromechanical actuators to reduce complexity. The layout of the hydraulic system is shown in Figure 20.6.

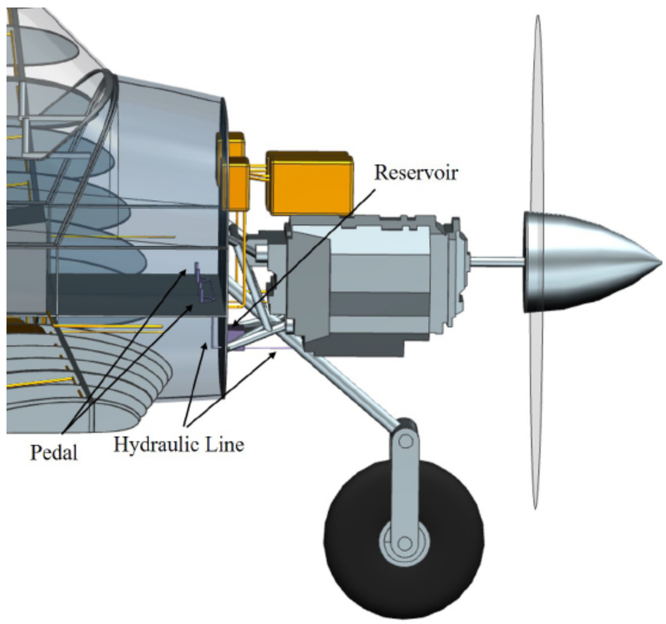

Figure 20.6 Hydraulic System (Not to Scale)

20.6. <u>Description of Environmental Control System</u>

Each aircraft in the aircraft family has cabin environmental controls for temperature. The system uses a heat exchanger to bring hot air from the exhaust to the cabin for cold temperature operations and windshield de-fogging. For cooling, two small vents located at the fore of the bottom canopy or a small side window can be opened.

20.7. Conflict Analysis

System layout adds significant complexity to the aircraft and certain interactions between systems must be addressed. Fuel tanks are in close proximity to the landing gear. If a tire were to rupture, a fuel system puncture would causing fire hazard as fuel is also stored directly behind the twin engines. Minor engine fires could quickly become severe with fuel nearby.

20.8. Summary and Recommendations

20.8.1. Summary

The conclude that the Super Aerial Bros family of aircraft is redundant in most major systems. The twin engine aircraft is fully redundant while the single engine is only redundant in-flight controls. The lack of redundancy in the single engine variant is mainly due to the limitations of a single engine and its accessories. Table 20.1 through 20.4 show all relevant information.

20.8.2. Recommendations

The authors recommend that the fuel system be moved to avoid damage from ruptured tires and engine malfunctions.

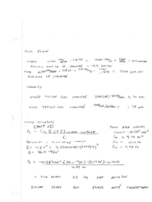

21. Sizing of the Landing Gear and Struts using Class II Methods

The purpose of this chapter is to perform a Class II sizing of the landing gear and struts for the single and twin aircraft outlined in Chapter 2 in Ref. 29.

21.1. Description of Major Landing Gear Components and Disposition

The landing gear for the two aircraft was sized to handle worst case landing loads. A vertical speed of 10 ft/s was used based off Ref. 29. The tires were sized for Class II condition static loads found and scaled by a factor of 1.25 to allow for aircraft growth. A dynamic load was calculated and compared to the static loads calculated. The load cases found were compared to the tires found in Table 2.5 in Ref. 29. The same tire was selected for the nose and main main gear for both aircraft. The tires were sized based off static loading. The tires on the twin aircraft requires width clearance of 1.25 in and a radial clearance of 2.75 in when retracted. The characteristics of the tire selected are shown in Table 21.1.

Table 21.1 Tire Characteristics

Description	6.00-6
Ply Rating	8
Tube/Tubeless	TT
D_o (in)	17.5
W (in)	6.3
Type	III
Max Loading (lbs)	2,350
Pressure (psi)	55
Max Speed (mph)	120
Loaded Radius (in)	6.9
Weight (lbs)	10

The landing gear struts were sized by stroke and diameter. The struts contain an air spring shock absorber. The struts were calculated with a load factor of 3 as the worst possible case. The strut dimensions are shown in Table 21.2.

Table 21.2 Strut Characteristics

		Strut Stroke (in)	Strut Diameter (in)
Single	Nose	0	1.57
	Main	3.5	1.57
Twin	Nose	0	1.79
	Main	3.6	1.79

The nose gear and main gear were mounted on the firewall and the aft spar respectively. The single engine aircraft has fixed landing gear with conventional disk brakes and nose gear steering. The twin engine retractable landing gear uses electromechanical actuators to retract and extend the gear. The nose gear uses a single actuator retracting the gear forward into the nose of the aircraft. The main gear uses an electromechanical system to rotate the gear 90 degrees and retract the gear forward into the engine cowling. The kinematic sweep of the twin engine landing gear is shown in Figure 21.4 below. The ground contact points for the single engine aircraft did not change. The twin engine changes and the stability is shown in Figure 21.1.

The force needed by the electromechanical actuation system of the landing gear to extend and retract is shown in Figure 21.2 and Figure 21.3.

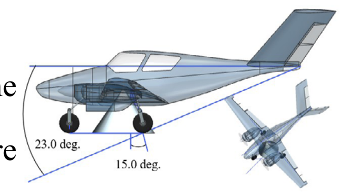

Figure 21.1 Stability Check Twin Engine

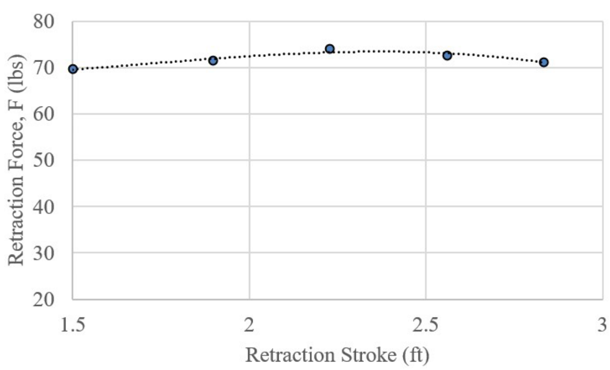

Figure 21.2 Nose Gear Retraction Force

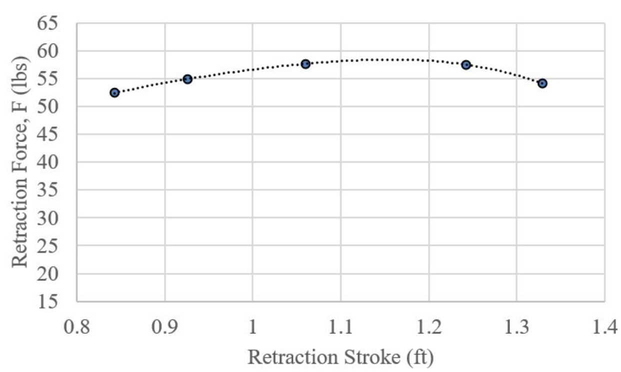

Figure 21.3 Main Gear Retraction Force

21.2. <u>CAD Drawing of Landing Gear Components, Disposition and Integration into Airframe</u>

Figure 21.3 represents the kinematic sweep of the twin engine retracting gear. A three view of the single engine aircraft, twin engine aircraft with gear retracted, and twin engine aircraft with gear extended are shown in Figure 21.5 through 21.7 respectively.

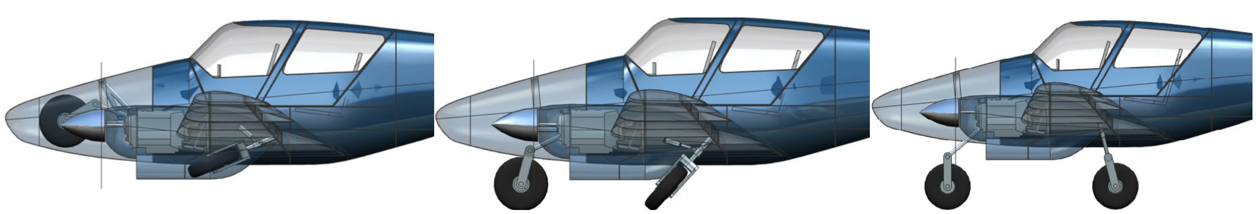

Figure 21.4 Retraction Sweep (Not to Scale)

Figure 21.5 Single Engine Landing Gear (Not to Scale)

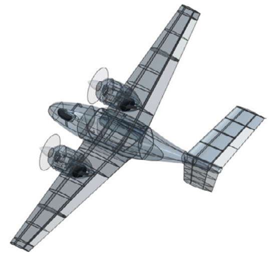

Figure 21.6 Twin Engine Landing Gear Retracted (Not to Scale)

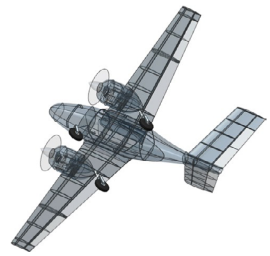

Figure 21.7 Twin Engine Landing Gear Extended (Not to Scale)

21.3. <u>Summary and Recommendations</u>

21.3.1. <u>Summary</u>

The authors conclude the following characteristics for the tire and struts used on the landing gear for the aircraft shown in Table 21.3.

Table 21.3 Summary Characteristics

	Single Engine		Twin Engine	
	Nose	Main	Nose	Main
Tire Diameter (in)	17.5	17.5	17.5	17.5
Tire Width (in)	6.3	6.3	6.3	6.3
Tire Pressure (in)	55	55	55	55
Strut Diameter	1.57	1.57	1.79	1.79
Strut Stroke (in)	0	3.5	0	3.6
Max Load (lbs)	905	1303	1414	1864
Max Retraction Force (lbf)	N/A	N/A	75	60

21.3.2. <u>Recommendations</u>

The authors recommend that:

i.) Mounting brackets are designed to connect the gear to the substructure;

ii.) A finite element model be created to optimize the landing gear layout;

iii.) Pants are designed to reduce drag on the single engine fixed gear;

iv.) The electromechanical system to rotate the main gear be designed.

22. Initial Structural Arrangement

This section details the initial structural arrangement of the aircraft following the procedure and recommendations of Roskam's Airplane Design Part II (Ref. 20), and Part III (Ref. 22).

22.1. Layout of Structural Components

The structural layout includes that of the fuselage, wing, powerplants, and empennage. Ref. 20 provides preliminary structural layout guidelines and various configuration examples including the size, spacing, and location of ribs, longerons, stringers, and spars.

22.1.1. Fuselage Structure

Figure 22.1 Diamond DA40 XLS Door Configuration (Ref. 30)

The fuselage skin is to be made from a composite material, either carbon fiber or fiberglass. This facilitates the manufacture of compound curvature featured in the fuselage design. Layout of cabin doors is similar to that of the Diamond DA40 XLS shown in Figure 22.1, but with an opposing second rear door. Frames are placed around windows and doors to reinforce the composite structure while longerons are not needed due to the composite nature of the fuselage. Bulkheads are located at the single aircraft engine bay/cabin interface and the tail/cabin interface of both aircraft. Ring frames provide the structural interface for empennage, wing, and single engine nose gear attachment. Fuselage structure is shown in blue in Figure 22.2 and Figure 22.3 for the single and twin-engine variants, respectively.

22.1.2. Wing Structural Layout

The wing's structural layout consists of 18 ribs and two spars. A corrugated aluminum skin was chosen to simplify design by eliminating stringers. Ribs are located at critical positions such as the control surfaces and fuel tank mounting positions. Additional ribs were located following the spacing recommendations stated in Ref. 22, with spacing no greater than 36 inches. The front spar is located at 25% chord length and the rear spar is located at 70% chord length, adjacent to the flaps and ailerons. Wings are integrated to the fuselage by bolting the wings in a carry-through section as in Figure 4.60 from Ref. 22. Wing structure is shown in red in Figure 22.2 and Figure 22.3 for the single and twin-engine variants, respectively.

22.1.3. Powerplant Structural Layout

Each engine is mounted via a truss to a firewall. Engine cowlings are composite to accommodate compound curvature and require no additional structure as they only experience aerodynamic loading. Engine structure is shown in green in Figure 22.2 and Figure 22.3 for the single and twin-engine variants, respectively.

22.1.4. Empennage Structural Layout

As with the wings, the V-tail skin will be corrugated aluminum. Two spars were placed in the V-tail along with five ribs. The front spar is located at 25% chord and the rear spar at 70% chord, adjacent to the ruddervator. The ribs are placed at the root and tip of the V-tail and at the sides of the ruddervator. Rib spacing is no greater than 36 in. as per Ref. 22.

To integrate the V-tail with the fuselage, the spars of the V-tail protrude straight down and are bolted to ring frames in the fuselage. Empennage structure is shown in red in Figure 22.2 and Figure 22.3 for the single and twin-engine variants, respectively.

22.2. CAD Drawing of Structural Layout

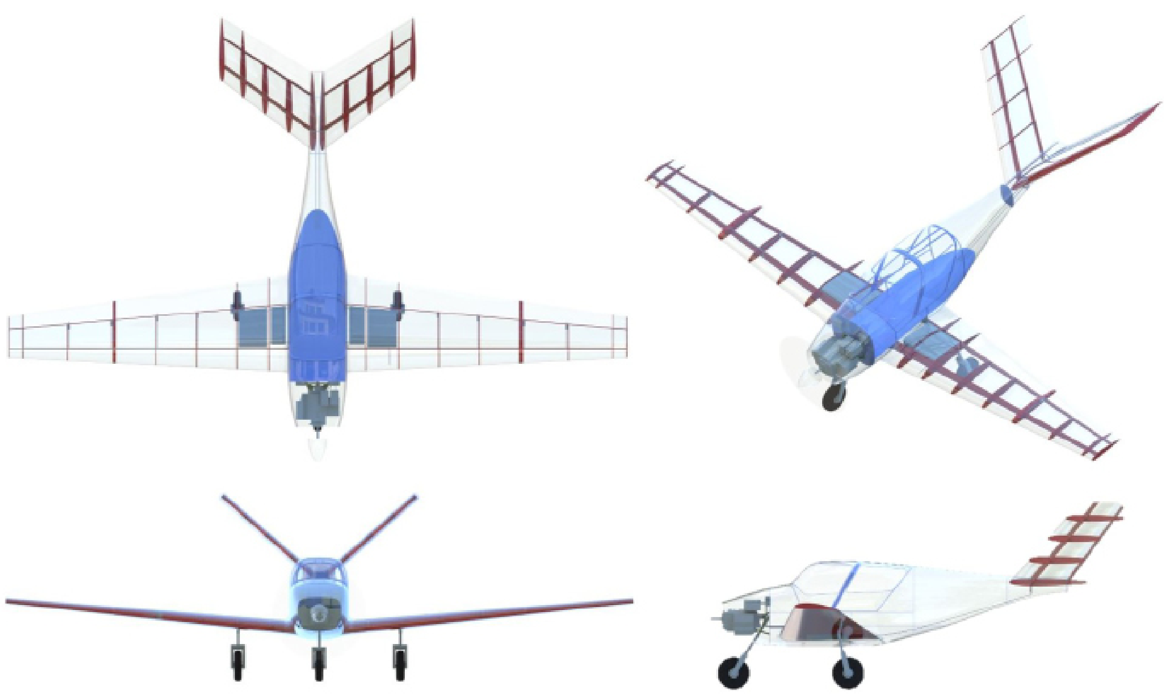

Figure 22.2 Single Engine Structural Layout (1:125)(in)

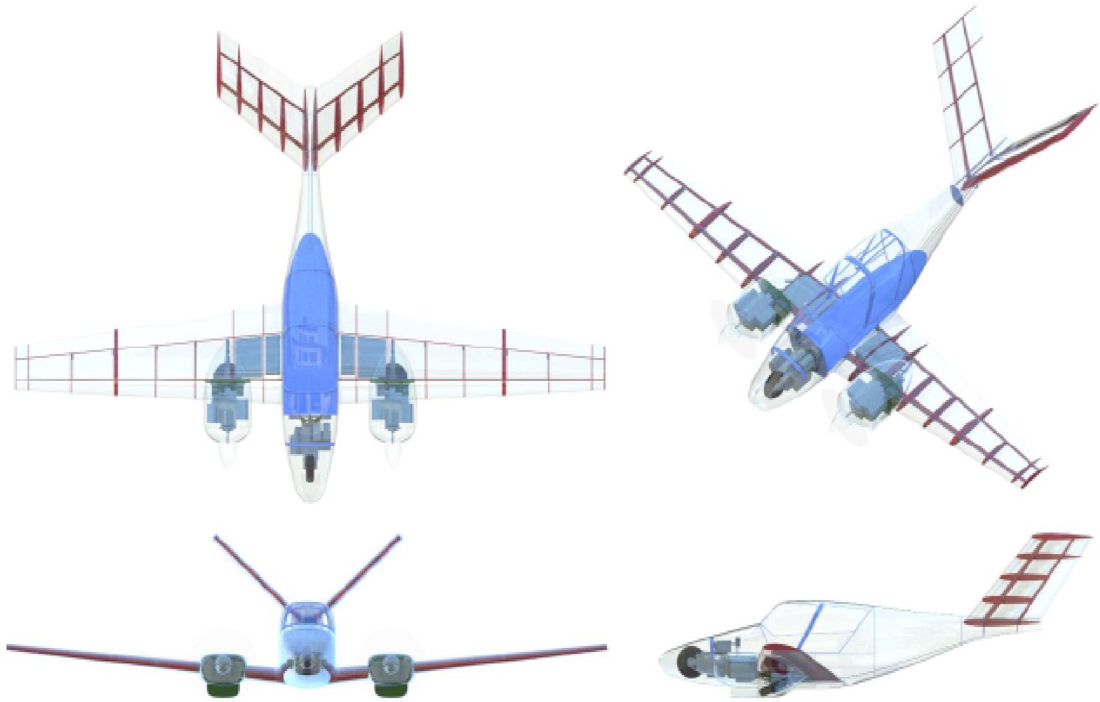

Figure 22.3 Twin Engine Structural Layout (1:125)(in)

22.3. Summary and Recommendations

22.3.1. Summary

The authors conclude that the fuselages and of the single and twin variants will be composite to accommodate compound curvature; the same applies to the twin variant engine nacelles. Wings and empennages will be aluminum with corrugated aluminum skins. Structure of the single and twin variants are shown in Figure 22.2 and Figure 22.3 for the single and twin-engine variants, respectively.

22.3.2. Recommendations

The authors recommend that:

i.) A method for preventing galvanic corrosion between the composite structures and aluminum structures be determined;

ii.) Lightening hole sizing and placement should be estimated to accommodate systems routing.

23. Class II Weight and Balance

The purpose of this chapter is to perform Class II weight and Balance using the methods found in Reference 20.

23.1. Class II Weight & Balance Calculations

All Class II weights were found using AAA Class II weight estimation method. A detailed component weight break down is found in Table 23.1 and Table 23.2 for the single and twin engine aircraft respectively

Table 23.1 Single Engine Component Weight Breakdown

#	Component	Weight (lbf)	F.S (in)	M_iX_i
1	Wing	270.0	195	52650
2	V-Tail	69.2	387	26789
3	Fuselage	284.0	170	48280
4	Nose Landing Gear	30.0	132	3960
5	Main Landing Gear	90.0	217	19530
6	Propeller	37.5	113	4238
7	Piston Engine	239.4	137	32798
8	Air Induction System	24.5	120	2940
9	Propulsion System	24.0	137	3288
10	Flight Control System	128.2	170	21788
11	Hydraulic System	10.5	173	1817
12	Instruments/Avionics	75.0	183	13725
13	Electrical System	127.8	151	19295
14	Furnishings	96.4	215	20727
15	Cargo Handling Equipment	18.0	263	4734
16	Other	15.0	200	3000
	Empty Weight	1539.5		
17	Trapped Fuel and Oil	14.8	201	2975
18	Fuel	240.0	198	47520
19	Crew	200.0	200	40000
20	Front Passenger	200	200	40000
21	Rear Passenger	400	240	96000
22	Baggage	160	260	41600
	Takeoff Weight	2034.3	X C.G (in)	187

Table 23.2 Twin Engine Component Weight Breakdown

#	Component	Weight (lbf)	F.S (in)	M_iX_i
1	Wing	330.0	195	64350
2	V-Tail	94.0	387	36378
3	Fuselage	284.0	161	45724
4	Nacelle	58.0	160	9280
5	Nose Landing Gear	80.0	132	10560
6	Main Landing Gear	250.0	215	53750
7	Propeller	77.0	136	10472
8	Piston Engine	600.0	161	96600
9	Fuel System	89.0	230	20470
10	Propulsion System	132.0	231	30492
11	Flight Control System	145.0	161	23345
12	Hydraulic System	10.5	173	1816.5
13	Instruments/Avionics	75.0	183	13725
14	Electrical System	151.0	175	26425
15	Furnishings	96.4	161	15521
16	Cargo Handling Equipment	18.0	263	4734
17	Other	10.0	161	1606
	Empty Weight	2499.9		
18	Trapped Fuel and Oil	30	201	6030
19	Fuel	464	201	93264
20	Crew	200	200	40000
21	Front Passenger	200	200	40000
22	Rear Passenger	400	244	97600
23	Baggage	160	263	42080
	Take off Weight	3954	X C.G (in)	198

23.2. Class II CG Positions on the Airframe, CG Excursion

The locations of each component system on its respective airframe is shown in Figure 23.1 and Figure 23.2 for singe engine and twin engine aircraft respectively

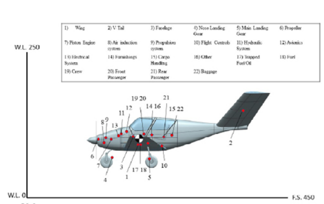

Figure 23.1 Single Engine Component Location

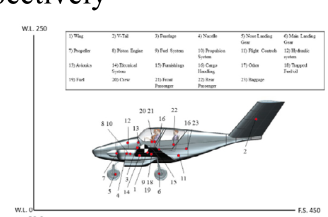

Figure 23.2 Twin Engine Component Location

For each loading condition Table 23.3 and Table 23.4 show aircraft weight, C.G location and MGC percentage.The CG excursion for the respective aircraft are found in Figure 23.3 and Figure 23.4.

Table 23.3 Single Engine Weight and Balance Summary

Weight and Balance Summary			
Condition	Weight (lbf)	CG location (in)	MGC %
Empty	1576	181.4	0.25
Operating empty weight	1794	185.0	0.31
Takeoff Weight	2034	187.0	0.34
2 occupants	2274	189.0	0.37
3 occupants	2514	194.0	0.45
4 occupants	2754.3	198.0	0.51
Minus Fuel	2514	198.8	0.52

Table 23.4 Twin Engine Weight and Balance Summary

Weight and Balance Summary			
Condition	Weight (lbf)	CG location (in)	MGC %
Empty	2499	186.0	0.32
Operating Empty Weight	2769	188.0	0.35
Take Off Weight	3233	190.0	0.38
2 Occupants	3474	191.0	0.40
3 Occupants	3714	195.0	0.46
4 Occupants	3954	198.0	0.51
Minus fuel	3489	197.0	0.49

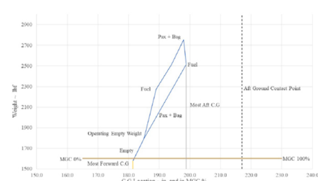

Figure 23.3 Single CG Excursion

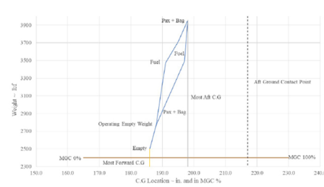

Figure 23.4 Single CG Excursion

23.3. <u>Summary and Recommendations</u>

23.3.1. <u>Summary</u>

Major findings from this chapter are:

- Class II weight analysis increased aircraft weight when compared to Class I estimations
- Overall C.G location moved forward from initial Class I calculations allowing for the twin engine aircraft to carry the full baggage payload.

23.3.2. <u>Recommendations</u>

The authors recommend that the weight could be estimated at a higher fidelity structural component estimations of thicknesses were applied. If done, material densities could be applied and more precise component weights could be found.

24. Class II Weight and Balance Analysis

The purpose of this chapter is to analyze the Class II weight and balance and determine the aircraft design feasibility. The procedures in Ref. 20 were used to determine aircraft design feasibility.

24.1. Class II Weight & Balance Analysis

The class II weight calculations were performed using AAA and based on the component weights computed, a completed systems list of weights was compiled. Each aircraft had an increase in empty weight; of 297 lbf and 339 lbf for the single and twin aircraft respectively. While this is an increase of more than 5%, Chapter 31 demonstrates that each aircraft is capable of meeting takeoff, climb, and service ceiling requirements defined by the RFP. The weight increase caused the C.G. to move slightly forward on each aircraft, allowing the twin engine aircraft to carry a full baggage load with four passenger. The C.G. excursion for each aircraft is within the outlined requirements of Ref. 20. The aircraft family satisfies tip over conditions.

24.2. Summary and Recommendations

24.2.1. Summary

The authors conclude that the current aircraft family meets the Class II weight and balance requirements outlined in Ref. 20.

24.2.2. Recommendations

The authors recommend that advanced technologies be investigated to limit C.G. excursion to 0 in. The authors also conclude additional design iterations be performed that could decrease the C.G. excursions of the aircraft.

25. Updated 3-View & Aircraft Family Summary

This section will provide an updated 3-view of the single and twin engine and a summary of geometric characteristics. The single variant has been named Odyssey and the twin engine variant has been named Sunshine.

25.1. Geometry Summary

Table 25.1 shows the characteristics of the wing and V-tail of the Odyssey and Sunshine. Table 25.2 presents a dimensional summary of the Odyssey, and Table 25.3 presents a dimensional summary of the Sunshine. The differences between the Odyssey and the Sunshine are found in the engine Wnumber and placement and in the landing gear type; the Odyssey has a single nose-mounted engine and fixed landing gear while the Sunshine has one engine mounted on each wing and retractable landing gear. The main structure of the fuselage, wing, and empennage remain the same between the two variants.

Table 25.1 Odyssey and Sunshine Wing and V-Tail Characteristics Summary

	Wing	V-Tail
Area (ft^2)	188	57.0
Span (ft)	39.6	12.4
MGC (ft)	4.98	4.62
X_{MGC} (ft)	0.439	1.85
Aspect Ratio (~)	8.51	2.70
Sweep Angle (deg)	0.00	30.0
Taper Ratio (–)	0.403	0.804
Thickness Ratio (%)	15.0	20.0
Airfoil (~)	NACA 4415	NACA 0012
Dihedral Angle (deg)	5.80	41.5
Incidence Angle (deg)	Root: 2.00	0.00
	Tip: -1.70	
Aileron Chord Ratio (%)	29.5	Ruddervator Chord Ratio:
Aileron Span Ratio (%)	28.8	31.9
Flap Chord Ratio (%)	29.5	Ruddervator Span Ratio:
Flap Span Ratio (%)	38.9	70.8

Table 25.2 Odyssey Dimensions Summary

	Fuselage	Cabin Interior	Overall
Length (ft)	25.3	14.7	28.8
Maximum Height (ft)	5.31	3.92	12.0
Maximum Width (ft)	3.83	3.66	39.6

Table 25.3 Sunshine Dimensions Summary

	Fuselage	Cabin Interior	Overall
Length (ft)	25.4	14.7	28.9
Maximum Height (ft)	5.31	3.92	12.0
Maximum Width (ft)	3.83	3.66	39.6

25.2. Updated 3-Views

The updated 3-views for the Odyssey and Sunshine are shown in Figures 25.1 and 25.2 respectively.

25.3. Summary and Recommendations

25.3.1. Summary

The authors conclude that the single engine variant has been named Odyssey, and the twin engine variant has been named Sunshine. Odyssey and Sunshine 3-views are shown in Figure 25.1 and Figure 25.2.

25.3.2. Recommendations

The authors recommend that a higher fidelity CAD model be produced to show opening of aircraft doors and cowlings.

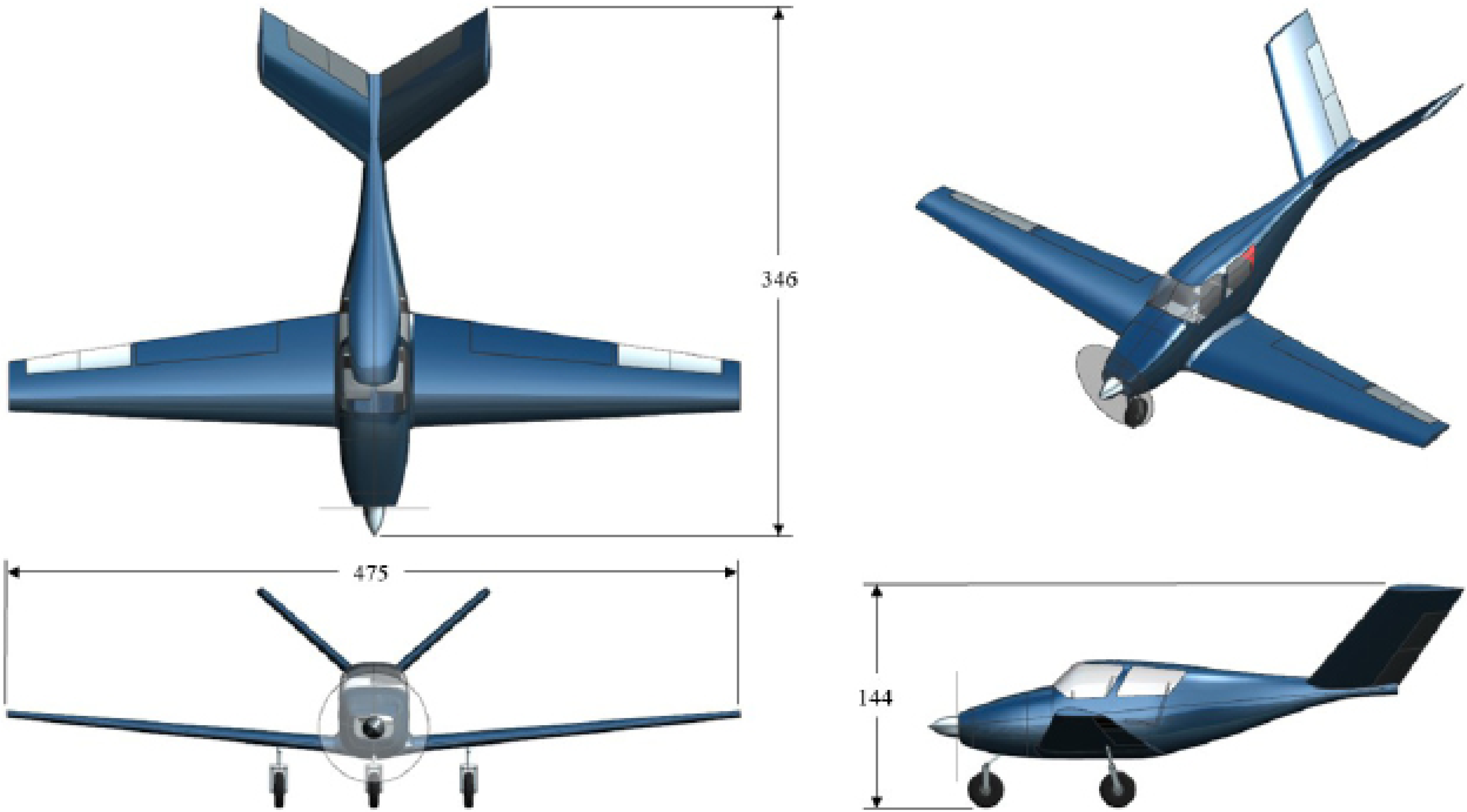

Figure 25.1 Odyssey 3-View (1:50)

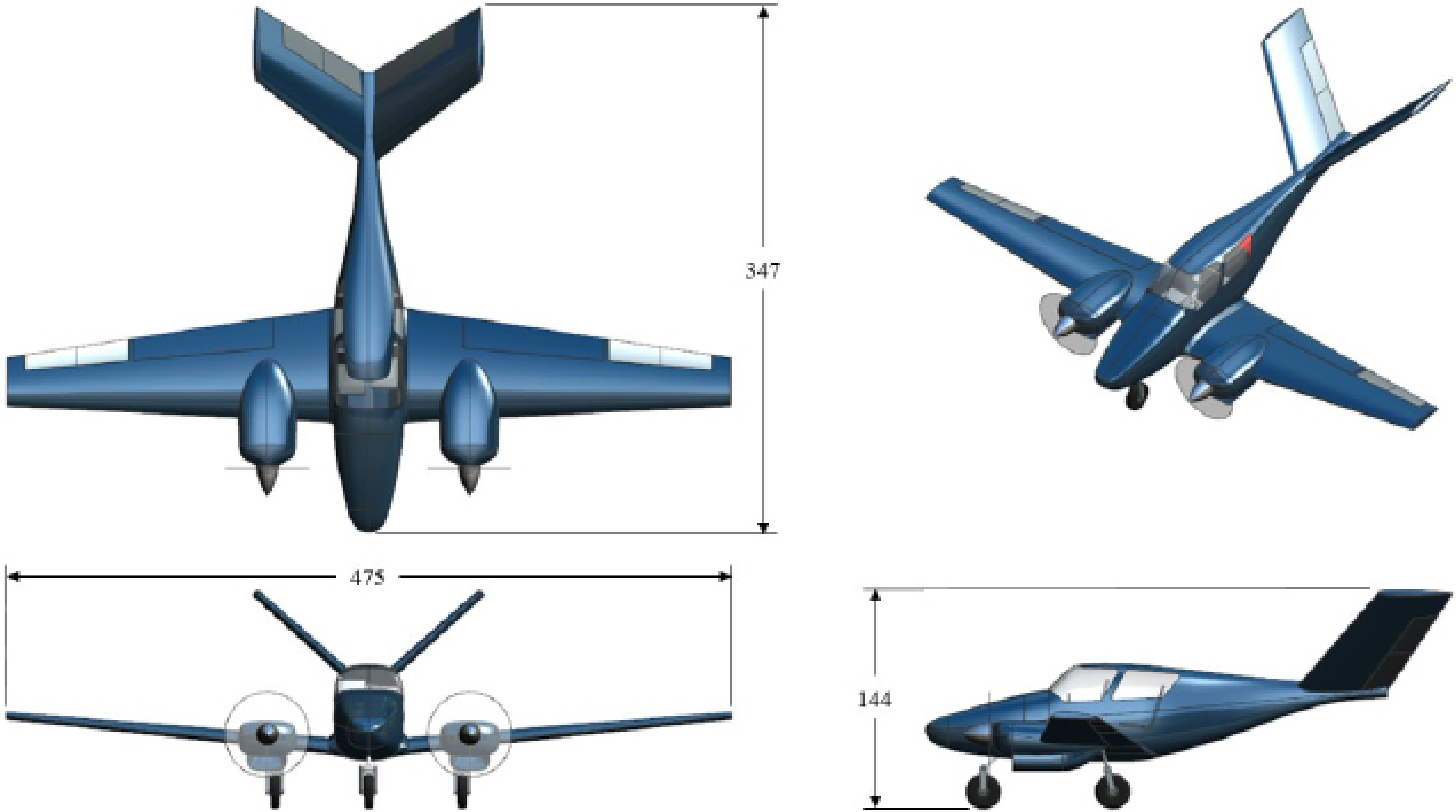

Figure 25.2 Sunshine 3-View (1:50)

26. Advanced Technologies

The purpose of this chapter is to outline advanced technologies that will be integrated into the aircraft family.

26.1. Fly by Wire

It was determined during the preliminary sizing of the aircraft that a fly-by-wire system would be used. The fly-by-wire system would save weight, increase the controllability of the aircraft, and reduce the pilot's input into the system, as stated in Chapter 20. Other than helping counter the coupling between yaw and roll generated by the butterfly tail, the particular advantage of implementing fly-by-wire is handling quality modification. In the system can simulate different flight types and conditions which would be useful for pilots in training. The flight control computers are able to have a series of handling quality modes providing for different flight conditions for a pilot to train on.

26.1.1. Handling Quality Modification

Fly =-by-wire is able to simulate different flight conditions by changing the gains of the control system of the aircraft to emulate the controls of a particular flight condition or even emulate handling qualities of other aircraft. The desired types of flight conditions and handling qualities can be programmed in the flight control computers and accessed at command. As such, the pilot is able to train in a safe environment for flight conditions that would otherwise be dangerous or inaccessible. For example, a pilot could simulate and train flying with an engine failure or experience a lightning strike.

More advantageous is the ability to emulate the handling quality of similar aircraft such as other popular trainer aircraft including the Cessna 172, Cirrus SR20, Diamond DA42, or Piper Seminole. Pilots would be able to change the handling quality by just inputting the desired handling quality in the flight control computer which would change the control system gains. As a result, the pilot would experience the feel of flying in a different aircraft. Different modes would also be incorporated such as an aerobatic mode in which the aircraft would be able to emulate the handling quality of aerobatic aircraft, limited only by the control surface authority. This would however be accounted for in the flight control computer to avoid maneuvers that could endanger the aircraft.

26.2. Advanced Airspeed Sensor

Figure 26.1 BAE System's Concept of LASSI (Ref. 31)

BAE systems is currently developing an advanced airspeed sensor based on bouncing an ultraviolet laser off air molecules Ref. 31,32. This system is similar to how roadside guns detect a car's speed and is based on the Doppler effect.

The airspeed works by reflecting ultraviolet light ahead of the aircraft. Once the ultraviolet light reflects from the air molecules, it undergoes a change in color based on the Doppler effect. The change in frequency physically changes the color of the light reflecting off the air molecules. The further away the reflection is from the color violet, the faster the aircraft is moving. The system, named Laser Air Speed Sensing Instrumentation (LASSI), measures the changes in color and calculates the airspeed of the aircraft. Figure 26.1 shows BAE System's concept of LASSI. Figure 26.2 portrays LASSI shooting ultraviolet beams on the twin engine aircraft, and Figure 26.3 shows the reflected beams being detected by the aircraft.

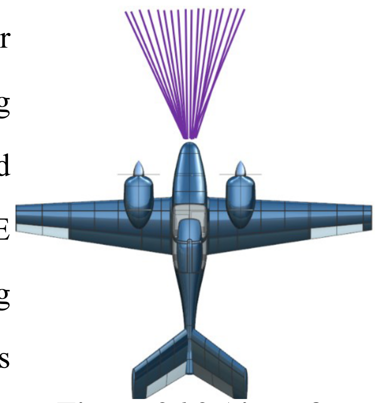

Figure 26.2 Aircraft Reflecting Ultraviolet Beams

LASSI has major advantages over conventional airspeed measuring systems such as pitot tubes. Wind tunnel testing by BAE Systems has shown that LASSI measures airspeed more accurately than pitot tubes, particularly at lower speeds. This would render LASSI more effective for the applications of trainer aircraft since they do not fly at high speeds. Moreover, since LASSI is completely integrated inside the aircraft, it is not susceptible to icing or foreign object damage. (Ref. 31) LASSI is also able to detect the airspeed at a distance, thus warning the pilot of turbulence ahead. BAE Systems expects LASSI to be available to the market by 2022 and thus would be able to be integrated into the aircraft within the service life.

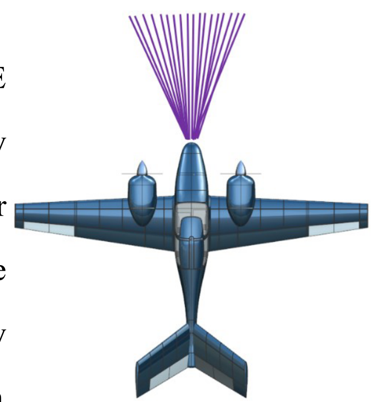

Figure 26.2 Aircraft Detecting Reflecting Ultraviolet Beams

27. Risk Mitigation

The fly-by-wire system itself counts for risk mitigation of the flight controls; however, to decrease the chances of catastrophic failure, a number of measures will be taken. In addition to LASSI, pitot tubes will still be integrated into the system. LASSI will be the main indicator for airspeed. In the case of an anomaly, the pitot tubes will be used as backup.

Separate Surface Stability Augmentation (SSSA) will be implemented. SSSA consists of splitting the control surfaces such as the aileron and rudder into two components (Ref. 34). Each component would be controlled by a single actuator, each of which would be connected to the two flight controllers. In the case one a flight control computer failure, the second flight control computer would still be operational and could still control the aircraft to land bsafety. LASSI alongside SSSA would ensure that system failures, such as the Boeing 737 Max incidents, would not be catastrophic and the stability of the system will not be lost.

Having two flight control computers would increase the price, however, this would be countered by the simplified certification process and decrease the insurance costs. The fly by wire system alongside LASSI and SSSA will decrease the chances of a crash thus flight absurdity can be guaranteed to the FAA. As such, the certification process can be accelerated and its related costs reduced. With the chances of a crash minimized, the insurance cost for the aircraft will also decrease thus obtaining two flight control computers becomes a viable and realistic option.

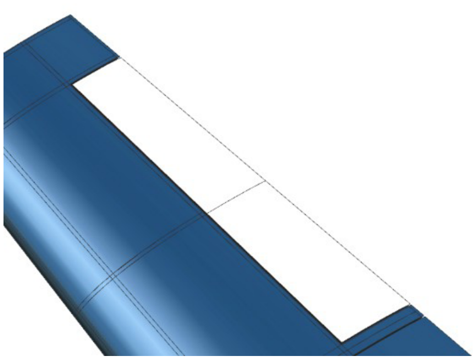

Figure 27.1 Split Aileron

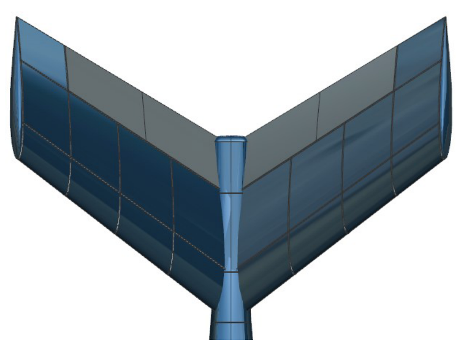

Figure 27.2 Split Ruddervator

28. Manufacturing Plan

The purpose of this chapter is to develop a manufacturing plan for the single and twin engine aircraft. The exploded views of the aircraft are shown in Figure 28.1 and Figure 28.2.

Figure 28.1 Single Engine Exploded View

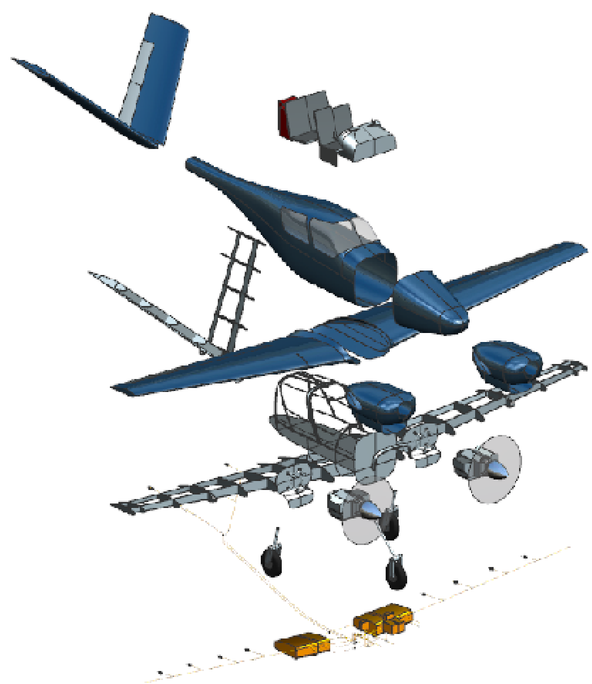

Figure 28.2 Twin Engine Exploded View

The design of the manufacturing process includes selecting materials and what manufacturer provides the parts for the aircraft. Super Aerial Bros will be manufacturing and making the majority of the parts. The parts will be either made at the assembly plant or at off site locations and shipped to the assembly plant by flatbed trucks. The bill of materials for the aircraft is found in Table 28.1.

Table 28.1 Bill of Material

Part	Material	Manufacturer
Wing	Aluminum	One Stone
Fuselage	Composites	One Stone
V-Tail	Aluminum	One Stone
Nacelles	Composites	One Stone
Enginges	~	Lycoming
Landing Gear	–	One Stone
Tires	Rubber	Goodyear
Avionics	~	Garmin

The wings and vertical tail are made from aluminum. The fuselage, nacelles, and nose cone for the aircraft are made from composites. The tooling needed for these composite parts are plugs. The parts will be manufactured with a fiber placement machine and a meltable inner mold. The inner molds for the composite parts are shown in Figure 28.3 to Figure 28.8.

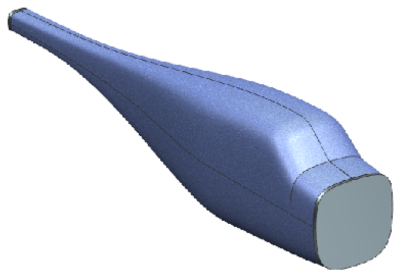

Figure 28.3 Fueselage Tool

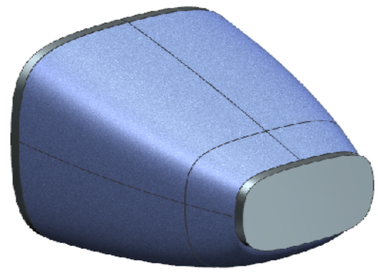

Figure 28.4 Single Nose Tool

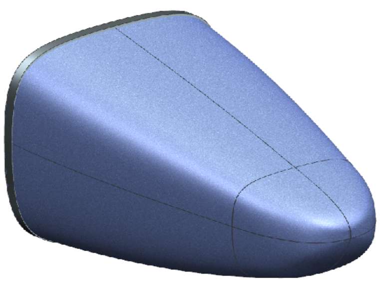

Figure 28.5 Twin Nose Tool

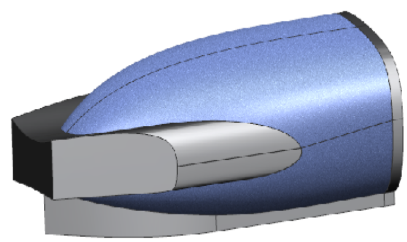

Figure 28.6 Nacelle Main Tool

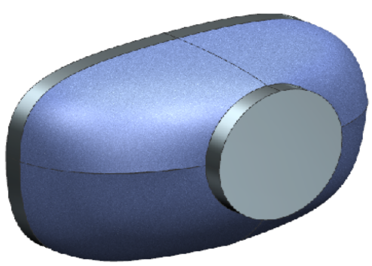

Figure 28.7 Nacelle Tip Tool

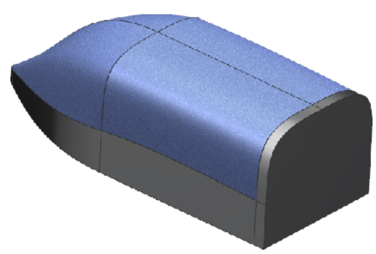

Figure 28.8 Nacelle Scoop Tool

The assembly of the single and twin engine aircraft will be performed in the same assembly plant. An overview of the manufacturing floor is shown in Figure 28.9.

The flow of the plant originates with the parts arriving at the two receiving dock. The parts will then be stored in the main storage area next to the receiving area. The assembly line for both aircraft begin the same. The wing assembly and the fuselage are assembled in their respective locations.and then transported to the wing fuselage assembly area for integration. Then the wing fuselage assembly will be supported by a custom cart as it is transported to Bay A1 or Bay A2. This point marks the divergence of the single and twin engine aircraft manufacturing processes. Line 1 is the assembly line for the single engine aircraft, and line 2 is the assembly line for the twin engine aircraft. Each bay contains the general part assembly area between the two lines. This area is for preparing the parts for installation on the aircraft in the respective bays. Each assembly area contains part and tool storage for relevant processes. When the storage or tools run low they contact the receiving team to deliver more parts to their section along the delivery path. The aircraft are rolled from bay to bay along the line until the aircraft is finished. Then the aircraft is rolled out a set of hangar doors at the end of the plant. The plant also contains break rooms (BR) and restrooms (RR) periodically along the side of the plant.

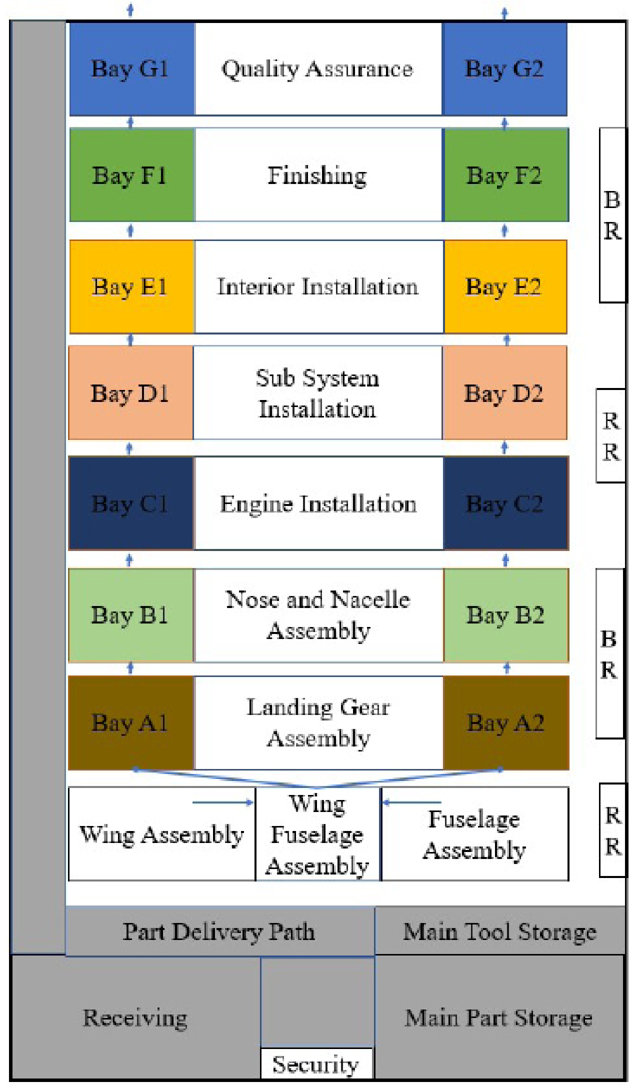

Figure 28.9Assembly Plant Floor

29. Cost

The purpose of this chapter is to analyze the cost associated with the single and twin engine aircraft using the methods from Ref. 37. AAA was used to calculate the cost. The costs calculated were the Research Development Test and Evaluation (RDTE) cost, acquisition cost, operating cost, and life cycle cost. The aircraft were analyzed assuming 6000 aircraft were manufactured with an operation life of 10 years each. The AAA calculations are shown in the hand calculations below. The cost for the single and twin engine aircraft are shown in Table 29.1.

Table 29.1 Aircraft Cost

	Single	Twin
RDTE	$ 43,945,000	$ 56,303,000
Acquisition	$ 588,000	$ 900,000
Operating	$ 8,400,463,000	$ 13,698,560,000
Life Cycle Cost	$ 12,050,412,000	$ 19,291,600,000

Hand Calculations

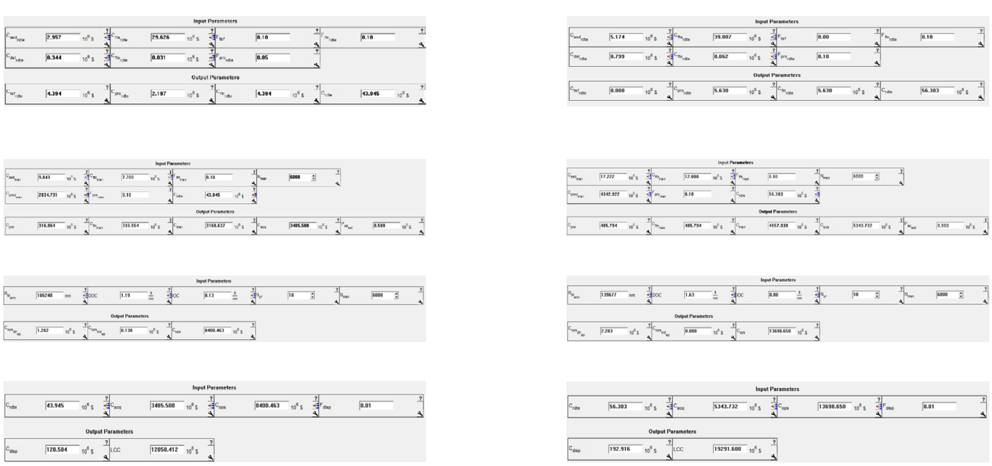

30. Class II Stability and Control

The purpose of this chapter is to perform a Class II Stability and Control analysis on the two aircraft using the methods depicted in Chapter 3 of Ref. 37. Both aircraft must meet FAR 23 requirements and have Level 1 stability requirements for flight conditions categorized as B and C (Ref. 37).

30.1. Static Longitudinal Stability

Longitudinal stability for both aircraft was reanalyzed as shown in the AAA popups. Table 30.1 contains the results of the analysis. The results show the aircraft are stable because they have a static margin ≥10%±1%.

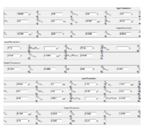

Click to Enlarge

Table 30.1 Static Longitudinal Stability Results

Aircraft	SM (%)	S_{vee} (ft^2)
Single Engine	9	57
Twin Engine	15	57

30.2. Static Directional Stability

Static Directional Stability was reanalyzed for each aircraft. No single engine out occurs for the single engine. The results are found in Table 30.2 and Table 30.3.

Table 30.2 Static Directional Stability Results

Aircraft	$C_{n,\beta}$ (rad^{-1})
Single Engine	0.0719
Twin Engine	0.0562

Click to Enlarge

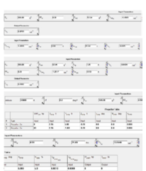

Table 30.3 Output Parameters for Single Engine Out

Minimum Controllable Speed, V_{mc} (kts)	85.2
Ruddervator Directional Deflection Angle, $\delta_{r,rv}$ (deg)	-4.07

30.3. Dynamic Longitudinal Stability

Both aircraft are classified as Class I aircraft with flight phases B and C (Ref. 37). As such, both aircraft must meet the following criteria in Table 30.4.

Table 30.4 Level 1 Requirements for Class 1 Aircraft

Mode	Undamped Natural Frequency, ω_n (rad/s)	Damping Ratio, ξ (~)
Phugoid	Low	$\xi > 0.04$
Short Period	High	$0.35 < \xi < 1.30$

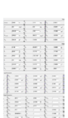
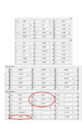


Click to Enlarge

30.4. Dynamic Lateral-Directional Stability

Within this section spiral mode, roll mode, and Dutch roll mode were investigated for each aircraft. Each aircraft must meet the requirements shown in Table 30.5 to be considered stable. AAA was used to model the three modes for both aircraft. The results are shown in Table 30.6 and Table 30.7.

Table 30.5: Lateral-Directional Stability Requirements

Spiral Mode		
Flight Phase	**Spiral Mode Time Constant, T_S (s)**	
B	$T_S>20$	
C	$T_S>12$	
Roll Mode		
Flight Phase	**Roll Mode Time Constant, T_R (s)**	
B	$T_R<1.4$	
C	$T_R<1.0$	
Dutch Roll Mode		
Flight Phase	**Undamped Natural Frequency, ω_n (rad/s)**	**Damping Ratio, ξ (~)**
B	$\omega_{n,D} > 0.4$	$\xi_D >0.08$
C	$\omega_{n,D} > 1.0$	$\xi_D > 0.08$

Click to Enlarge

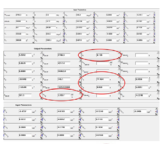

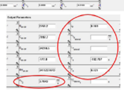

Table 30.6: Lateral-Directional Stability Results (Single Engine)

Spiral Time Constant, T_S (s)	77.5
Roll Time Constant, T_S (s)	0.069
Dutch Roll Undampened Natural Frequency, $\omega_{n,D}$ (rad/s)	3.20
Dutch Roll Damping Ratio, ξ_{D} (~)	0.139

Table 30.7: Lateral-Directional Stability Results (Twin Engine)

Spiral Time Constant, T_S (s)	192.3
Roll Time Constant, T_S (s)	0.121
Dutch Roll Undampened Natural Frequency, $\omega_{n,D}$ (rad/s)	3.78
Dutch Roll Damping Ratio, ξ_{D} (~)	0.169

30.5. Roll Rate Coupling

Roll rate coupling needs to meet the following criteria to be considered stable:

$$\left(\frac{M_q * N_r}{M_\alpha} + \frac{I_{yy}-I_{xx}}{I_{zz}} + \frac{N_\beta (I_{xx}-I_{zz})^2}{M_\alpha * I_{yy}}\right)^2 - 4\left(\frac{I_{yy}-I_{xx}}{I_{zz}}\right)\left(\frac{N_\beta (I_{xx}-I_{zz})}{M_\alpha * I_{yy}}\right) < 0 \qquad \text{Ref. 37}$$

AAA was used to analyze these criteria. The results show that there is no critical roll rate.


Click to Enlarge
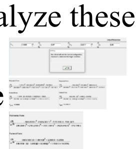

30.6. Summary and Recommendations

30.6.1. Summary

The authors conclude that:

i.) The single engine aircraft is inherently stable for all conditions;

ii.) The twin Engine is inherently stable for static conditions, but de facto stable for dynamic conditions;

iii.) No pitch coupling exists;

iv.) No critical roll rate occurs for either aircraft;

v.) The following tables:

Table 30.8: Longitudinal Dynamic Stability Values (Single Engine)

Mode	Undamped Natural Frequency, ω_n (rad/s)	Damping Ratio, ξ (~)
Phugoid	0.19	0.10
Short Period	3.29	0.67
Both	Load Factor to angle-of-attack, n_α (g/rad)	10.49

Table 30.9: Longitudinal Dynamic Stability Values (Twin Engine)

Mode	Undamped Natural Frequency, ω_n (rad/s)	Damping Ratio, ξ (~)
Phugoid	0.18	0.24
Short Period	2.18	0.67
Both	Load Factor to angle-of-attack, n_α (g/rad)	10.49

Table 30.10: Feedback Gains for Twin Engine (Static)

Airspeed Feedback, k_u (ft/s/ft/s)	Angle of Attack Feedback, k_α (deg/deg)	Pitch rate Feedback, k_Θ (deg/deg)
673	-0.312	-2.35

Table 30.11: Lateral-Directional Stability Values (Single Engine)

Spiral Time Constant, T_S (s)	77.5
Roll Time Constant, T_S (s)	0.069
Dutch Roll Undampened Natural Frequency, $\omega_{n,D}$ (rad/s)	3.20
Dutch Roll Damping Ratio, ξ_D (~)	0.14

Table 30.12: Lateral-Directional Stability Values (Twin Engine)

Spiral Time Constant, T_S (s)	192
Roll Time Constant, T_S (s)	0.12
Dutch Roll Undampened Natural Frequency, $\omega_{n,D}$ (rad/s)	3.78
Dutch Roll Damping Ratio, ξ_D (~)	0.17

Table 30.13: Feedback Gain for Dynamic Stability (Twin Engine)

Sideslip Gain, k_β (deg/deg)	Yawrate Gain, k_Φ (deg/deg)	Rollrate Gain, k_Ψ (deg/deg)
4.19	369	40.3

30.6.2. Recommendations

The authors recommend a more advanced controller than a basic PID-controller. This will enhance the flight characteristics of the twin engine aircraft as well as adapt to nonlinear external disturbances.

31. Performance

The following chapter uses the step-by-step analysis given in Chapter 5 of Ref. 37 to determine the performance characteristics of both aircraft. AAA was used to calculate any necessary values. All requirements have been set by FAR 23 and/or the RFP for both aircraft.

31.1. Stall

Stall conditions were determined for max weight at cruise, takeoff, and landing. FAR 23 aircraft must maintain a stall speed lower than 61 kts in all conditions. Stall characteristics can be found in Table 31.1.

Table 31.1: Stall Characteristics for Aircraft

Aircraft-Condition	$C_{L,Max,S}$ (~)	$\alpha_{CL,Max,S}$ (deg)	V_S (kn)
Single- Takeoff, Landing	1.7, 1.7	15.7, 15.7	43.6, 46.1
Single- Clean	1.5	15.8	53.6
Twin- Takeoff, Landing	1.8, 1.8	14.5, 14.5	48.7, 44.0
Twin- Cruise	1.5	15.5	67.7

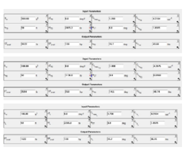

Click to Enlarge

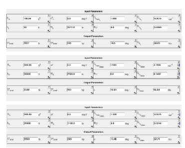

31.2. Takeoff

Ground takeoff distance must be less than 1500 ft to meet the requirements of the RFP. The results are found in Table 31.2.

Table 31.2: Takeoff Characteristics

Aircraft	Stall Speed at Takeoff, $V_{S,TO}$ (kn)	Speed at Liftoff, V_{LOF} (kn)	Takeoff Field Length, S_{TO} (ft)	Takeoff ground Run, S_{TOG} (ft)
Single	43.7	52.4	1537	737
Twin	48.7	55.5	869	423

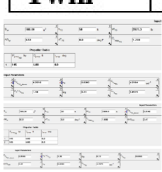

Click to Enlarge

31.3. Climb

The minimum rate of climb requirement for both aircraft is 100 ft/min. The results are shown in Table 31.3.

Table 31.3: Climb Characteristics of Aircraft

Aircraft	Time to Ceiling, t_{Cl} (min)	Rate of Climb, RC (ft/min)
Single Engine	7.90	1512
Twin Engine	15.6	1495

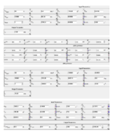

Click to Enlarge

31.4. Cruise, Range, and Payload-Range Performance

Both aircraft must meet the requirements by the RFP shown in Table 1.1. The results are shown in Table 31.4.

Table 31.4: Range Results

Aircraft	MTOW Range (nmi)	Full Passenger Range (nmi)	Max Ferry Range (nmi)
Single	797	998	1176
Twin	963	1124	1226

Click to Enlarge

31.5. Endurance

The single engine aircraft must have an endurance loiter of at least 3 hours per the RFP, and the twin engine aircraft must have an endurance loiter of at least 4 hours per the RFP. The results are shown in Table 31.5.

Table 31.5: Endurance Characteristics

Aircraft	Endurance at Constant Altitude, $E_{CR,h=const}$ (hr)
Single	4.3
Twin	4.5

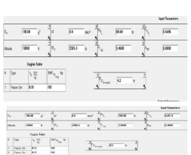

Click to Enlarge

31.6. Dive

No dive requirements exist in the RFP for either aircraft, but the aircraft are limited to the values shown due to their V-n diagram. The results are shown in Table 31.6.

Table 31.6: Dive Characteristics

Aircraft	α (deg)	γ (deg)	Max Dive Speed, V_d (ft/s)
Single	-4.12	8.8	253
Twin	-2.58	23.2	363

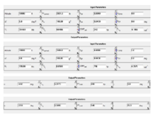

Click to Enlarge

31.7. Maneuvering

Both aircraft must be able to maintain a steady level turn. These aircraft are not meant to withstand a sudden pull-up or pushover maneuver; therefore, so it was not investigated. The results are shown in Table 31.7.

Table 31.7: Sustained Turn Characteristics

Aircraft	V_M (kts)	Turn Rate (rad/s)	n_{turn} (g)	Φ (deg)	R_{turn} (ft)
Single	66.8	0.542	2.15	62.3	208
Twin	63.4	0.353	1.55	49.7	302.9

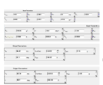

Click to Enlarge

31.8. Landing

The single engine must land within 1500 feet, and the twin engine must land within 2500 ft. The average deceleration must be between 0.30-0.35 ft/s^2. The landing distance was calculated as 424 ft and 642 ft for the single and twin engine aircraft respectively.

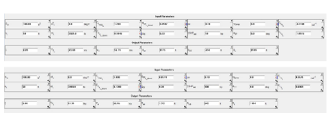

Click to Enlarge

31.9. Summary and Recommendations

The authors conclude that required values are in Tables 31.1 to 31.7 and the following figures. Additionally, both aircraft can reach their ceiling requirements shown in Figure 31.1 and Figure 31.2. Both aircraft meet the requirements for the RFP and FAR 23 standards.

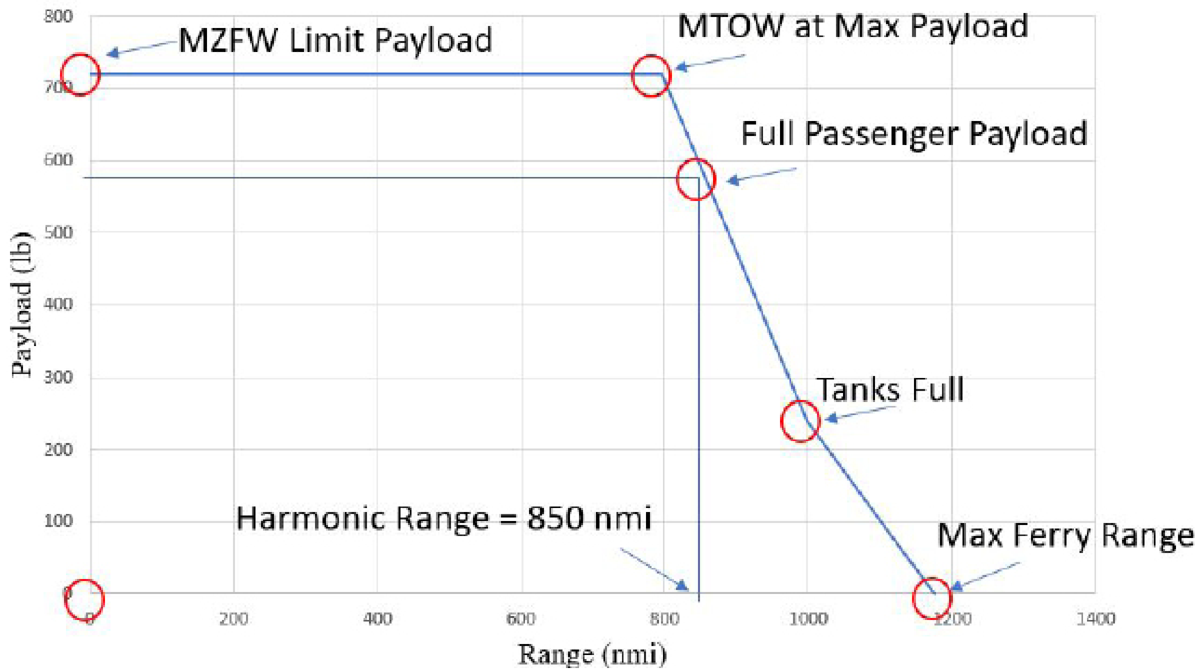

Figure 31.1: Payload-Range Diagram (Single Engine)

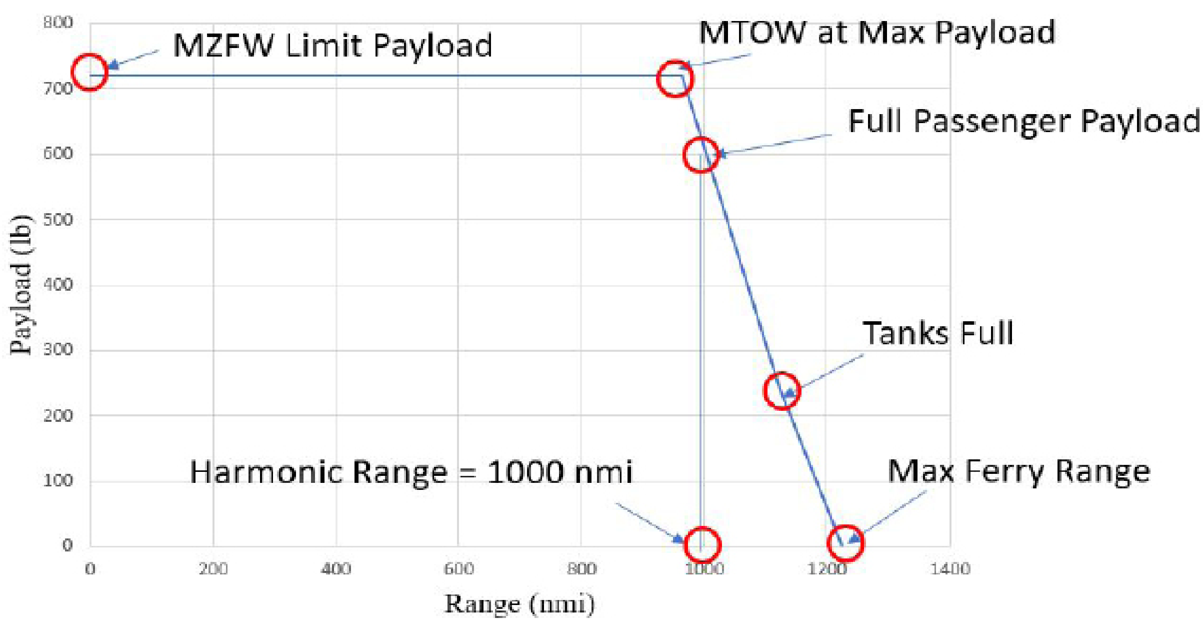

Figure 31.2: Payload-Range Diagram (Twin Engine)

32. Specification Compliance

The purpose of this section if to display the compliance to the requirements provided by the RFP. Table 32.1 shows the compliance the RFP requirements.

Table 32.1 RFP Compliance

RFP Requirement			Aircraft Characteristic		Requirement Met?		Page #
	Single	Twin	Single	Twin	Single	Twin	
Capable of taking off and landing from runways (asphalt or concrete)	~		Land on Hard Surface	Land on Hard Surfaces	Yes	Yes	56-58
Capable of VFR and IFR flight	~		Fly by wire system with avionics package	Fly by wire system with avionics package	Yes	Yes	50,
Meets applicable certifacation rules in FAA 14 CFR Part 23	–		FAA 14 CFR Part 23 Desinged	FAA 14 CFR Part 23 Desinged	Yes	Yes	15,16,46
Engine/ppropulsion systemn assumptions documented	~		IO-360, Dual Fixed Pitch Prop	IO-360, Three Blade Fixed Speed Prop	Yes	Yes	14-14
Crew	1 Pilot Required, 2-Pilot (Dual Instruction) Capable		Dual Capable	Dual Capable	Yes	Yes	19-21
Passengers	1+	3+	3	3	Yes	Yes	19-21
Takeoff Distance	< 1500 ft	< 2500 ft	737 ft	869 ft	Yes	Yes	82-84
Landing Distance	< 1500 ft	< 2500 ft	424 ft	642 ft	Yes	Yes	82-84
Endurance	> 3 hr	> 4 hr	4.3 hrs	4.5 hrs	Yes	Yes	82-84
Ferry Range	> 800 nmi	> 1000 nmi	1176 nmi	1226 nmi	Yes	Yes	82-84
Service Ceiling	> 12,000 ft	> 18,000 ft	>12,000 ft	>18,000 ft	Yes	yes	82-84
Certification Category	Utility	Normal	Normal	Normal	Yes	Yes	82-84

33. Marketing Plan and Path Forward

This section will briefly discuss the Super Aerial Bros marketing plan for the Odyssey and the Sunshine and the path forward.

33.1. Marketing Plan

A marketing brochure for each aircraft, the Odyssey and the Sunshine, are shown at the end of this report.

33.2. Path Foward

In the future, new aircraft options could be offered. These could be diesel engine variants or an electric variant as battery technology advances. Augmented reality features could be integrated as the technology matures to ease pilot workload.

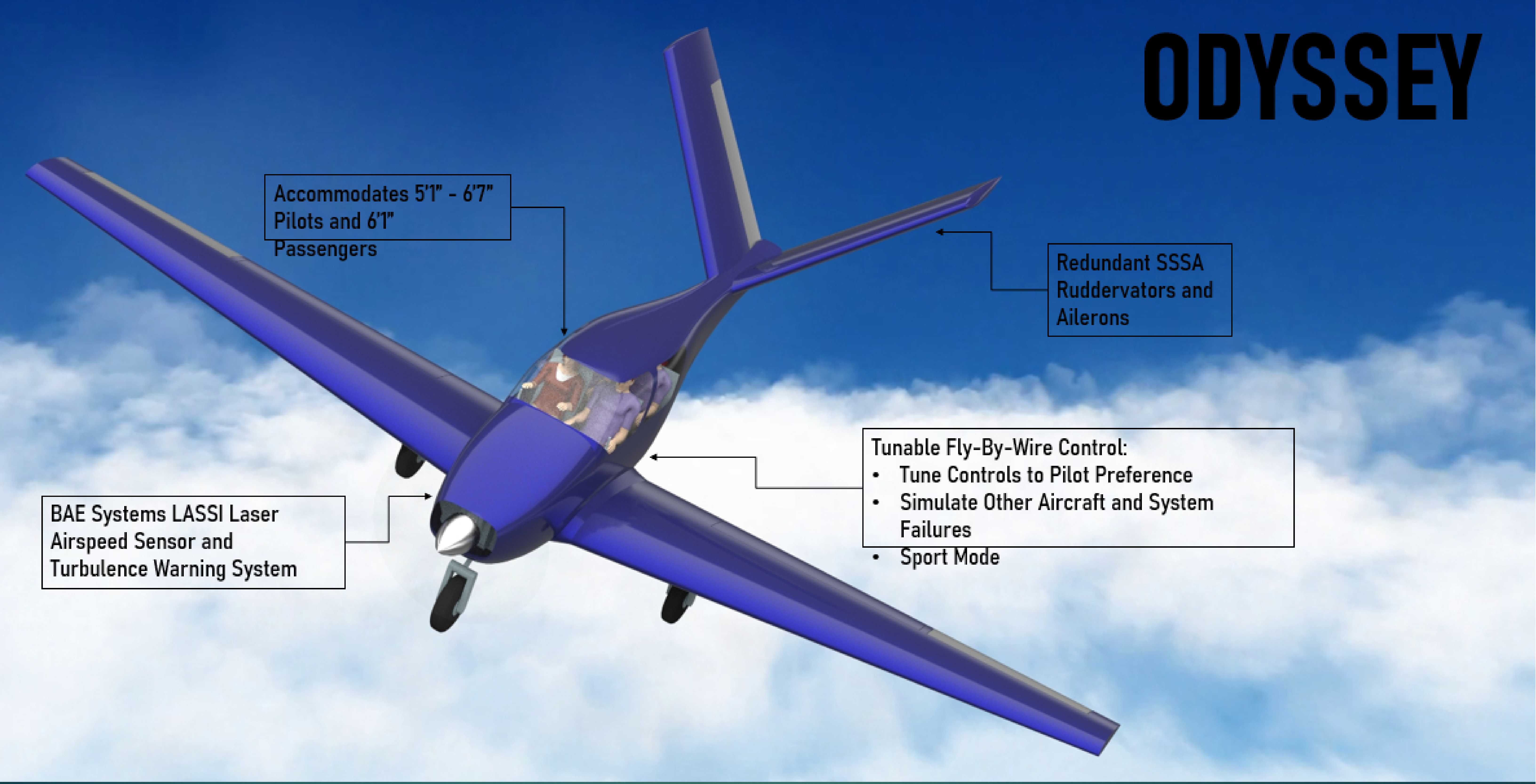

Acquisition Cost: $558,000

Stall Speed Takeoff: 43.6 kn

Takeoff Ground Run: 737 ft

Rate of Climb: 1512 ft/min

Stall Speed Landing: 46.1 kn

Ferry Range: 1176 nm

Endurance: 4.3 hrs

Rate of Climb: 1512 ft/min

Useful Payload: 960 lbf

Fuel Consumption: 0.319 lbf-hp/hr

SUNSHINE

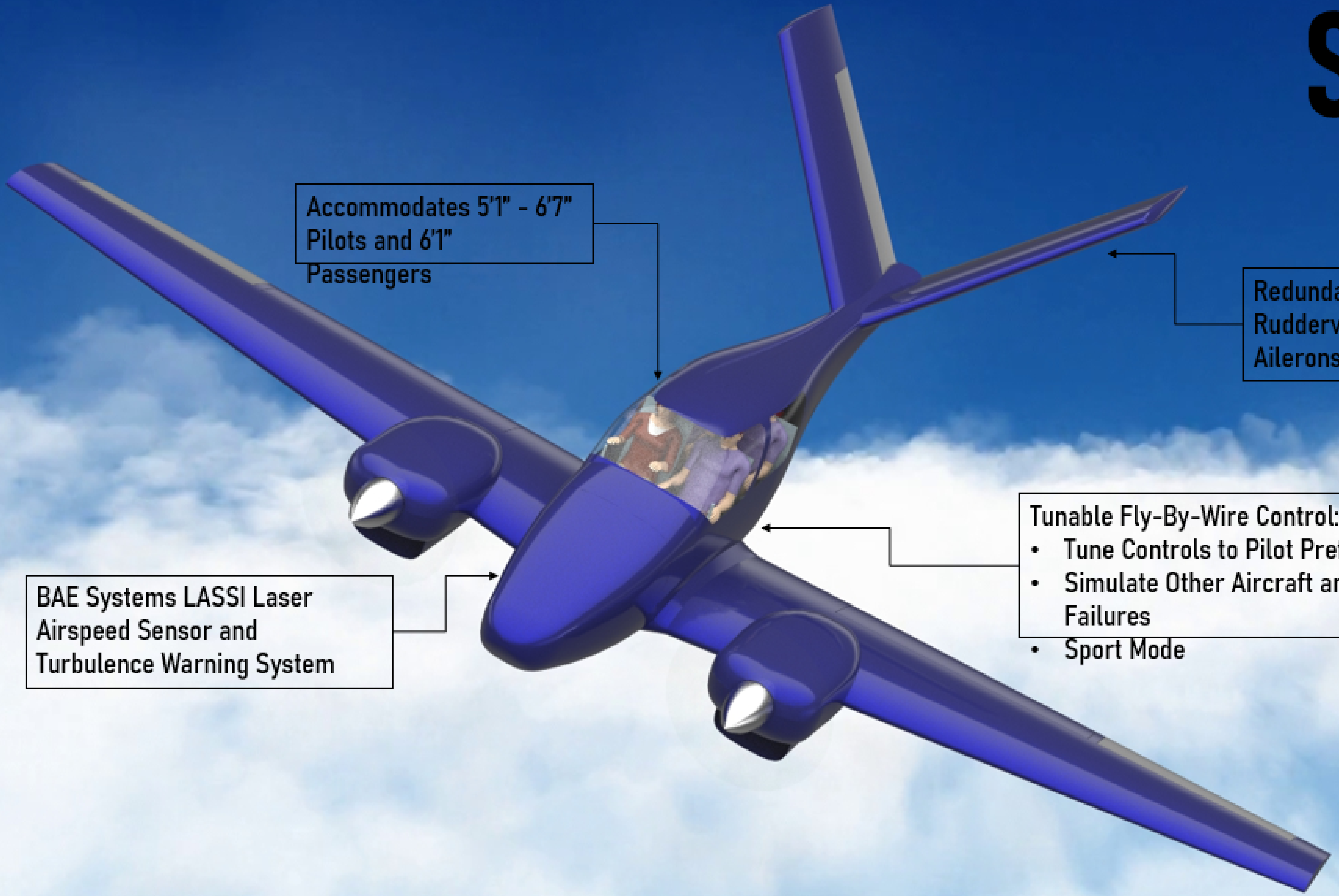

Acquisition Cost: $900,000

Stall Speed Takeoff: 48.7 kn

Takeoff Ground Run: 423 ft

Rate of Climb: 1495 ft/min

Stall Speed Landing: 44.0 kn

Ferry Range: 1226 nm

Endurance: 4.5 hrs

Rate of Climb: 1495 ft/min

Useful Payload: 1185 lbf

Fuel Consumption: 0.319 lbf-hp/hr

34. References

1. Anon., "General Aviation Trainer Aircraft Family; Request for Proposal," 2019-2020 AIAA Foundation Graduate Competition, pp. [online RFP], URL: https://www.aiaa.org/designcompetitions/ [26 August 2018].

2. Anon., "Fair Treatment of Experience Pilots Act," *Web Site* [https://www.faa.gov/other_visit/aviation_industry/airline_operators/airline_safety/info/all_infos/media/age65_qa.pdf] September 2019.

3. Anon.," Pilot Outlook by Region," *Boeings Market outlook Pilot and Technician Outlook Web Site* [https://www.boeing.com/commercial/market/pilot-technician-outlook/] P. O. Box 3707 Seattle, Washington 98124, September 2019.

4. Roskam, J., "Airplane Design: Part I, Preliminary Sizing of Airplanes," DARcorporation, Lawrence, KS, 2005.

5. Anon., "Cessna Skyhawk," *Cessna Textron Aviation Web Site* [https://cessna.txtav.com/en/piston/cessna-skyhawk] Textron Aviation, 11 September 2019.

6. Anon., "Embry-Riddle To Buy 60 Cessna Skyhawks," *Aircraft Owners and Pilots Association Web Site* [https://www.aopa.org/news-and-media/all-news/2019/july/25/embry-riddle-to-buy-60-cessna-skyhawks] AOPA, 421 Aviation Way Frederick, MD, 21701, 14 September 2019.

7. "2018 Annual Report" General Aviation Manufacturers Association., 1400 K Street, NW Suite 801 Washington, DC 20005.

8. Anon., "Professional Flight Fees" *Purdue Polytechnic Institute Web Site* [https://polytechnic.purdue.edu/degrees/professional-flight/fees] Purdue University - Purdue Polytechnic Institute, 401 N Grant Street, West Lafayette, IN 47907, September 2019.

9. Anon., "Aircraft and Equipment," *Western Michigan University College of Aviation Web Site* [https://wmich.edu/aviation/future/why/aircraft] Western Michigan University, Kalamazoo, MI 49008, September 2019.

10.Anon.," Aviation Consumer: Cirrus Safety Record Just Average," *AVweb Web Site* [https://www.avweb.com/news/aviation-consumer-cirrus-safety-record-just-average/] Aviation Publishing Group, September 2019.

11. Anon., "CGCC Aero Fleet," *University of North Dakota Aerospace Web Site* [http://phoenix.aero.und.edu/fleet/airplanes.aspx] University of North Dakota, Grand Forks, ND, September 2019.

12. Anon., "Explore the SR20," *Cirrus Aircraft Web Site* [https://cirrusaircraft.com/aircraft/sr20/] Cirrus Design Corporation d/b/a Cirrus Aircraft, September 2019.

13. Anon., "DA42 Technical Specifications," *Diamond Aircraft Web Site* [https://www.diamondaircraft.com/en/private-pilots/aircraft/da42/tech-specs/] Diamond Aircraft Industries, N. A. Otto-Strasse 5 2700 Wiener Neustadt Austria, September 2019.

14. Anon., "Welcome to the Seminole," *Piper Web Site* [https://www.piper.com/aircraft/trainer-class/seminole/] Piper Aircraft, 2926 Piper Drive, Vero Beach, FL 32960, September 2019.

15. Krueger, N "Discussion of Favorable Trainer Aircraft Characteristics," Lawrence Municipal Airport, 20 September 2019

16. Barrett, R., "Statistical Time and Market Predictive Engineering Design (STAMPED) Techniques for Aerospace System Preliminary Design," Journal of Aeronautics & Aerospace Engineering., Volume 3 Issue 1.

17. Anon., "Janes all the worlds aircraft," *IHS Markit Web Site* [https://janes.ihs.com/janes/home] Jane's Information Group London, England, 8 September 2019.

18. Anon., "Part 23-Airworthiness Standards: Normal Category Airplanes," *Electronic Code of Federal Regulations Web Site* [https://www.ecfr.gov/cgi-bin/text-idx?SID=685dc1ae97ae3f5e5569e47880fab01e&mc=true&node=pt14.1.23#se14.1.23_12000] 11 September 2019.
19. Anon., "Aircraft Weight and Balance Control," Advisory Circular, FAA, AC 120-27E, Washington, DC, 2005.
20. Roskam, J., Airplane Design: Part II, Preliminary Configuration Design and Integration of the Propulsion System, DARcorporation, Lawrence, KS, 2005
21. Anon.," 14 CFR 61.1," *Electronic Code of Federal Regulations, Web Site* [https://www.ecfr.gov/cgi-bin/text-idx?pitd=20160829&node=se14.1.61_11&rgn=div8] 2 October 2019
22. Roskam, J., Airplane Design: Part III, Layout Design of Cockpit, Fuselage, Wing and Empennage: Cutaways and Inboard Profiles, DARcorporation, Lawrence, KS, 2005
23. tsatips, "Carry On Luggage Size: TSA and Airline Dimensions," *TSA Travel Tips, TSA Travel Tips Web Site* [https://tsatraveltips.us/] TSA, 13 June 2018.
24. Lycoming, "Operator's Manual O-360, HO-360, IO-360, AIO-360, HIO-360 & TIO-360 Series," Lycoming, Williamsport, Penselvania, October 2005.
25. Anon., "NACA 4415," *Airfoil Tools* [http://airfoiltools.com/airfoil/details?airfoil=naca4415-il] Airfoil Tools, October 2019.
26. "Aircraft Spotlight: The V-Tail Bonanza – A Cross Country Head Turner", AOPA Foundation
27. Pope, S., "We Fly: Cirrus SF50 Vision Jet", Flying
28. Roskam, J., Airplane Design: Part V, Component Weight Estimation, DARcorporation, Lawrence, KS, 2005
29. Roskam, J., Airplane Design: Part IV, Layout of Landing Gear and Systems, DARcorporation, Lawrence, KS, 2005 30
30. Lee, M., "Diamond DA40 XLS," *Plane & Pilot, Plane & Pilot Web Site* [https://www.planeandpilotmag.com/article/diamond-da40-xls2/#.XeSr4uhKiUl], 24 February 2009.
31. Laycock, L., "Our ground-breaking laser airspeed sensor means more accurate data and a safer more comfortable flight," *BAE Systems Corporate Blog,* July 27, 2016.
32. "BAE claims aviation first laser airspeed sensor", *The Engineer*, July 13th, 2016.
33. "The Doppler Effect", *the Physics Classroom.*
34. Jenks, G., Henry, H., Roskam, J., "Flight Test Results for a Separate Surface Stability", KU-FRL-364, NASA-CR-143839, April 1977
35. "Boeing 737 Max Lion Air crash caused by a series of failures", *BBC News*, October 2019
36. Roskam, J., Airplane Design: Part VIII, Airplane Cost Estimation: Design, Development, Manufacturing and Operating, DARcorporation, Lawrence, KS,2005 30.
37. Roskam, J., Airplane Design: Part VII, Determination of Stability, control, and Performance Characteristics: Far and Military Requirements , DARcorporation, Lawrence, KS,2005 30.